

APPENDIX A-1
Hydrodynamic Model Equations

HYDRODYNAMIC MODEL EQUATIONS

INTRODUCTION

The physics of the model and the techniques employed to solve the governing equations have been described in detail by Blumberg and Mellor (1983, 1987) and by Blumberg and Herring (1987).

The most important prognostic/diagnostic variables computed by the model are:

1. Water surface elevation (η)
2. ξ_1 component of the velocity vector (U)
3. ξ_2 component of the velocity vector (V)
4. Vertical component of the velocity vector (W)
5. Salinity (S)
6. Temperature (Θ)
7. Density (ρ)
8. Turbulence kinetic energy (q^2)
9. Turbulence macroscale (λ)
10. Vertical eddy viscosity (K_M)
11. Vertical eddy diffusivity (K_H)
12. ξ_1 component of the bottom stress vector (WUBOT)
13. ξ_2 component of the bottom stress vector (WWBOT)

DESCRIPTION OF THE MODEL

The model described in this primer is the time-dependent, three-dimensional, estuarine and coastal circulation model of Blumberg and Mellor (see Blumberg and Mellor, 1980 and 1987). This model has been used in numerous studies on various important natural water systems; among them works by Blumberg and Mellor (1983) on the South Atlantic Bight, Oey et al. (1985a,b,c,d) on the Hudson-Raritan estuary, Blumberg and Mellor (1985) on the Gulf of Mexico, Galperin and Mellor (1990a,b) on Delaware Bay, River and adjacent continental shelf, Blumberg and Goodrich (1990) on Chesapeake Bay and most recently Blumberg, Signell and Jenter (1993) on Massachusetts Bay. In all these studies the model skills were assessed via extensive comparisons with data and a confidence has been established that the predominant physics are realistically reproduced by the model.

THE BASIC EQUATIONS

The basic equations may be expressed as,

$$\frac{\partial U}{\partial x} + \frac{\partial V}{\partial y} + \frac{\partial W}{\partial z} = 0 \quad (1)$$

$$\begin{aligned} \frac{\partial U}{\partial t} + \frac{\partial U^2}{\partial x} + \frac{\partial UV}{\partial y} + \frac{\partial UW}{\partial z} - fV + g \frac{\partial \eta}{\partial x} \\ = \frac{\partial}{\partial z} \left(K_M \frac{\partial U}{\partial z} \right) - \frac{g}{\rho_0} \frac{\partial}{\partial x} \int_z^n \rho dz + F_x \end{aligned} \quad (2)$$

$$\begin{aligned} \frac{\partial V}{\partial t} + \frac{\partial UV}{\partial x} + \frac{\partial V^2}{\partial y} + \frac{\partial VW}{\partial z} + fU + g \frac{\partial \eta}{\partial y} \\ = \frac{\partial}{\partial z} \left(K_M \frac{\partial V}{\partial z} \right) - \frac{g}{\rho_0} \frac{\partial}{\partial y} \int_z^n \rho dz + F_y \end{aligned} \quad (3)$$

$$\frac{\partial \Theta}{\partial t} + \frac{\partial \Theta U}{\partial x} + \frac{\partial \Theta V}{\partial y} + \frac{\partial \Theta W}{\partial z} = \frac{\partial}{\partial z} \left(K_H \frac{\partial \Theta}{\partial z} \right) + F_\Theta \quad (4)$$

$$\frac{\partial S}{\partial t} + \frac{\partial SU}{\partial x} + \frac{\partial SV}{\partial y} + \frac{\partial SW}{\partial z} = \frac{\partial}{\partial z} \left(K_H \frac{\partial S}{\partial z} \right) + F_S \quad (5)$$

$$\begin{aligned} \frac{\partial q^2}{\partial t} + \frac{\partial Uq^2}{\partial x} + \frac{\partial Vq^2}{\partial y} + \frac{\partial Wq^2}{\partial z} = \frac{\partial}{\partial z} \left(K_q \frac{\partial q^2}{\partial z} \right) \\ + 2K_M \left[\left(\frac{\partial U}{\partial z} \right)^2 + \left(\frac{\partial V}{\partial z} \right)^2 \right] + \frac{2g}{\rho_0} K_H \frac{\partial \rho}{\partial z} - 2 \frac{q^3}{\Lambda_1} + F_q \end{aligned} \quad (6)$$

$$\frac{2q^2\lambda}{\partial t} + \frac{\partial U q^2 \lambda}{\partial x} + \frac{\partial V q^2 \lambda}{\partial y} + \frac{\partial W q^2 \lambda}{\partial z} = \frac{\partial}{\partial z} \left(K_q \frac{\partial q^2 \lambda}{\partial z} \right) + E_1 \lambda \left\{ K_M \left[\left(\frac{\partial U}{\partial z} \right)^2 + \left(\frac{\partial V}{\partial z} \right)^2 \right] + \frac{q D^3}{\rho_o} K_H \frac{\partial \rho}{\partial z} \right\} - \frac{q^3}{B_1} \tilde{W} + F_\lambda \quad (7)$$

The horizontal viscosity and diffusion terms are defined according to:

$$F_x = \frac{\partial}{\partial x} (\tau_{xx}) + \frac{\partial}{\partial y} (\tau_{xy}) \quad (8a)$$

$$F_y = \frac{\partial}{\partial x} (\tau_{xy}) + \frac{\partial}{\partial y} (\tau_{yy}) \quad (8b)$$

with

$$\tau_{xx} = 2A_M \frac{\partial U}{\partial x} \quad (9a)$$

$$\tau_{xy} = \tau_{yx} = A_M \left[\frac{\partial U}{\partial y} + \frac{\partial V}{\partial x} \right] \quad (9b)$$

$$\tau_{yy} = 2A_M \frac{\partial V}{\partial y} \quad (9c)$$

Also

$$F_\phi = \frac{\partial}{\partial x} (q_x) + \frac{\partial}{\partial y} (q_y) \quad (10)$$

$$q_x = A_H \frac{\partial \phi}{\partial x} \quad (11a)$$

$$q_y = A_H \frac{\partial \phi}{\partial y} \quad (11b)$$

where ϕ now represents Θ , S , q^2 or $q^2\lambda$.

Vertical Boundary Conditions

The vertical boundary conditions on (1) are

$$W(-H) = 0 \quad (12)$$

The boundary conditions on (2) and (3) are

$$K_M \left| \frac{\partial U}{\partial z}, \frac{\partial V}{\partial z} \right| = - (\langle wu(\eta) \rangle, \langle wv(\eta) \rangle), \quad z \rightarrow \eta \quad (13a,b)$$

where the right hand side of (13a,b) corresponds to the input values of the surface wind stress (divided by ρ_0), and

$$K_M \left| \frac{\partial U}{\partial z}, \frac{\partial V}{\partial z} \right| = C_z (U^2 + V^2)^{1/2} (U, V), \quad z \rightarrow -H \quad (13c,d)$$

where

$$C_z = \text{MAX} \left[\frac{k^2}{(\ln(z/z_o))^2}, \text{BFRIC} \right] \quad (13e)$$

$k = 0.4$ is the von Karman constant, z_o is the roughness parameter and BFRIC is user-specified. Numerically, (13c, d, e) is applied to the first grid point nearest the bottom. It

can be derived by matching the numerical solution to the "law of the wall". Where the bottom is not well resolved (z/z_0 is large), (13e) reverts to an ordinary drag coefficient formulation.

The boundary conditions on (4) and (5) are

$$K_H \left[\frac{\partial T}{\partial z}, \frac{\partial S}{\partial z} \right] = - (\langle w\theta(\eta) \rangle, \langle ws(\eta) \rangle), \quad z \rightarrow \eta \quad (14a,b)$$

$$K_M \left[\frac{\partial T}{\partial z}, \frac{\partial S}{\partial z} \right] = (0, 0), \quad z \rightarrow -H \quad (14c,d)$$

The boundary conditions on (6) and (7) are

$$(q^2(\eta), q^2\lambda(\eta)) = (B_1^{2/3} u_r^2(\eta), 0) \quad (15a,b)$$

$$(q^2(-H), q^2\lambda(-H)) = (B_1^{2/3} u_r^2(-H), 0) \quad (15c,d)$$

where B_1 is one of the turbulence closure constants and u_r is the friction velocity at the top and bottom as denoted.

An important advantage of the present model over that used earlier is the use of a horizontal, orthogonal, curvilinear coordinate system. These equations in the mass flux conservative form are:

The Continuity Equation

$$\frac{\partial}{\partial \xi_1} (h_2 U_1) + \frac{\partial}{\partial \xi_2} (h_1 U_2) + h_1 h_2 \frac{\partial W}{\partial z} = 0 \quad (16a)$$

Free Surface Equation

Integrating the continuity equation (16a) over the depth and using a kinematic boundary condition at the free surface leads to an important auxillary equation, the free surface equation

$$h_1 h_2 \frac{\partial \eta}{\partial t} + \frac{\partial}{\partial \xi_1} \int_{-H}^n (U_1 h_2) dz + \frac{\partial}{\partial \xi_2} \int_{-H}^n (U_2 h_1) dz = 0 \quad (16b)$$

The Reynolds Equations

$$\begin{aligned} & \frac{\partial (h_1 h_2 U_1)}{\partial t} + \frac{\partial}{\partial \xi_1} (h_2 U_1^2) + \frac{\partial}{\partial \xi_2} (h_1 U_1 U_2) + h_1 h_2 \frac{\partial (W U_1)}{\partial z} \\ & + U_2 \left(- U_2 \frac{\partial h_2}{\partial \xi_1} + U_1 \frac{\partial h_1}{\partial \xi_2} - h_1 h_2 f \right) \\ \therefore & = - g h_2 \left(\frac{\partial \eta}{\partial \xi_1} + \frac{\partial H_o}{\partial \xi_1} \right) - \frac{g D h_2}{\rho_o} \int_z^n \frac{\partial \rho}{\partial \xi_1} dz \\ & - \frac{h_2}{\rho_o} \frac{\partial P_a}{\partial \xi_1} + \frac{\partial}{\partial \xi_1} \left(2 A_M \frac{h_2}{h_1} \frac{\partial U_1}{\partial \xi_1} \right) + \frac{\partial}{\partial \xi_2} \left(A_M \frac{h_1}{h_2} \frac{\partial U_1}{\partial \xi_2} \right) \\ & + \frac{\partial}{\partial \xi_2} \left(A_M \frac{\partial U_2}{\partial \xi_1} \right) + h_1 h_2 \frac{\partial}{\partial z} \left(K_M \frac{\partial U_1}{\partial z} \right) \end{aligned} \quad (17)$$

$$\begin{aligned}
& \frac{\partial(h_1 h_2 U_2)}{\partial t} + \frac{\partial}{\partial \xi_1} (h_2 U_1 U_2) + \frac{\partial}{\partial \xi_2} (h_1 U_2^2) + h_1 h_2 \frac{\partial (WU_2)}{\partial z} \\
& + U_1 \left(- U_1 \frac{\partial h_1}{\partial \xi_2} + U_2 \frac{\partial h_2}{\partial \xi_1} + h_1 h_2 f \right) \\
= & - gh_1 \left(\frac{\partial \eta}{\partial \xi_2} + \frac{\partial H_o}{\partial \xi_2} \right) - \frac{gDh_1}{\rho_o} \int_z^n \frac{\partial \rho}{\partial \xi_2} dz \\
& - \frac{h_1}{\rho_o} \frac{\partial P_a}{\partial \xi_2} + \frac{\partial}{\partial \xi_2} \left(2A_M \frac{h_1}{h_2} \frac{\partial U_2}{\partial \xi_2} \right) + \frac{\partial}{\partial \xi_1} \left(A_M \frac{h_2}{h_1} \frac{\partial U_2}{\partial \xi_1} \right) \\
& + \frac{\partial}{\partial \xi_1} \left(A_M \frac{\partial U_1}{\partial \xi_2} \right) + h_1 h_2 \frac{\partial}{\partial z} \left(K_M \frac{\partial U_2}{\partial z} \right)
\end{aligned} \tag{18}$$

Transport of Temperature

$$\begin{aligned}
& h_1 h_2 \frac{\partial \theta}{\partial t} + \frac{\partial}{\partial \xi_1} (h_2 U_1 \theta) + \frac{\partial}{\partial \xi_2} (h_1 U_2 \theta) + h_1 h_2 \frac{\partial (W\theta)}{\partial z} \\
= & \frac{\partial}{\partial \xi_1} \left(\frac{h_2}{h_1} A_H \frac{\partial \theta}{\partial \xi_1} \right) + \frac{\partial}{\partial \xi_2} \left(\frac{h_1}{h_2} A_H \frac{\partial \theta}{\partial \xi_2} \right) + h_1 h_2 \frac{\partial}{\partial z} \left(K_H \frac{\partial \theta}{\partial z} \right)
\end{aligned} \tag{19}$$

Transport of Salinity

$$\begin{aligned}
 & h_1 h_2 \frac{\partial s}{\partial t} + \frac{\partial}{\partial \xi_1} (h_2 U_1 s) + \frac{\partial}{\partial \xi_2} (h_1 h_2 s) + h_1 h_2 \frac{\partial (ws)}{\partial z} \\
 &= \frac{\partial}{\partial \xi_1} \left(\frac{h_2}{h_1} A_H \frac{\partial s}{\partial \xi_1} \right) + \frac{\partial}{\partial \xi_2} \left(\frac{h_1}{h_2} A_H \frac{\partial s}{\partial \xi_2} \right) + h_1 h_2 \frac{\partial}{\partial z} \left(K_H \frac{\partial s}{\partial z} \right)
 \end{aligned} \tag{20}$$

Transport of Turbulent Kinetic Energy

$$\begin{aligned}
 & h_1 h_2 \frac{\partial q^2}{\partial t} + \frac{\partial}{\partial \xi_1} (h_2 U_1 q^2) + \frac{\partial}{\partial \xi_2} (h_1 U_2 q^2) + h_1 h_2 \frac{\partial (wq^2)}{\partial z} \\
 &= h_1 h_2 \left\{ 2K_M \left[\left(\frac{\partial U_1}{\partial z} \right)^2 + \left(\frac{\partial U_2}{\partial z} \right)^2 \right] + \frac{2g}{\rho_o} K_H \frac{\partial \rho}{\partial z} - \frac{2q^3}{\Lambda_1} \right\} \\
 &+ \frac{\partial}{\partial \xi_1} \left(\frac{h_2}{h_1} A_H \frac{\partial q^2}{\partial \xi_1} \right) + \frac{\partial}{\partial \xi_2} \left(\frac{h_1}{h_2} A_H \frac{\partial q^2}{\partial \xi_2} \right) + h_1 h_2 \frac{\partial}{\partial z} \left(K_q \frac{\partial q^2}{\partial z} \right)
 \end{aligned} \tag{21}$$

Transport of Turbulent Macroscale

$$\begin{aligned}
 & h_1 h_2 \frac{\partial (q^2 \lambda)}{\partial t} + \frac{\partial}{\partial \xi_1} (h_2 U_1 q^2 \lambda) + \frac{\partial}{\partial \xi_2} (h_1 U_2 q^2 \lambda) + h_1 h_2 \frac{\partial (wq^2 \lambda)}{\partial z} \\
 &= h_1 h_2 \left\{ \lambda E_1 K_M \left[\left(\frac{\partial U_1}{\partial z} \right)^2 + \left(\frac{\partial U_2}{\partial z} \right)^2 \right] + \frac{\lambda E_1 g}{\rho_o} K_H \frac{\partial \rho}{\partial z} - \frac{q^3}{B_1} \tilde{w} \right\}
 \end{aligned}$$

$$\begin{aligned}
& + \frac{\partial}{\partial \xi_1} \left(\frac{h_2}{h_1} A_H \frac{\partial (q^2 \lambda)}{\partial \xi_1} \right) + \frac{\partial}{\partial \xi_2} \left(\frac{h_1}{h_2} A_H \frac{\partial (q^2 \lambda)}{\partial \xi_2} \right) \\
& + h_1 h_2 \frac{\partial}{\partial z} \left(K_q \frac{\partial (q^2 \lambda)}{\partial z} \right)
\end{aligned} \tag{22}$$

where ξ_1 and ξ_2 are arbitrary horizontal curvilinear orthogonal coordinates. The horizontal viscosity in the present model is given according to the Smagorinsky (1963) formulation and, in the simulations conducted here, the coefficient varied between 1 and 50 $m^2 s^{-1}$. However, for numerical stability the model limits the maximum horizontal viscosity to 1000 $m^2 s^{-1}$. The vertical mixing (eddy) coefficients (K_M , K_H and K_q) are evaluated using the level 2-1/2 turbulence closure model of Mellor and Yamada (1982) as modified by Galperin et al. (1988).

The coefficients are given by:

$$K_M = q \lambda S_M, \quad K_H = q \lambda S_H \text{ and } K_q = 0.2 q \lambda \tag{23a,b,c}$$

where the stability functions, S_M and S_H , are analytically derived, algebraic relations.

CHARACTERISTICS OF THE MODEL

Non-linear

The model is fully non-linear. Linear momentum equation options are also available and are useful for debugging purposes.

Coriolis Parameter

A variable Coriolis parameter is incorporated into the model and is determined from latitude, which is user specified.

Finite Difference

The equations which form the circulation model, together with their boundary conditions, are solved by finite difference techniques. A horizontally and vertically staggered lattice of grid points is used for the computations. An implicit numerical scheme in the vertical direction (Roache, 1972;) and a semi-implicit scheme in the horizontal direction (Cassuli, 1990). The finite difference equations conserve energy, mass and momentum.

Diagnostic Variables

The diagnostic variables include the horizontal and vertical eddy viscosity, and the horizontal and vertical eddy diffusivity. Global integrals and budgets of various properties such as total kinetic energy, available potential energy, total mass, heat and salt content are also computed.

Prognostic Variables

ECOMsiz is a three-dimensional, primitive equation, time-dependent estuarine, coastal

and open ocean circulation model. The prognostic variables are the free surface elevation, the three components of velocity, temperature, salinity (hence density through an equation of state), and two quantities which characterize the turbulence, turbulence kinetic energy and turbulence macroscale. Prognostic equations governing the thermodynamic quantities, temperature and salinity, account for water mass variations brought about by highly time-dependent coastal upwelling processes, for example.

Free Surface

Free surface elevation is calculated prognostically so that tides and storm surge events can be simulated.

Hybrid-Level Model

ECOMsiz is a multi-level model whose equation set is obtained from the continuous governing equations by replacing the vertical derivatives by finite differences and locating the vertical grid level (or points) at $z = z_k$, $k = 0, 1, \dots, KB$, such that $z_0 = \eta$ (surface) and $z_{KB} = -H$ (bottom).

Time Stepping

The semi-implicit treatment used in ECOMsiz is patterned after Cassuli (1990) and Casulli and Cheng (1992). Basically, the treatment involves taking the free surface gradient in the momentum equations (17) and (18) and solving the velocity divergence in the continuity equation (16b) implicitly. Consider the Reynolds equations (17 and 18) in the form:

$$\frac{\partial U_1}{\partial t} + ADVU_1 + \frac{g}{h_1} \frac{\partial \eta}{\partial \xi_1} = 0 \quad (24)$$

$$\frac{\partial U_2}{\partial t} + ADVU_2 + \frac{g}{h_2} \frac{\partial \eta}{\partial \xi_2} = 0 \quad (25)$$

where $ADVU_1$ and $ADVU_2$ represent all the remaining terms in equation (17) and (18). The time differencing leads to:

$$(U_1)^{n+1} = F(U_1) - \frac{g}{h_1} \frac{\partial \eta^{n+1}}{\partial \xi_1} \quad (26)$$

$$(U_2)^{n+1} = F(U_2) - \frac{g}{h_2} \frac{\partial \eta^{n+1}}{\partial \xi_2} \quad (27)$$

and

$$h_1 h_2 \frac{\partial \eta}{\partial t} + \frac{\partial}{\partial \xi_1} \int_{-H}^H (h_2 U_1)^{n+1} dz + \frac{\partial}{\partial \xi_2} \int_{-H}^H (h_1 U_2)^{n+1} dz = 0 \quad (28)$$

The $F(\cdot)$ terms in equations (26) and (27) represent the solution to Equations (24) and (25) at time level $n+1$ where the contribution from the $\partial \eta / \partial \xi_1$ and $\partial \eta / \partial \xi_2$ terms has been deferred until now (operator splitting). Substituting the momentum equations (26) and (27) into the free surface equation (16b), leads to a linear five diagonal system which is solved for the water surface elevation at time level $n+1$ over the domain of interest. Such a linear system is symmetric, positive definite and is solved by an efficient preconditioned conjugate gradient method (Casulli and Cheng, 1992).

Surface Fronts

The physical processes involved in the formation and maintenance of fronts are incorporated into the modeling framework by providing sufficient horizontal and vertical resolution for resolving the front and by calculating vertical entrainment/detrainment

processes according to a second-moment turbulence closure submodel.

Variable Grid Size

ECOMsiz allows considerable latitude in the design of a computational grid network. This freedom is accomplished through the use of an orthogonal, curvilinear coordinate system on the horizontal coordinate surfaces. When cast in these coordinates, the governing equations retain much of the analytical simplicity of the familiar Cartesian equations and require only marginally greater computer resources for their solution.

Realistic Topography

The model physics and solution techniques have been formulated such that realistic coastline and bottom topography are readily accommodated. Novel computational procedures have been formulated to cope gracefully with the large baroclinic and topographic variability found, among other locations, along a shelf break.

Inclusion of Passive Tracers

The computational design of the model permits the direct inclusion of passive tracers with little difficulty. This is because the model already solves four transport equations (temperature, salinity and two turbulence quantities) by sharing various subroutines and other computational code. However, previous efforts modeling water quality and oil spill impacts using ECOM in various regions have shown that it is more computationally efficient to separate the circulation component of the problem from the passive tracer component. The circulation component computes the transport and mixing suitably averaged in time and stores these data for subsequent use. The tracer component (water quality model) then takes this information and performs the desired tracer computations.

Open Boundary Condition Scheme

The treatment of the open boundaries of a limited area model domain continues to be an evolving area of research. These boundaries must be prescribed with special care, since the environment exterior to the relevant domain must be parameterized. While there has been much activity in the literature concerning open boundary conditions for wind forced barotropic coastal ocean models, relatively little attention has been devoted to the much more difficult problem of including both barotropic and baroclinic wave and mean motions. It is clear from the many applications of the Blumberg and Mellor (1987) code that the more that is known about the exterior domain the better the interior results become. For the solution of "real" three-dimensional problems, some knowledge of the hydrography and mean surface elevation along the open boundaries is essential. The different types of open boundary conditions available with this version of the model are:

Clamped - On the open boundaries of the domain, the surface elevation is specified by the user. The velocities on the boundary are then computed using the elevation and a linearized set of momentum equations.

P.Clamp - The surface elevation is specified by the user on the open boundaries, and a relaxation formulation based on a user specified TLAG and the Sommerfeld condition is used to calculate the surface elevation at the boundary.

Closed - The open boundaries are treated as solid walls.

Zero Gradient - The transport normal to the open boundary side of each open boundary grid cell is equal to the transport computed along the opposite side of the boundary grid cell (i.e., within the model domain).

Reid and Bodine - The velocity normal to open boundary grid cell (u) is specified as

$$u = \pm (\eta_T - \eta) (g/H)^{1/2} \quad (29)$$

where η_T is the surface height amplitude of the tidal forcing specified in the run_data input file, η is the first interior surface height in the model domain, g is the acceleration due to gravity, and H is the open boundary grid cell depth (Reid and Bodine, 1968). The user should note that if no tidal forcing is specified in the run_data input file (all amplitudes are set to zero), this boundary condition reduces to the standard longwave radiation condition of

$$u = \pm \eta (g/H)^{1/2} \quad (30)$$

Reid and Bodine with Shulman Modification - The same as the standard Reid and Bodine open boundary formulation except for the incorporation of a multiplier which optimizes the fit between the η_T specified and the η computed. The optimization is based on the total mechanical energy passing through the open boundaries.

Mixed - Open boundaries in water depths less than 75 m use zero gradient and those in depths greater than 75 m use Reid and Bodine.

All of the above open boundary conditions specify temperature and salinity in the same manner at the boundary. When inflow occurs along the open boundaries, temperature and salinity are user provided from data sets. On the outflow portions, they are determined from their full equations using an upwind advection scheme.

Types of Forcing

The model responds to forcing due to non-hydrostatic wind waves and swell, surface wind stress, heat flux (total of the sensible, latent, long wave and net solar radiation components), salinity flux (essentially evaporation minus precipitation) and the specification of tidal forcing, freshwater discharge and other lateral boundary conditions.

The code is configured to accept computer generated tidal forcing for up to six harmonic constituents according to the following:

$$\eta = E_{\text{mean}} + \sum_{i=1}^6 a_i \cos(\omega_i t - \phi_i) \quad (31)$$

where

- a_i = amplitude of the i^{th} tidal constituent
- ω_i = frequency of the i^{th} tidal constituent
- ϕ_i = phase lag of the i^{th} tidal constituent (relative to GMT)
- E_{mean} = mean water level with reference to the undisturbed water level of the model.

It is through the stipulation of the open lateral boundary conditions that the region outside of the domain of interest imposes itself.

Subgrid Scale Parameterization

Horizontal mixing coefficients for both momentum and heat/salinity are used to parameterize all processes which are not resolved on the numerical grid. Typically, these mixing coefficients are chosen such that they are sufficient to provide minimal smoothing without excessive damping of real oceanographic processes. Since the numerical grid can be non-uniform, the mixing coefficients must vary proportionally in order to maintain a uniform grid Reynolds number. The parameterization suggested by Smagorinsky (1963), which also depends on the horizontal grid spacing, has been used in the model.

The terms in the governing equations related to small-scale mixing processes not directly resolved by the model are parameterized as horizontal diffusion:

$$F_2 = \frac{\partial}{\partial y} \left(2A_M \frac{\partial V}{\partial y} \right) + \frac{\partial}{\partial x} \left[A_M \left(\frac{\partial U}{\partial y} + \frac{\partial V}{\partial x} \right) \right] \quad (33)$$

$$F_1 = \frac{\partial}{\partial x} \left(2A_M \frac{\partial U}{\partial x} \right) + \frac{\partial}{\partial y} \left[A_M \left(\frac{\partial U}{\partial y} + \frac{\partial V}{\partial x} \right) \right] \quad (32)$$

$$F_{T,S} = \frac{\partial}{\partial x} \left(A_H \frac{\partial (T,S)}{\partial x} \right) + \frac{\partial}{\partial y} \left(A_H \frac{\partial (T,S)}{\partial y} \right) \quad (34)$$

where the horizontal viscosity, A_M , is calculated according to Smagorinsky (1963):

$$A_M = C \Delta x \Delta y \left[\left(\frac{\partial U}{\partial x} \right)^2 + \left(\frac{\partial V}{\partial y} \right)^2 + \frac{1}{2} \left(\frac{\partial U}{\partial y} + \frac{\partial V}{\partial x} \right)^2 \right]^{1/2} \quad (35)$$

and where the notation is based upon Cartesian coordinates and variable names are those used conventionally. The parameter C is typically equal to 0.10 and has ranged from 0.01 to 0.5 in various applications. Here $A_H = A_M$, but the code has provisions to relax this constraint.

Advection Algorithms

Accurately simulating the transport of salinity and temperature can be difficult, particularly in hydrodynamic problems involving the propagation of steep gradients, or fronts. In estuarine and coastal problems, the propagation of fronts is important, particularly in the zone where freshwater and saltwater mix. Three algorithms, each of which may provide distinct advantages for a particular problem, are available for use in ECOMsiz: central difference, upwind difference and the Multidimensional Positive Definite Advection Transport Algorithm (MPDATA).

The central difference algorithm is second-order accurate, generates no numerical diffusion and is computationally efficient. However, this method is not positive definite and

negative salinities/ temperatures, which are physically impossible, may be generated in certain types of hydrodynamic problems. In addition, numerical ripples may be generated ahead of and behind fronts. Upwind differences are only first-order accurate and may introduce significant numerical diffusion into a solution depending upon typical current speeds and grid sizes. An advantage of upwind transport is that the algorithm is positive definite and the most computationally efficient of any of the advective schemes.

An improvement over both the central and upwind methods, particularly with regard to the transport of fronts, is MPDATA, which is described in detail by Smolarkiewicz (1984), Smolarkiewicz and Clark (1986) and Smolarkiewicz and Grabowski (1990). The general concept used in MPDATA is the successive application of an upwind transport algorithm, which is first-order accurate and positive definite, such that numerical diffusion, generated by a first-order truncation error, is minimized. A correction to the first-order truncation error is made by reapplying the upwind algorithm, after the initial upwind step, using an "anti-diffusion" velocity that is based on the local first-order truncation error. The corrective step may be applied an arbitrary number of times, resulting in a successive reduction in the numerical diffusion generated by the initial upwind step. This procedure yields an advection algorithm that is second-order accurate, and positive definite. Furthermore, MPDATA preserves the local monotone character of the advection field, such that, the field is free of numerically-generated ripples, provided that the anti-diffusion velocities are properly bounded. The greatest drawback to routine use of MPDATA is its large demand for computational resources. The execution time for a typical simulation can double the time required for a case involving central or upwind differences. On vector computers this factor is even larger because of the unavoidable many "IF" statements needed in the computer code.

CHARACTERISTICS OF THE COMPUTER CODE

The equations of the hydrodynamic model, together with their boundary conditions, are solved by finite difference techniques. The computational grid arrangement of points (as shown on Figure 1) has U at points $\pm h_1/2$ away from the point where the water depth, H, and the free surface elevation, η , are defined, and V at points $\pm h_2/2$ away from the H and η points. The metrics h_1 and h_2 are defined at the center point. Figure 2 shows the

locations of the variables on the finite difference grid.

For economy of computer storage, each variable array has its own allocation of subscripts in relation to the grid element location. A particular combination of subscripts (i, j), therefore, refers to a unique grid element location depending on the value of the subscript variable concerned. The convention adopted here is that all variables at the lower left corner, the left side and the lower side of the grid element have the same subscripts as those at the center. This means, for example, that the transport through the right side of the grid element has an i -index which is one higher than the center-index of this grid element, and which is equal to the center-index of the adjacent grid element on the right.

The overall grid mesh has a rectangular shape. In principle, the dimensions of the arrays, H and η referred to as elevation points, can be one less than the dimensions of U and V , which are called current points, because the number of grid element sides is one greater than the number of grid element squares. To avoid this kind of complication, all variable arrays are given the same dimension, namely (IM, JM) , where (IM, JM) represents the maximum number of elevation points. In order to simplify the computer code, it is convenient if the grid is surrounded by two dummy rows and two dummy columns of zero depths, H .

The shape and bathymetry of the region being modeled are completely determined by the depth array, H . Depths equal zero on land, on islands and in those areas outside the region of interest. The shorelines of the basin coincide locally with either one of the sides of the grid elements, resulting in a staircase boundary. Given the depths of the grid elements, the computer program determines which element side is part of the shoreline by checking if one of the two adjacent element depths is zero and the other non-zero. In order to locate open boundaries at the entrance or exit of rivers, the depths of grid elements located in such rivers must be set equal to zero while the transport normal to the boundary of the basin must be prescribed at such a river entrance or exit.

There are no restrictions on the shape of the domain or on any islands in the domain.

Channels may be as narrow as one single grid element. However, no dynamical connection exists between adjacent grid elements unless they have at least one side in common. Thus, two elements which touch each other in one corner only are essentially disconnected.

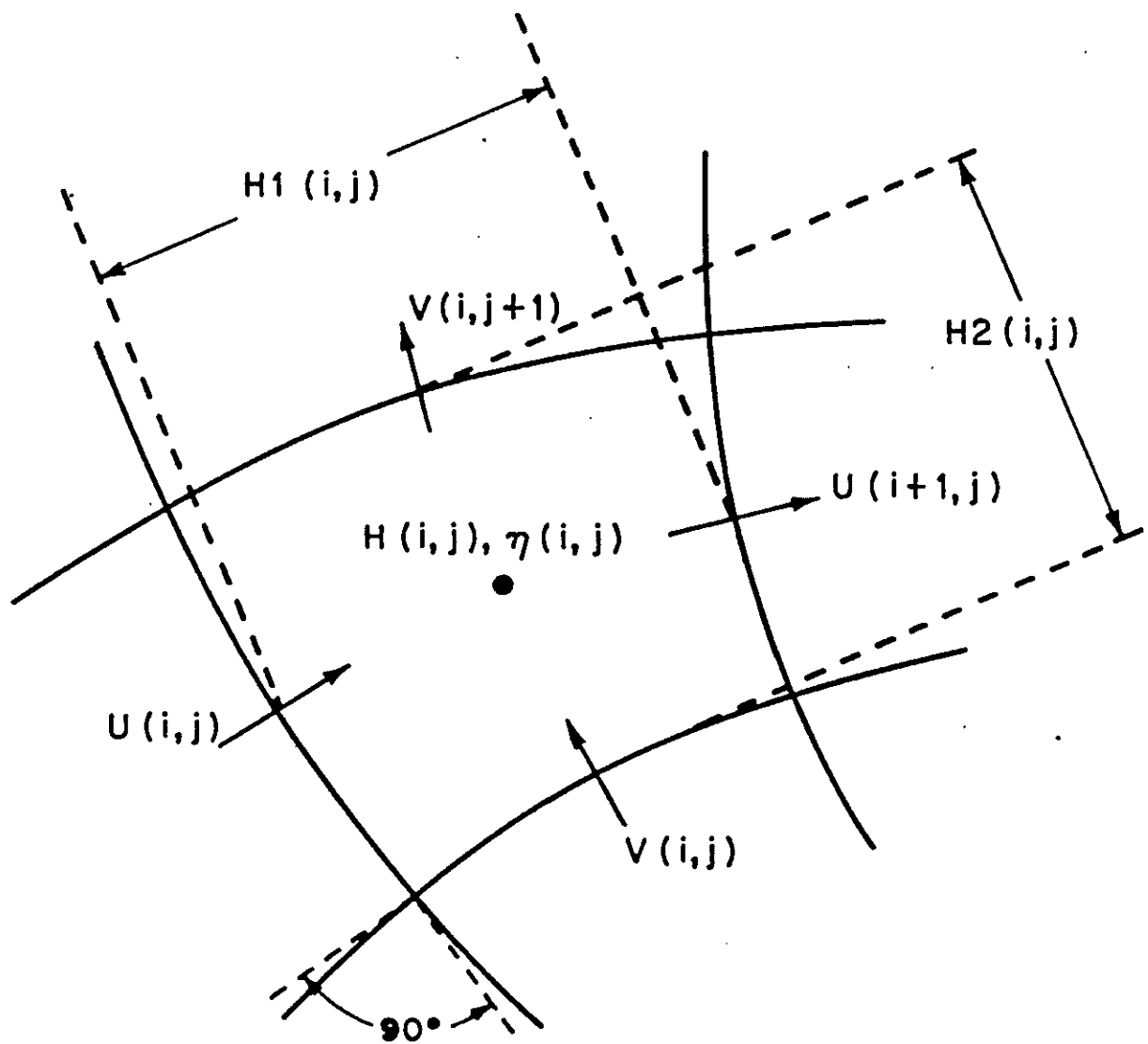


FIGURE 1. THE LOCATION OF MODEL VARIABLES ON THE COMPUTATIONAL GRID

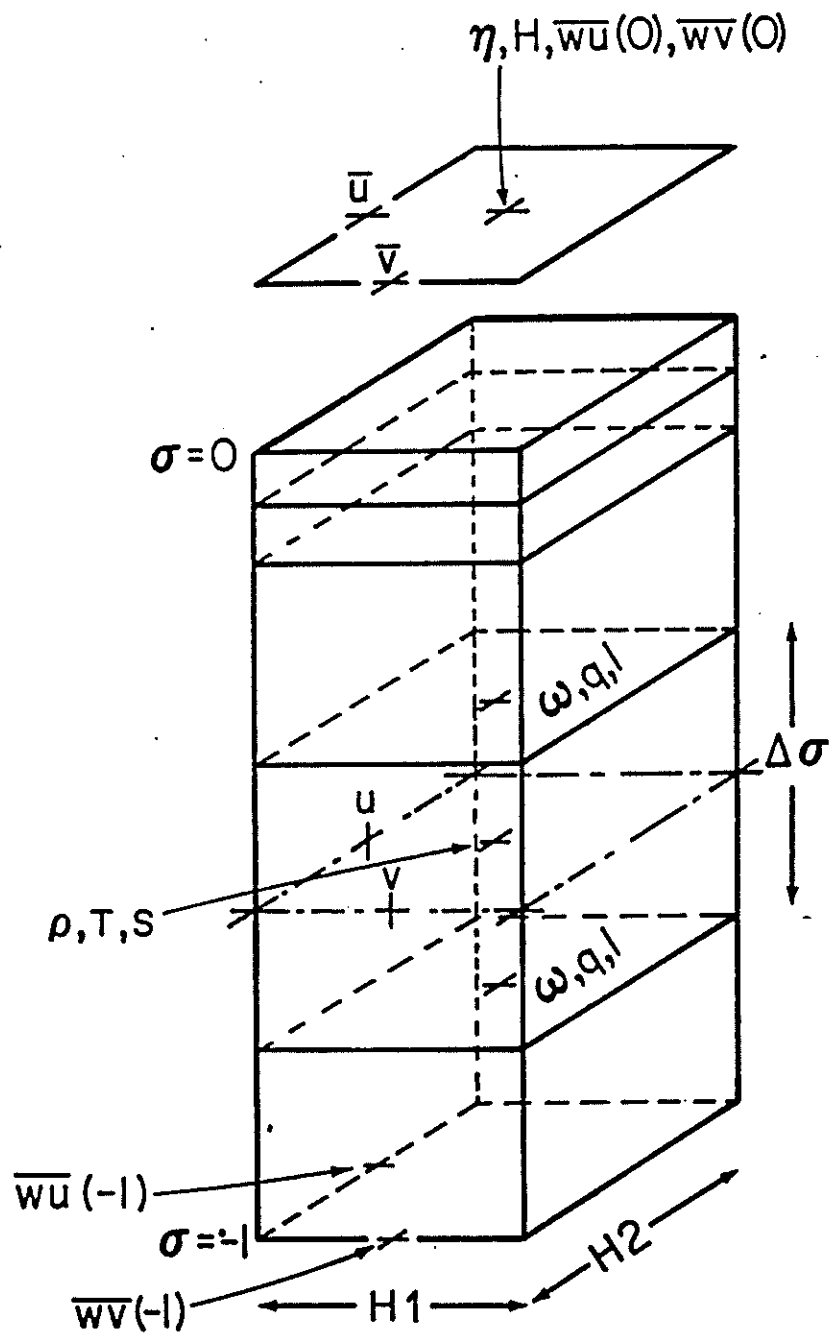


FIGURE 2. THE LOCATION OF MODEL VARIABLES ON THE FINITE DIFFERENCE GRID

APPENDIX B-1
Water Quality Model Equations

WATER COLUMN KINETICS

Table A-1. STATE SYSTEM VARIABLES, COUPLED EUTROPHICATION/CHEMICAL EQUILIBRIA MODEL

- 1 - Salinity (SAL)
- 2 - Total Suspended Solids (TSS)
- 3 - Phytoplankton (PHYT)
- 4 - Particulate Organic Phosphorus (POP)
- 5 - Dissolved Organic Phosphorus (DOP)
- 6 - Dissolved Inorganic Phosphorus (PO₄)
- 7 - Particulate Organic Nitrogen (PON)
- 8 - Dissolved Organic Nitrogen (DON)
- 9 - Ammonia Nitrogen (NH₃)
- 10 - Nitrite + Nitrate (NO₂3)
- 11 - Particulate Biochemical Oxygen Demand - Slow Reacting (PBODS)
- 12 - Dissolved Biochemical Oxygen Demand - Slow Reacting (DBODS)
- 13 - Particulate Biochemical Oxygen Demand - Fast Reacting (PBODF)
- 14 - Dissolved Biochemical Oxygen Demand - Fast Reacting (DBODF)
- 15 - Dissolved Oxygen (DO)

TABLE A-2. PHYTOPLANKTON NET GROWTH EQUATIONS

Net Growth Rate

$$G_p = G_{Pmax} \times G_T(T) \times G_I(I) \times G_N(N) \times P_c \quad \begin{array}{l} \text{Phytoplankton Growth} \\ \\ \end{array}$$

$$- k_{PR}(T) \times P_c \quad \begin{array}{l} \text{Endogenous Respiration} \\ \\ \end{array}$$

$$- k_{SP}(T) \times P_c \quad \begin{array}{l} \text{Algal Settling} \\ \\ \end{array}$$

$$- k_{grz}(T) \times P_c \quad \begin{array}{l} \text{Grazing} \\ \\ \end{array}$$

Temperature Correction

$$G_T(T) = e^{-\beta_1(T-T_{opt})^2} \quad T \leq T_{opt}$$

$$G_T(T) = e^{-\beta_2(T_{opt}-T)^2} \quad T > T_{opt}$$

Light Reduction

$$G_I(I) = \frac{e}{k_e H} \left[\exp \left(\frac{-I_o(t)}{I_s} e^{-k_e H} \right) - \exp \left(\frac{-I_o(t)}{I_s} \right) \right]$$

$$I_{surf}(t) = \frac{I_{tot}}{0.635 f} \sin \left[\frac{\pi (t_d - t_{sunrise})}{f} \right]$$

$$I_o(H) = I_{surf} \exp^{-k_e H}$$

Nutrient Uptake

$$G_N(N) = \text{Min} \left(\frac{\text{DIN}}{K_{mN} + \text{DIN}}, \frac{\text{DIP}}{K_{mP} + \text{DIP}} \right)$$

DIN = dissolved inorganic nitrogen = $\text{NH}_3 + \text{NO}_2 + \text{NO}_3$
 DIP = dissolved inorganic phosphorus

(Numbered variables refer to the variable list in Table A-1)

**TABLE A-2. PHYTOPLANKTON NET GROWTH EQUATIONS
(Continued)**

Algal Settling

$$k_{SP} = \frac{V_{SPb}}{H} \times \theta_{SP}^{(T-20)} + \frac{V_{SPn}}{H} \times [1 - G_N(N)] \times \theta_{SP}^{(T-20)}$$

Endogenous Respiration

$$k_{PR} = 0.04 + 0.38 S_p$$

Grazing

$$k_{grz}(T) = k_{grz}(20^{\circ}C) \times \theta_{grz}^{(T-20)}$$

<u>Notation</u>	<u>Exogenous Variables</u>
<u>Description</u>	
P_c	Phytoplankton Population as Carbon
k_e	Total Extinction Coefficient
k_{ebase}	Base Extinction Coefficient
I_o	Surface Solar Radiation
T	Temperature
H	Segment Depth
I_{tot}	Total daily incident solar radiation
f	fraction of daylight (daylight hours/24),
t_d	time of day
$t_{sunrise}$	time of sunrise

(Numbered variables refer to the variable list in Table A-1)

**TABLE A-2. PHYTOPLANKTON NET GROWTH EQUATIONS
(Continued)**

<u>Notation</u>	<u>Rate Constants</u>
G_{Pmax}	Maximum Specific Growth Rate at 20°C
θ_P	Growth Rate Temperature Coefficient
k_c	Phytoplankton Self-Light Attenuation
K_{mN}	Half-Saturation Constant for Nitrogen
K_{mP}	Half-Saturation Constant for Phosphorus
k_{PR}	Algal Endogenous Respiration Rate
θ_{RR}	Temperature Coefficient
v_{sPb}	Base Algal Settling Rate
v_{sPn}	Nutrient Dependent Algal Settling Rate
θ_{sP}	Temperature Coefficient
k_{grz}	Loss Due to Zooplankton Grazing
θ_{grz}	Temperature Coefficient
a_{cchl}	Carbon/Chlorophyll Ratio
I_s	Saturating Light Intensity

(Numbered variables refer to the variable list in Table A-1)

TABLE A-3. PHOSPHORUS REACTION EQUATIONS

Particulate Organic Phosphorus (POP)

$$S_4 = a_{PC} \times f_{POP} \times [k_{PR}(G_P) + k_{grz}(T)] \times P_c$$

Algal Respiration and Recycle

$$- k_{4,5}\theta_{4,5}^{(T-20)} \times POP \times \frac{P_c}{K_{mP_c} + P_c}$$

Hydrolysis

$$- \frac{v_{sPOM}(T)}{H} \times POP$$

Settling

Dissolved Organic Phosphorus (DOP)

$$S_5 = a_{PC} \times f_{DOP} \times [k_{PR}(G_P) + k_{grz}(T)] \times P_c$$

Algal Respiration and Recycle

$$+ k_{4,5}\theta_{4,5}^{(T-20)} \times POP \times \frac{P_c}{K_{mP_c} + P_c}$$

Hydrolysis

$$- k_{5,6}\theta_{5,6}^{(T-20)} \times DOP \times \frac{P_c}{K_{mP_c} + P_c}$$

Mineralization

Dissolved Inorganic Phosphorus (PO₄)

$$S_6 = a_{PC} \times f_{PO_4} \times [k_{PR}(G_P) + k_{grz}(T)] \times P_c$$

Algal Respiration and Recycle

$$+ k_{5,6}\theta_{5,6}^{(T-20)} \times DOP \times \frac{P_c}{K_{mP_c} + P_c}$$

DOP Mineralization

$$- a_{PC} \times G_P \times P_c \times \frac{P_c}{K_{mP_c} + P_c}$$

Uptake by Phytoplankton

$$\pm J PO_4$$

Sediment Flux

(Numbered variables refer to the variable list in Table A-1)

TABLE A-3. PHOSPHORUS REACTION EQUATIONS
(Continued)

<u>Notation</u>	<u>Description</u>
P_c	Phytoplankton Biomass
$k_{PR}(G_P)$	Temperature Corrected Algal Respiration Rate
$k_{grz}(T)$	Temperature Corrected Grazing Rate
G_P	Specific Phytoplankton Growth Rate
K_{mPc}	Half Saturation Constant for Phytoplankton Limitation
a_{PC}	Phosphorus to Carbon Ratio
	Fraction of Grazed Algal Phosphorus Recycled to
f_{POP}	the POP pool
f_{DOP}	the DOP pool
f_{PO_4}	the PO_4 pool
$k_{4,5}$	POP Hydrolysis Rate at 20°C
$\theta_{4,5}$	Temperature Coefficient
v_{sPOM}	Base Settling Rate of POM (POP)
$k_{5,6}$	DOP Mineralization Rate at 20°C
$\theta_{5,6}$	Temperature Coefficient

(Numbered variables refer to the variable list in Table A-1)

TABLE A-4. NITROGEN REACTION EQUATIONS

Particulate Organic Nitrogen (PON)

$$S_7 = a_{NC} \times f_{PON} \times [k_{PR}(G_P) + k_{grz}(T)] \times P_c \quad \begin{matrix} \text{Algal Respiration and} \\ \text{Recycle} \end{matrix}$$

$$- k_{7,8} \theta_{7,8}^{(T-20)} \times PON \times \frac{P_c}{K_m P_c + P_c} \quad \begin{matrix} \text{Hydrolysis} \\ \text{Settling} \end{matrix}$$

$$- \frac{V_s POM(T)}{H} \times PON \quad \begin{matrix} \text{Settling} \end{matrix}$$

Dissolved Organic Nitrogen (DON)

$$S_8 = a_{NC} \times f_{DON} \times [k_{PR}(G_P) + k_{grz}(T)] \times P_c \quad \begin{matrix} \text{Algal Respiration and} \\ \text{Recycle} \end{matrix}$$

$$+ k_{7,8} \theta_{7,8}^{(T-20)} \times PON \times \frac{P_c}{K_m P_c + P_c} \quad \begin{matrix} \text{Hydrolysis} \\ \text{Mineralization} \end{matrix}$$

$$- k_{8,9} \theta_{8,9}^{(T-20)} \times DON \times \frac{P_c}{K_m P_c + P_c} \quad \begin{matrix} \text{Mineralization} \end{matrix}$$

(Numbered variables refer to the variable list in Table A-1)

**TABLE A-4. NITROGEN REACTION EQUATIONS
(Continued)**

Ammonia Nitrogen ($\text{NH}_3 - \text{N}$)

$$\begin{aligned}
 S_9 &= a_{NC} \times f_{NH_3} \times [k_{PR}(G_P) + k_{grz}(T)] \times P_c && \text{Algal Respiration and Recycle} \\
 &+ k_{8,9}\theta_{8,9}^{(T-20)} \times DON \times \frac{P_c}{K_{MP_c} + P_c} && \text{DON Mineralization} \\
 &- a_{NC} \times a_{NH_3} \times G_P \times P_c \times \frac{P_c}{K_{MP_c} + P_c} && \text{Uptake by Phytoplankton} \\
 &- k_{9,10}\theta_{9,10}^{(T-20)} \times NH_3 \times \frac{DO}{K_{nitr} + DO} && \text{Nitrification} \\
 &\pm J NH_3 && \text{Sediment Flux}
 \end{aligned}$$

Nitrite + Nitrate Nitrogen ($\text{NO}_2 + \text{NO}_3$)

$$\begin{aligned}
 S_{10} &= k_{9,10}\theta_{9,10}^{(T-20)} \times NH_3 \times \frac{DO}{K_{nitr} + DO} && \text{Nitrification} \\
 &- a_{NC} \times (1 - a_{NH_3}) \times G_P \times P_c && \text{Uptake by Phytoplankton} \\
 &- k_{10,0}\theta_{10,0}^{(T-20)} \times (\text{NO}_2 + \text{NO}_3) \times \frac{K_{NO_3}}{K_{NO_3} + DO} && \text{Denitrification} \\
 &\pm J NO_{23} && \text{Sediment Flux}
 \end{aligned}$$

(Numbered variables refer to the variable list in Table A-1)

TABLE A-4. NITROGEN REACTION EQUATIONS
(Continued)

<u>Notation</u>	<u>Description</u>
P_c	Phytoplankton Biomass
$k_{PR}(G_p)$	Temperature Corrected Algal Respiration Rate
$k_{grz}(T)$	Temperature Corrected Grazing Rate
G_p	Specific Phytoplankton Growth Rate
K_{mPc}	Half Saturation Constant for Phytoplankton Limitation
a_{NC}	Nitrogen to Carbon Ratio
	Fraction of Respired and Grazed Algal Nitrogen Recycled to
f_{PON}	the PON pool
f_{DON}	the DON pool
f_{NH_3}	the NH_3 pool
v_{sPOM}	Base Settling Rate of POM (PON)
$k_{7,8}$	Hydrolysis Rate at 20°C for PON
$\theta_{7,8}$	Temperature Coefficient
$k_{8,9}$	Mineralization Rate at 20°C for DON
$\theta_{8,9}$	Temperature Coefficient
$k_{9,10}$	Nitrification Rate at 20°C
$\theta_{9,10}$	Temperature Coefficient
K_{nitr}	Half Saturation Constant for Nitrification Oxygen Limitation
$k_{10,0}$	Denitrification Rate at 20°C
$\theta_{10,0}$	Temperature Coefficient
K_{NO_3}	Michaelis Constant for Denitrification
a_{NH_3}	Ammonia Preference Term for Nitrogen Uptake

(Numbered variables refer to the variable list in Table A-1)

TABLE A-5. BIOCHEMICAL OXYGEN DEMAND REACTION EQUATIONS

Particulate Biochemical Oxygen Demand - Slow Reacting (PBODS)

$$S_{11} = a_{oc} \times f_{PBODS} \times k_{grz}(T) \times P_c \quad Recycle$$

$$- k_{11,12} \theta_{11,12}^{(T-20)} \times PBODS \quad Hydrolysis$$

$$- \frac{V_{sPBODS}}{H} \times PBODS \quad Settling$$

Dissolved Biochemical Oxygen Demand - Slow Reacting (DBODS)

$$S_{12} = a_{oc} \times f_{DBODS} \times k_{grz}(T) \times P_c \quad Recycle$$

$$+ k_{11,12} \theta_{11,12}^{(T-20)} \times PBODS \quad Hydrolysis$$

$$- k_{12,0} \theta_{12,0}^{(T-20)} \times DBODS \times \frac{DO}{K_{DO} + DO} \quad Oxidation$$

Particulate Biochemical Oxygen Demand - Fast Reacting (PBODF)

$$S_{13} = a_{oc} \times f_{PBODF} \times k_{grz}(T) \times P_c \quad Recycle$$

$$- k_{13,14} \theta_{13,14}^{(T-20)} \times PBODF \quad Hydrolysis$$

$$- \frac{V_{sPBODF}}{H} \times PBODF \quad Settling$$

Dissolved Biochemical Oxygen Demand - Fast Reacting (DBODF)

$$S_{14} = a_{oc} \times f_{DBODF} \times k_{grz}(T) \times P_c \quad Recycle$$

$$+ k_{13,14} \theta_{13,14}^{(T-20)} \times PBODF \quad Hydrolysis$$

$$- k_{14,0} \theta_{14,0}^{(T-20)} \times DBODF \times \frac{DO}{K_{DO} + DO} \quad Oxidation$$

(Numbered variables refer to the variable list in Table A-1)

TABLE A-5. BIOCHEMICAL OXYGEN DEMAND REACTION EQUATIONS
(Continued)

<u>Notation</u>	<u>Description</u>
a_{oc}	Oxygen to Carbon Ratio
P_c	Phytoplankton Biomass
	Fraction of Grazed Phytoplankton Recycled to:
f_{PBODS}	the PBODS pool
f_{DBODS}	the DBODS pool
$k_{11,12}$	Hydrolysis Rate for PBODS
$\theta_{11,12}$	Temperature Coefficient
v_{PBODS}	Base Settling Rate of PBODS
$k_{13,14}$	Hydrolysis Rate for PBODF
$\theta_{13,14}$	Temperature Coefficient
$V_s \text{ PBODF}$	Base Settling Rate of PBODF
H	Segment depth
$k_{12,0}$	Oxidation Rate of DBODS
$\theta_{12,0}$	Temperature Coefficient
$k_{14,0}$	Oxidation Rate DBODF
$\theta_{14,0}$	Temperature Coefficient
K_{DO}	Half Saturation for Oxygen Limitation of Organic Carbon Oxidation
DO	Dissolved Oxygen

(Numbered variables refer to the variable list in Table A-1)

TABLE A-6. DISSOLVED OXYGEN REACTION EQUATIONS

Dissolved Oxygen (DO)

$$\begin{aligned}
 S_{16} = & [a_{OC} \times a_{NH_3} + a_{NO_3C} \times (1 - a_{NH_3})] \times G_p \times P_c && \text{Phytoplankton Photosynthesis} \\
 & + k_a \theta_a^{(T-20)} \times (DO_{sat} - DO) && \text{(Ammonia and Nitrite Derived)} \\
 & - a_{OC} \times k_{PR}(G_p) \times P_c && \text{Atmospheric Reaeration} \\
 & - 2 \times a_{ON} \times k_{9,10} \theta_{9,10}^{(T-20)} \times NH_3 \times \frac{DO}{K_{nitr} + DO} && \text{Nitrification} \\
 & - k_{12,0} \theta_{12,0}^{(T-20)} \times DBODS \times \frac{DO}{K_{DO} + DO} && \text{DBODS Oxidation} \\
 & - k_{14,0} \theta_{14,0}^{(T-20)} \times DBODF \times \frac{DO}{K_{DO} + DO} && \text{DBODF Oxidation} \\
 & - SOD && \text{Sediment Oxygen Demand}
 \end{aligned}$$

(Numbered variables refer to the variable list in Table A-1)

TABLE A-6. DISSOLVED OXYGEN AND AQUEOUS SEDIMENT OXYGEN EQUIVALENT REACTION EQUATIONS
(Continued)

<u>Notation</u>	<u>Description</u>
P_c	Phytoplankton Biomass
G_p	Specific Phytoplankton Growth Rate
a_{NO3C}	Oxygen to Carbon Ratio for Nitrate Uptake
a_{OC}	Oxygen to Carbon Ratio
k_a	Reaeration Rate at 20°C ($K_a = K_L/H$)
θ_a	Temperature Coefficient
K_L	Oxygen Transfer Coefficient
DO_{sat}	Dissolved Oxygen Saturation
$k_{12,0}$	Oxidation Rate for DBODS at 20°C
$\theta_{12,0}$	Temperature Coefficient
$k_{14,0}$	Oxidation Rate for DBODF at 20°C
$\theta_{14,0}$	Temperature Coefficient
$k_{9,10}$	Oxidation Rate for NH3 (Nitrification) at 20°C
$\theta_{9,10}$	Temperature Coefficient
σ_{NH3}	Ammonia Preference Term for Nitrogen Uptake
K_{nitr}	Half Saturation for Nitrification Oxygen Limitation
K_{DO}	Half Saturation for Oxidation Oxygen Limitation
DO	Dissolved Oxygen
a_{on}	Oxygen to Nitrogen
$K_{PR}(G_p)$	Algal Endogenous Respiration Rate

(Numbered variables refer to the variable list in Table A-1)

APPENDIX B-2
Water Quality Model Parameter & Constants

1995 AND 1991 WATER QUALITY MODEL PARAMETERIZATION

**CONSTANTS, 2-D PARAMETERS (SPATIALLY VARIABLE CONSTANTS),
AND TIME-VARIABLE FUNCTIONS USED IN THE
DELAWARE RIVER-ESTUARY WATER QUALITY MODEL.**

CONSTANTS

<u>NAME</u>	<u>DESCRIPTION</u>	<u>UNITS</u>	<u>VALUE (RANGE)</u>
<u>PHYTOPLANKTON KINETICS</u>			
K1C	SATURATED PHYTOPLANKTON GROWTH RATE (AT 25°C)	1/DAY	2.00
K1T	TEMPERATURE COEFFICIENT		1.068
IS1	SATURATING ALGAL LIGHT INTENSITY	LY/DAY	350
KMN1	HALF SATURATION CONSTANT FOR NITROGEN	MG N/L	0.01
KMP1	HALF SATURATION CONSTANT FOR PHOSPHOROUS	MG P/L	0.001
K1GRZT	TEMPERATURE COEFFICIENT		1.068
<u>CARBON RATIOS</u>			
CCHL1	CARBON TO CHLOROPHYLL RATIO	MG C/MG CHLA	40
CRBP11	CARBON TO PHOSPHORUS RATIO	MG C/MG P	40
CRBN11	CARBON TO NITROGEN RATIO	MG C/MG N	5.67
XKC	CHLOROPHYLL SELF-SHADING EXT.COEFF.	M ² /MG CHLA	0.017
KMPHYT	HALF SATURATION CONSTANT FOR PHYTOPLANKTON	MG C/L	0.0
KMDO	BOD OXIDATION;HALF SAT CONSTANT FOR DO	MG O ₂ /L	1.0
<u>RECYCLE FRACTIONS</u>			
FPOP	REFRACTORY PARTICULATE ORGANIC PHOSPHOROUS		0.375
FDOP	REFRACTORY DISSOLVED ORGANIC PHOSPHOROUS		0.375
FPO4	DISSOLVED INORGANIC PHOSPHOROUS		0.250
FPON	REFRACTORY PARTICULATE ORGANIC NITROGEN		0.375
FDON	REFRACTORY DISSOLVED ORGANIC NITROGEN		0.375
FNH3	AMMONIA		0.25
FPBDS	PARTICULATE BOD - SLOW REACTING		0.50
FDBDS	DISSOLVED BOD - SLOW REACTING		0.50
<u>PHOSPHORUS HYDROLYSIS/MINERALIZATION RATES AT 20 DEG C</u>			
K45C	HYDROLYSIS RATE OF POP TO DOP	1/DAY	0.040
K45T	TEMPERATURE COEFFICIENT		1.080
K56C	MINERALIZATION RATE OF DOP TO PO ₄	1/DAY	0.040
K56T	TEMPERATURE COEFFICIENT		1.080
<u>NITROGEN HYDROLYSIS/MINERALIZATION RATES AT 20 DEG C</u>			
K78C	HYDROLYSIS RATE OF PON TO DON	1/DAY	0.040
K78T	TEMPERATURE COEFFICIENT		1.080
K89C	MINERALIZATION RATE OF DON TO NH ₃	1/DAY	0.040
K89T	TEMPERATURE COEFFICIENT		1.080
<u>NITRIFICATION/DENITIFICATION RATES</u>			
K910C	NITRIFICATION RATE AT 20 DEG C	1/DAY	0.10-1.00
K910T	TEMPERATURE COEFFICIENT		1.080
KNIT	HALF SATURATION CONSTANT FOR NITRIFICATION (OXYGEN) LIMITATION	MG O ₂ /L	1.0
K100C	DENITRIFICATION RATE AT 20 DEG C	1/DAY	0.0
K100T	TEMPERATURE COEFFICIENT		1.045
KNO3	MICHAELIS CONSTANT FOR DENITRIFICATION (OXYGEN) LIMITATION	MG O ₂ /L	0.10

	<u>BOD HYDROLYSIS RATES AT 20 DEG C</u>			
K1112C	HYDROLYSIS RATE OF PBODS TO DBODS	1/DAY	0.05	
K1112T	TEMPERATURE COEFFICIENT		1.080	
K1314C	HYDROLYSIS RATE OF PBODF TO DBODF	1/DAY	0.05	
K1314T	TEMPERATURE COEFFICIENT		1.080	
	<u>BOD/OXIDATION RATES AT 20 DEG C</u>			
K120C	DBODS OXIDATION RATE AT 20 DEG C	1/DAY	0.05	
K120T	TEMPERATURE COEFFICIENT		1.047	
K140C	DBODF OXIDATION RATE AT 20 DEG C	/DAY	0.05	
K140T	TEMPERATURE COEFFICIENT		1.047	
KAT	TEMPERATURE CORRECTION COEFFICIENT FOR ATMOSPHERIC REAERATION		1.024	
	<u>SETTLING RATES</u>			
VSBASE	BASE ALGAL SETTLING RATE	M/DAY	0.10	
VSNUTR	NUTRIENT STRESSED ALGAL SETTLING RATE	M/DAY	0.0	
VSBAST	TEMPERATURE CORRECTION		1.029	
VSPOM	PARTICULATE ORGANIC MATTER SETTLING RATE	M/DAY	0.10	
VSPMT	TEMPERATURE CORRECTION		1.029	
VSSEDT	TEMPERATURE CORRECTION FOR DEPOSITION TO SEDIMENT		1.029	
VSTSS	TOTAL SUSPENDED SOLIDS SETTLING RATE	M/DAY	1.00	
VSPBDS	SLOW REACTING PARTICULATE BOD SETTLING RATE	M/DAY	0.10	
VSPBDF	FAST REACTING PARTICULATE BOD SETTLING RATE	M/DAY	0.10	
VKMSAL	SALINITY BASED PHYTO GROWTH REDUCTION FACTOR	PSU	0.50	

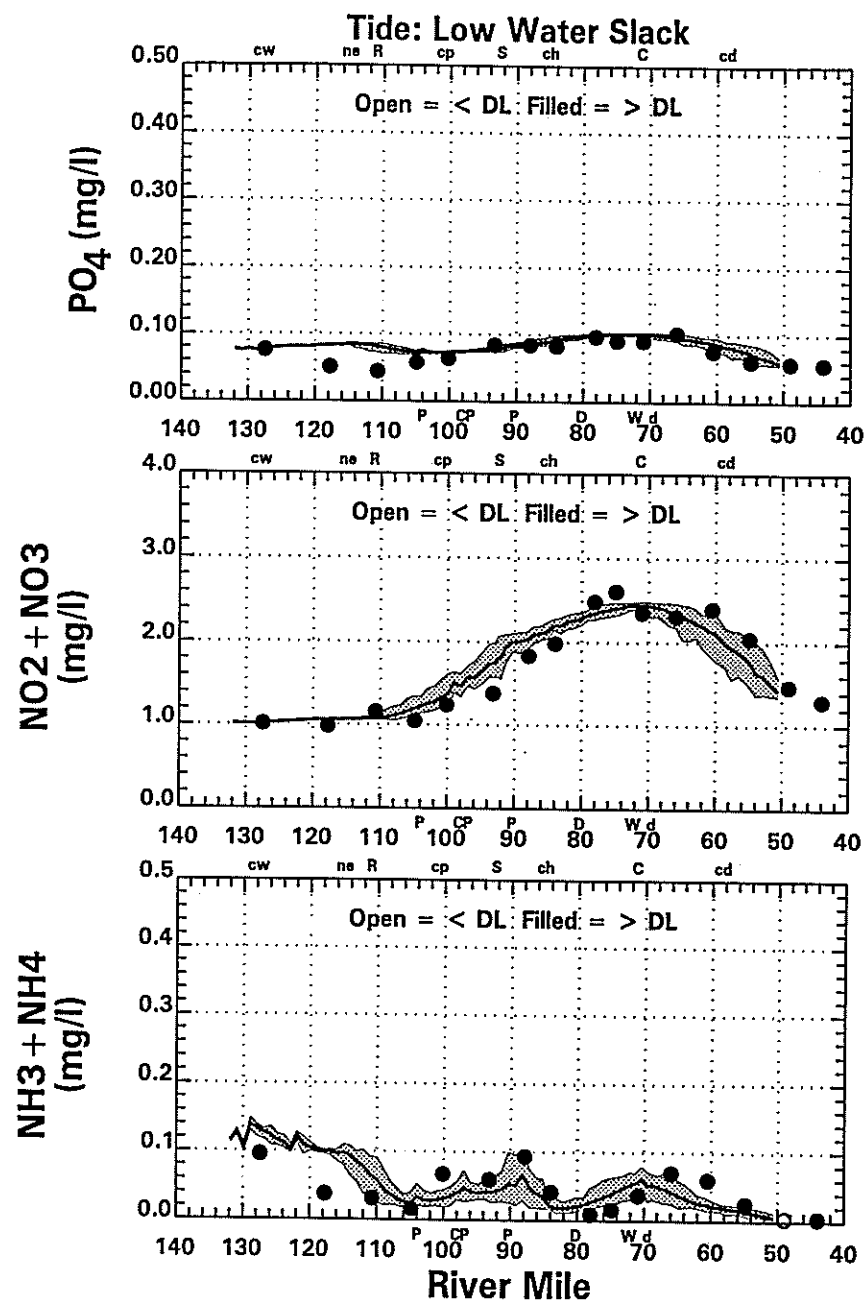
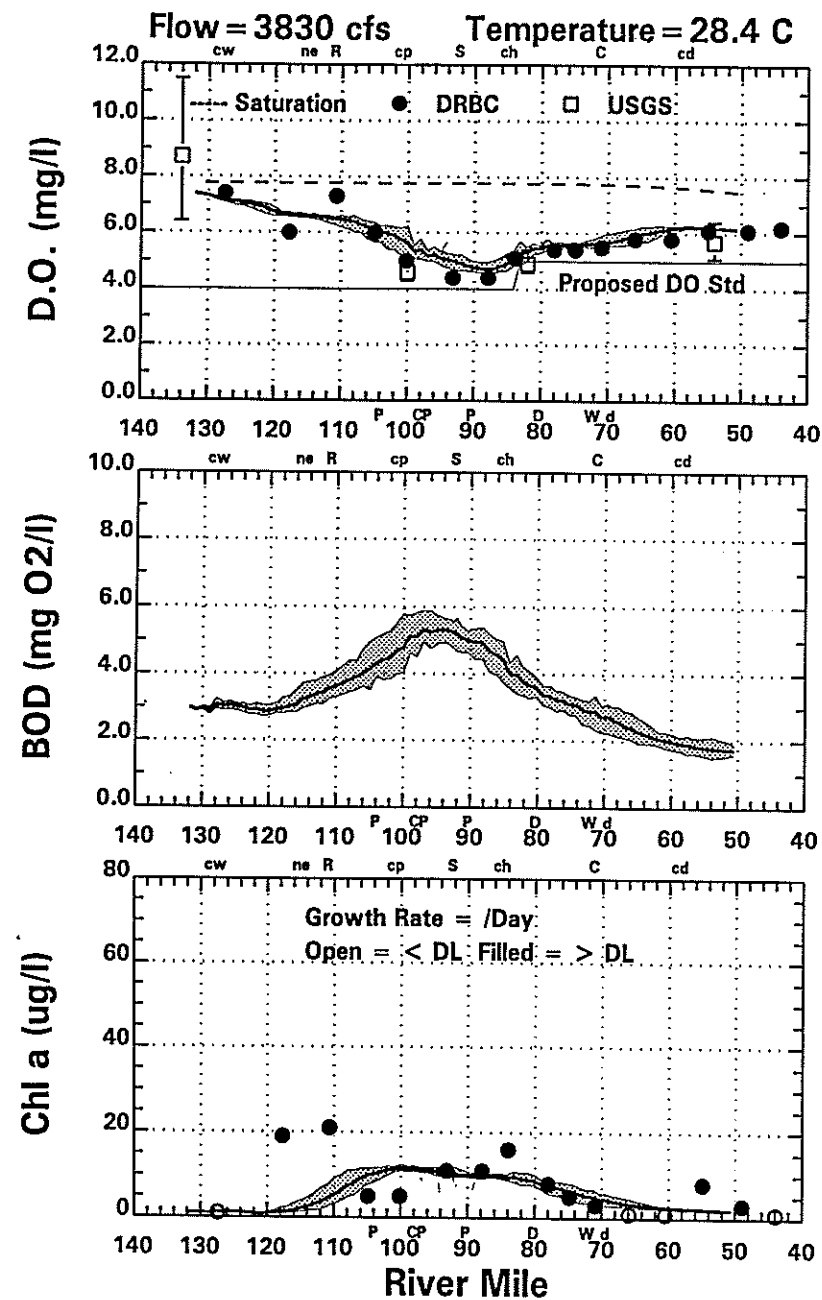
2-D PARAMETERS

KL	TRANSFER COEFFICIENT FOR REAERATION	M/DAY	0.40-1.40	
VSNET1	SCALE FACTOR FOR NET SETTLING RATE FROM WATER COLUMN TO THE BED FOR ALGAL		1.00	
VSNET2	SCALE FACTOR FOR NET SETTLING RATE FROM WATER COLUMN BED FOR NON-LIVING POM		1.00	
KEBASE	BASE (CHL-A CORRECTED) EXTINCTION COEFF (SINCE KE'S ARE TIME-VARIABLE, THEY WILL BE READ FROM A SERIES OF INPUT FILES)	/METER	f(time-location)	
SODS	SEDIMENT OXYGEN DEMAND	GM O ₂ /M ² -DAY	0.50	
JNH3	NH3 SEDIMENT FLUX	GM N/M ² -DAY	0.00	
JPO4	PO4 SEDIMENT FLUX	GM P/M ² -DAY	0.00	
JN03	NO3 SEDIMENT FLUX	GM N/M ² -DAY	0.00	
K1GRZC	DEATH RATE DUE TO GRAZING	1/DAY	0.025-0.150	

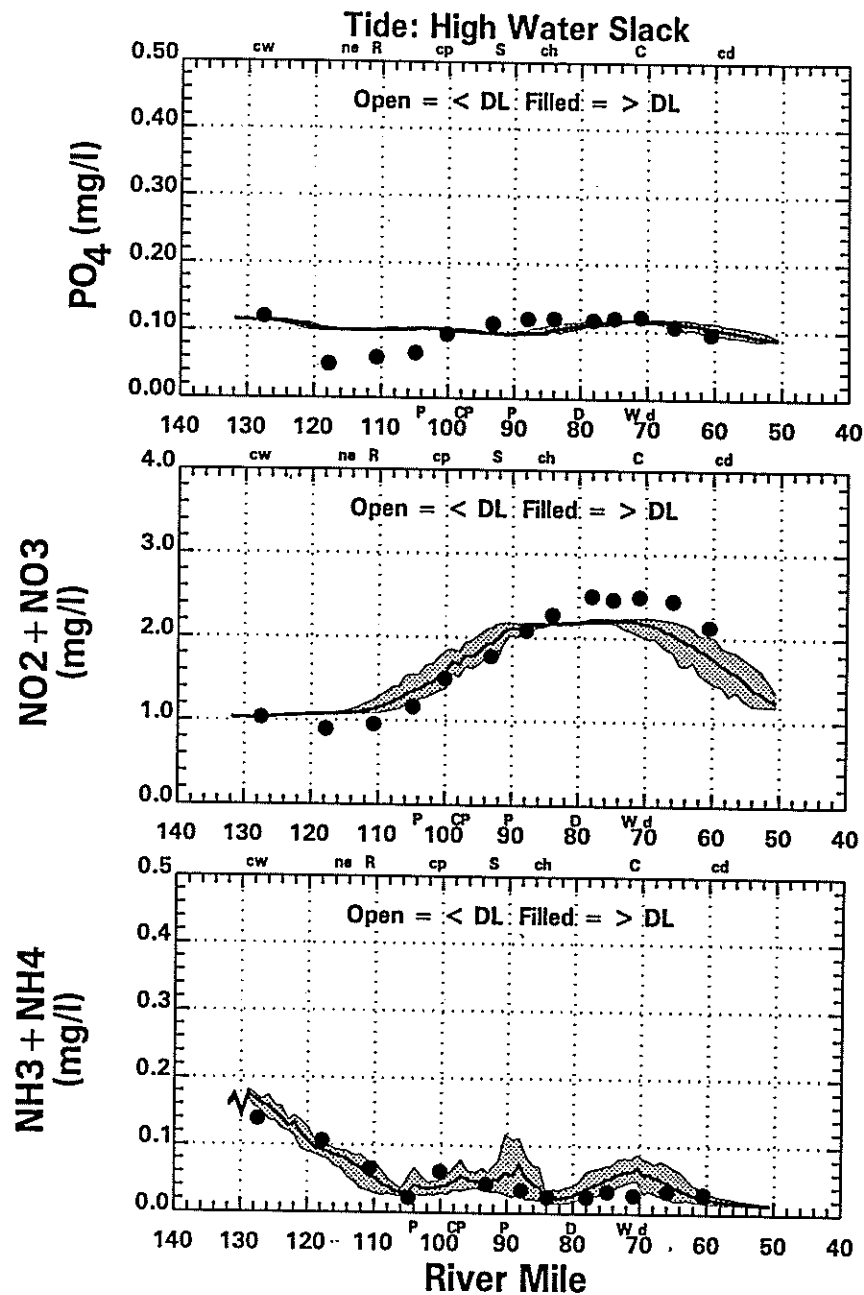
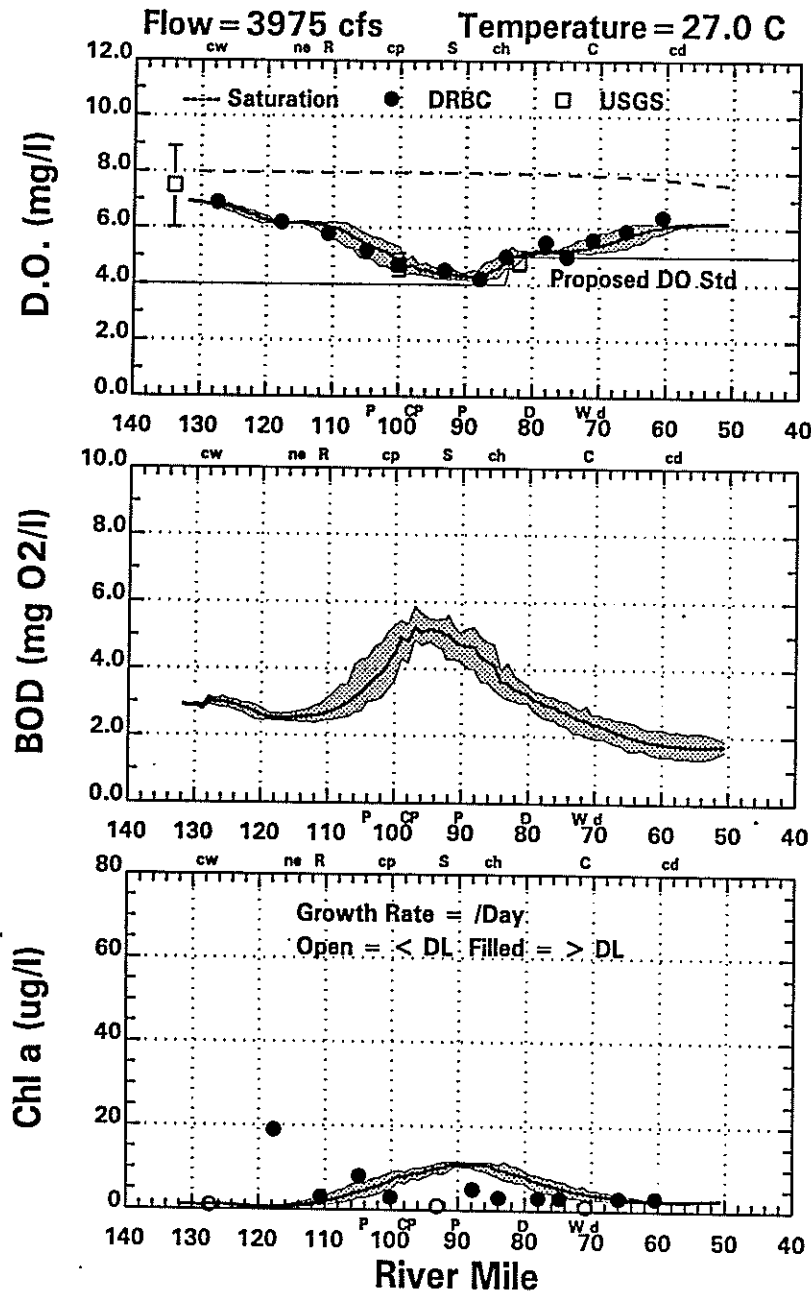
TIME-VARIABLE FUNCTIONS

ITOTSF	TOTAL DAILY SOLAR RADIATION	LY/DAY	f(time)
F	FRACTION OF DAYLIGHT	DAY	f(time)

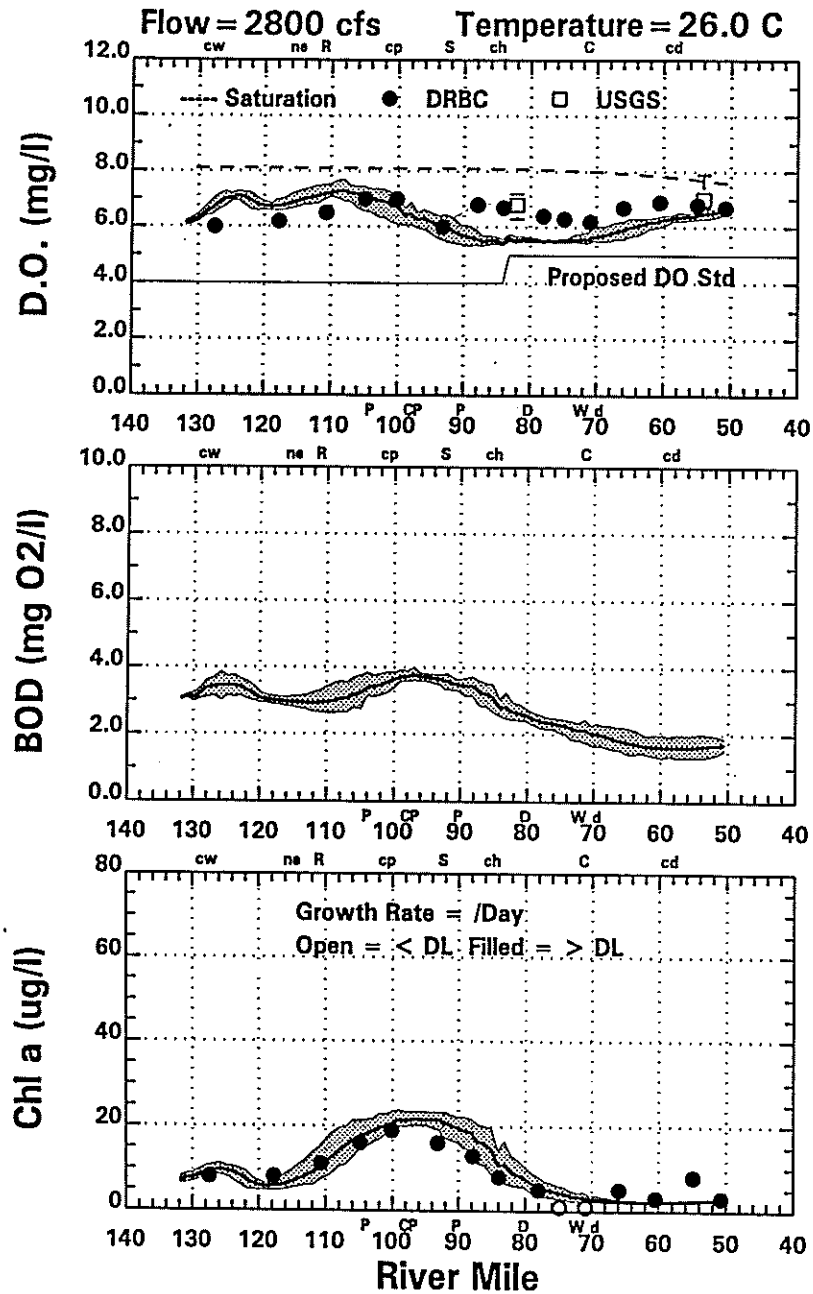
APPENDIX B-3
1995 Water Quality Model Runs



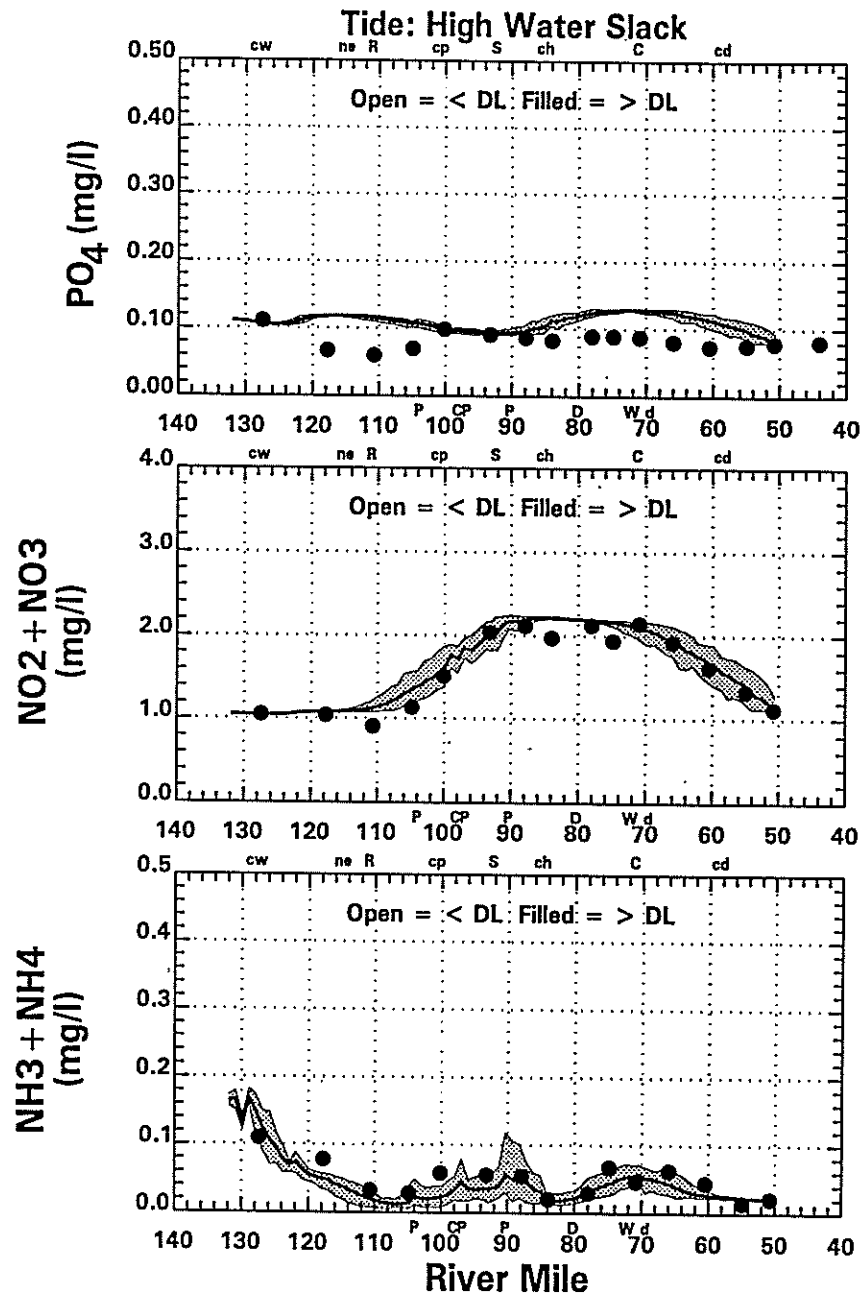
Delaware River Data (●) & Model (—) 7/25/95 (Model Day 8)
 [Daily Average & Shaded Area = Range over the Day]

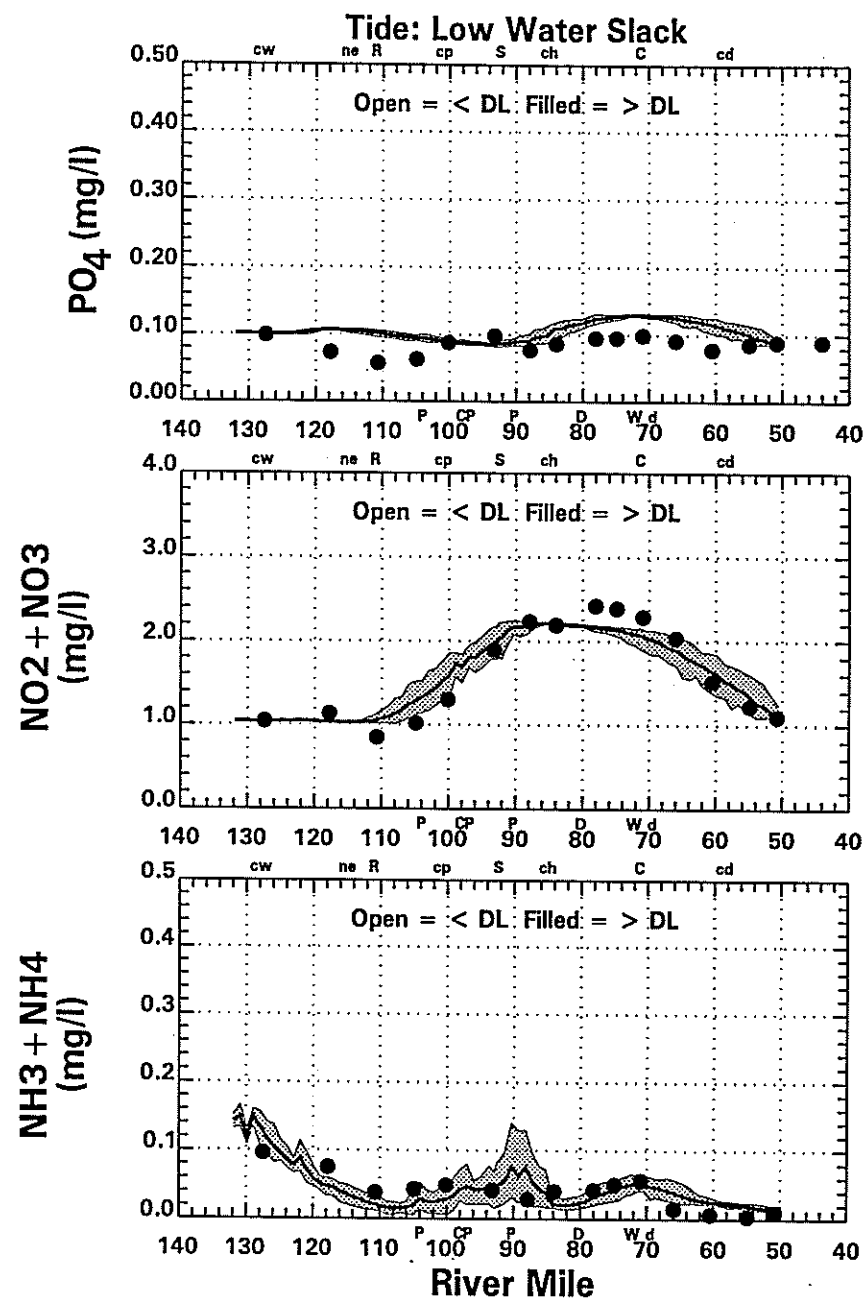
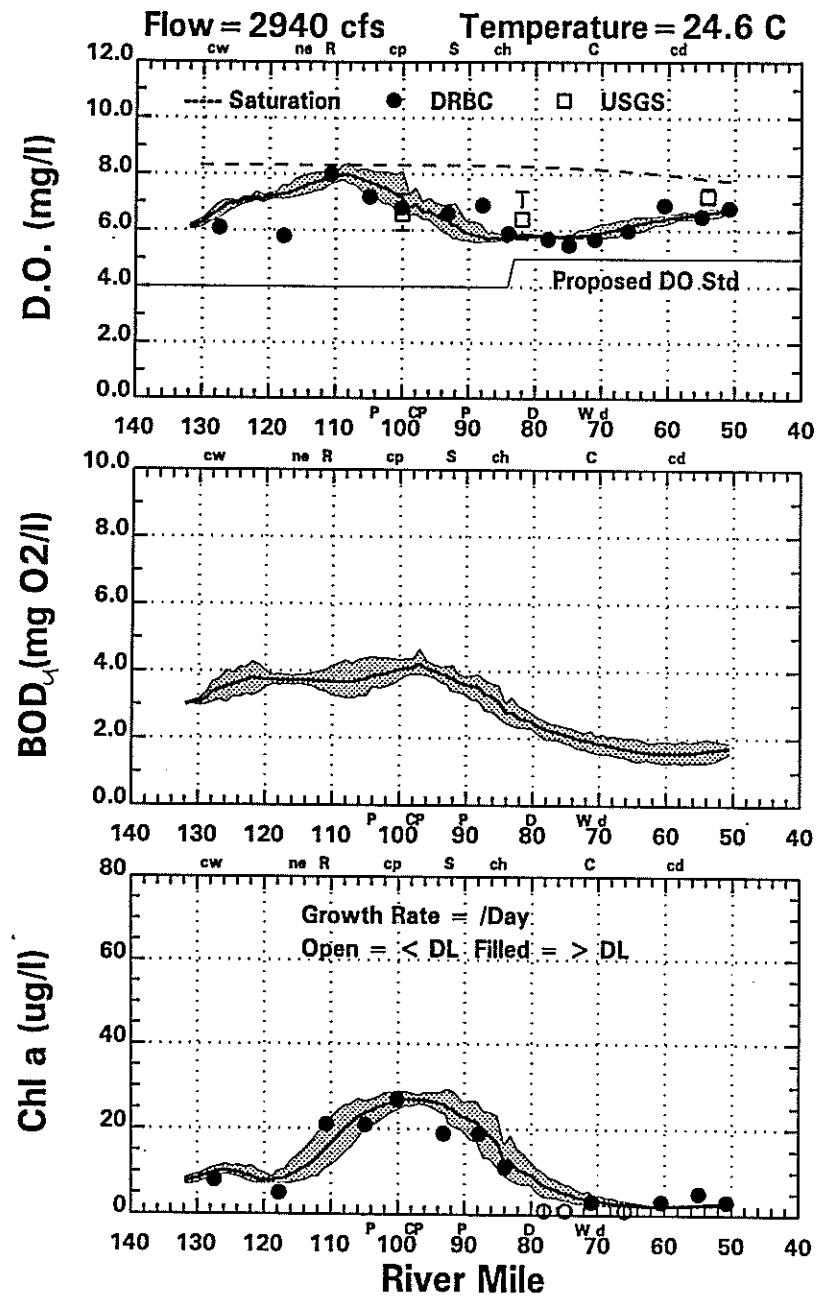


Delaware River Data (●) & Model (—) 8/8-9/95 (Model Day 23)
 [Daily Average & Shaded Area = Range over the Day]

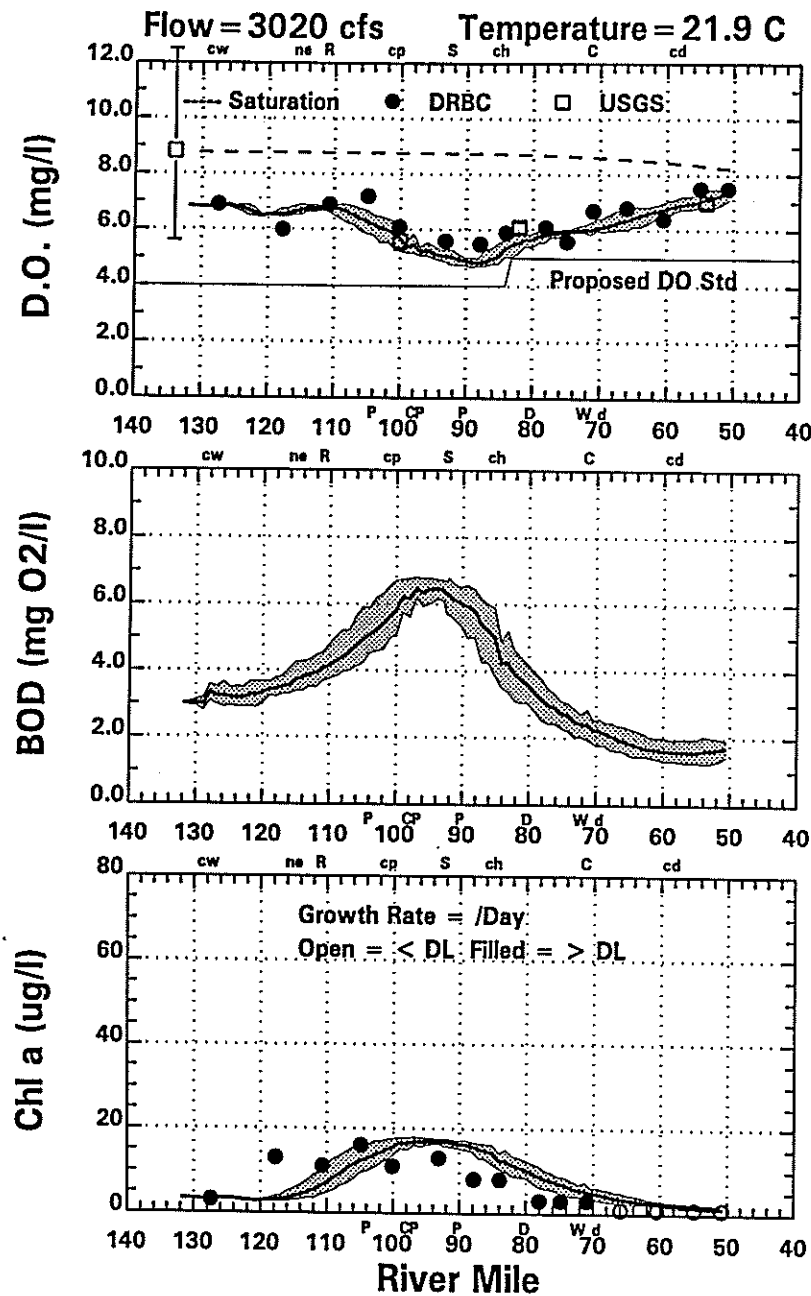


Delaware River Data (●) & Model (—) 8/29/95 (Model Day 43)
[Daily Average & Shaded Area=Range over the Day]

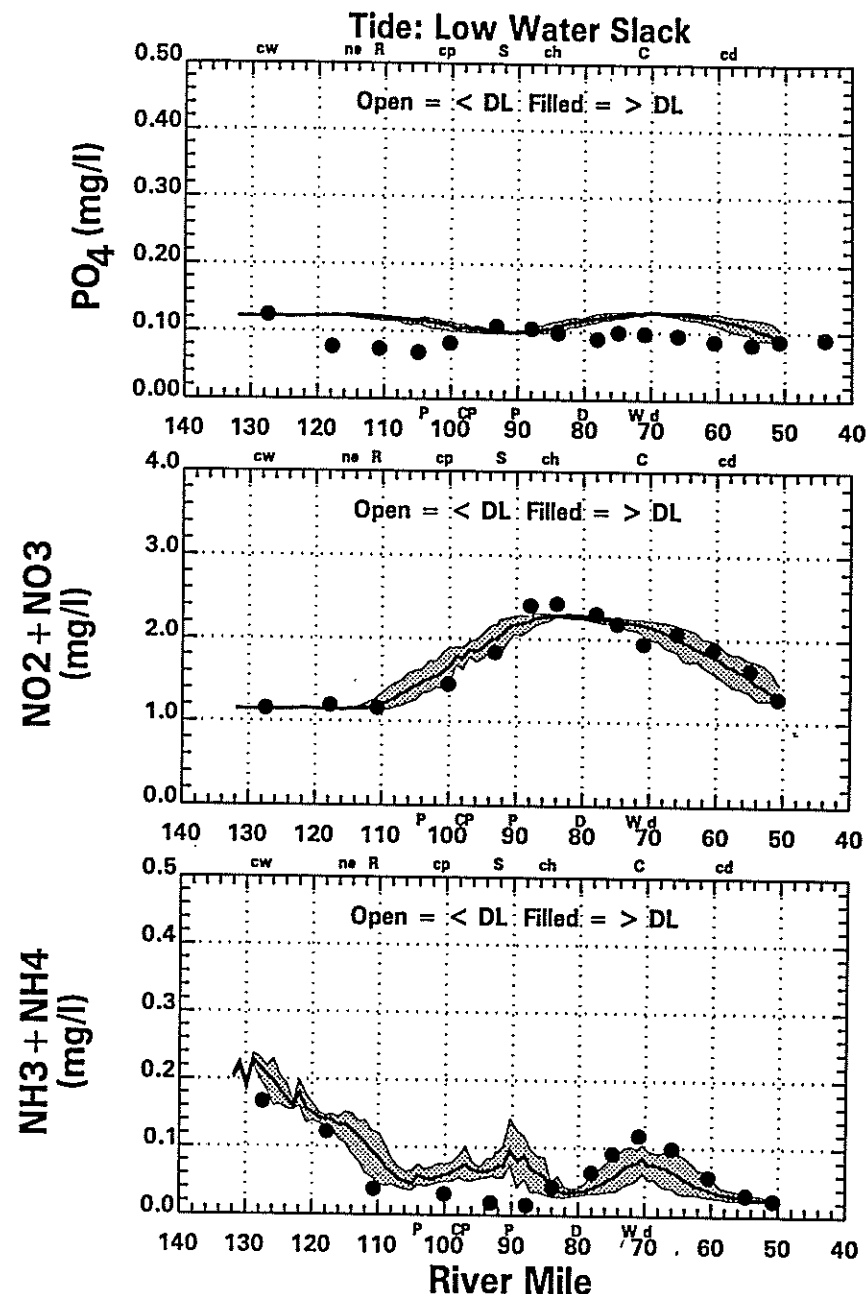


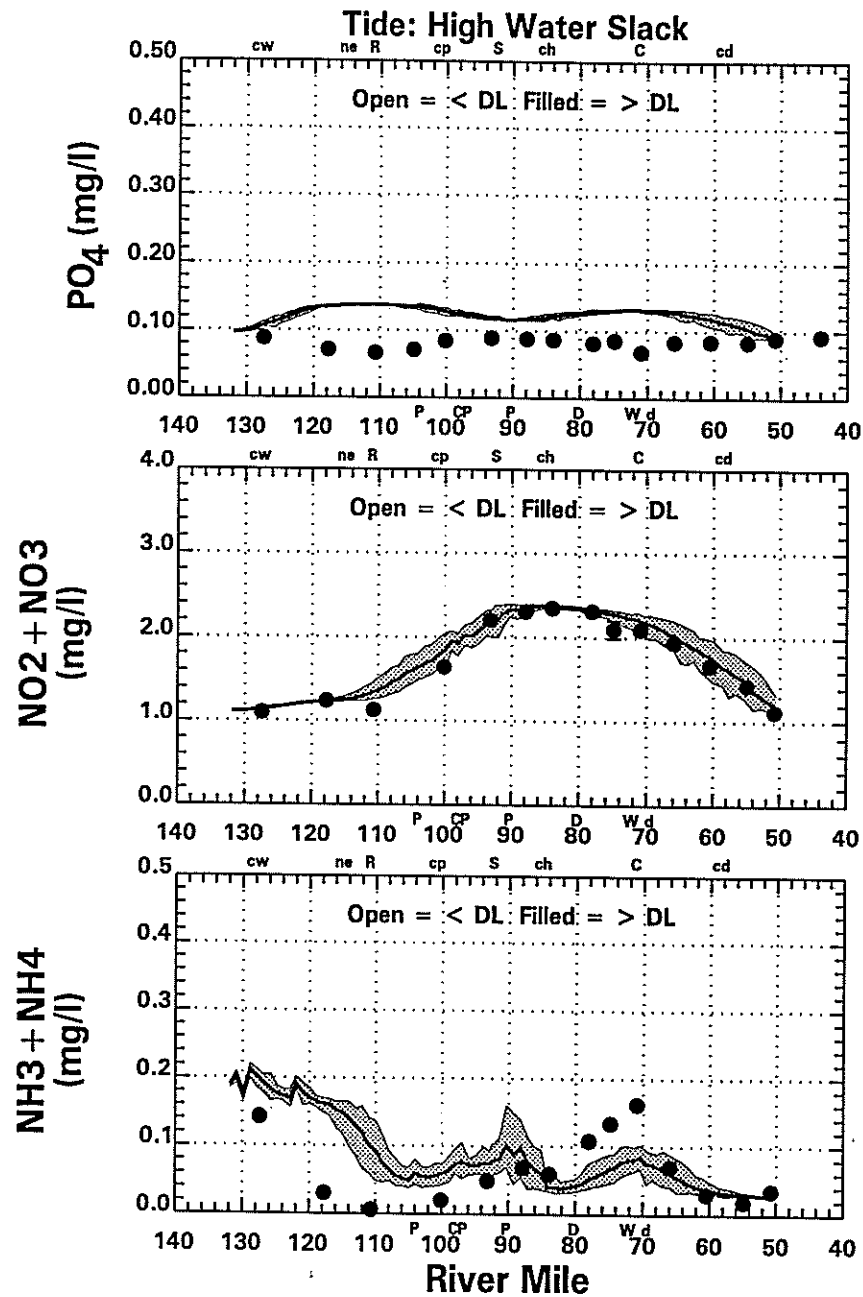
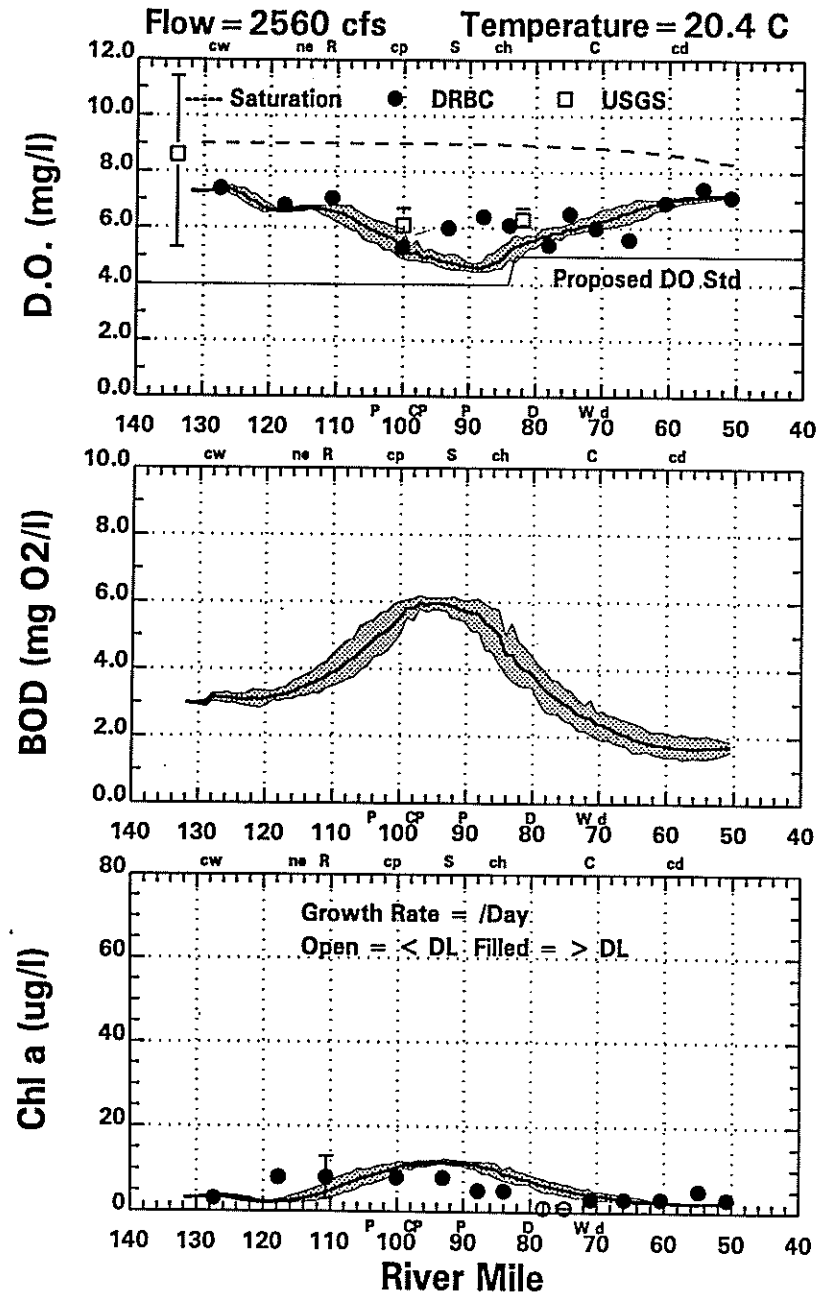


Delaware River Data (●) & Model (—) 9/5/95 (Model Day 50)
 [Daily Average & Shaded Area = Range over the Day]

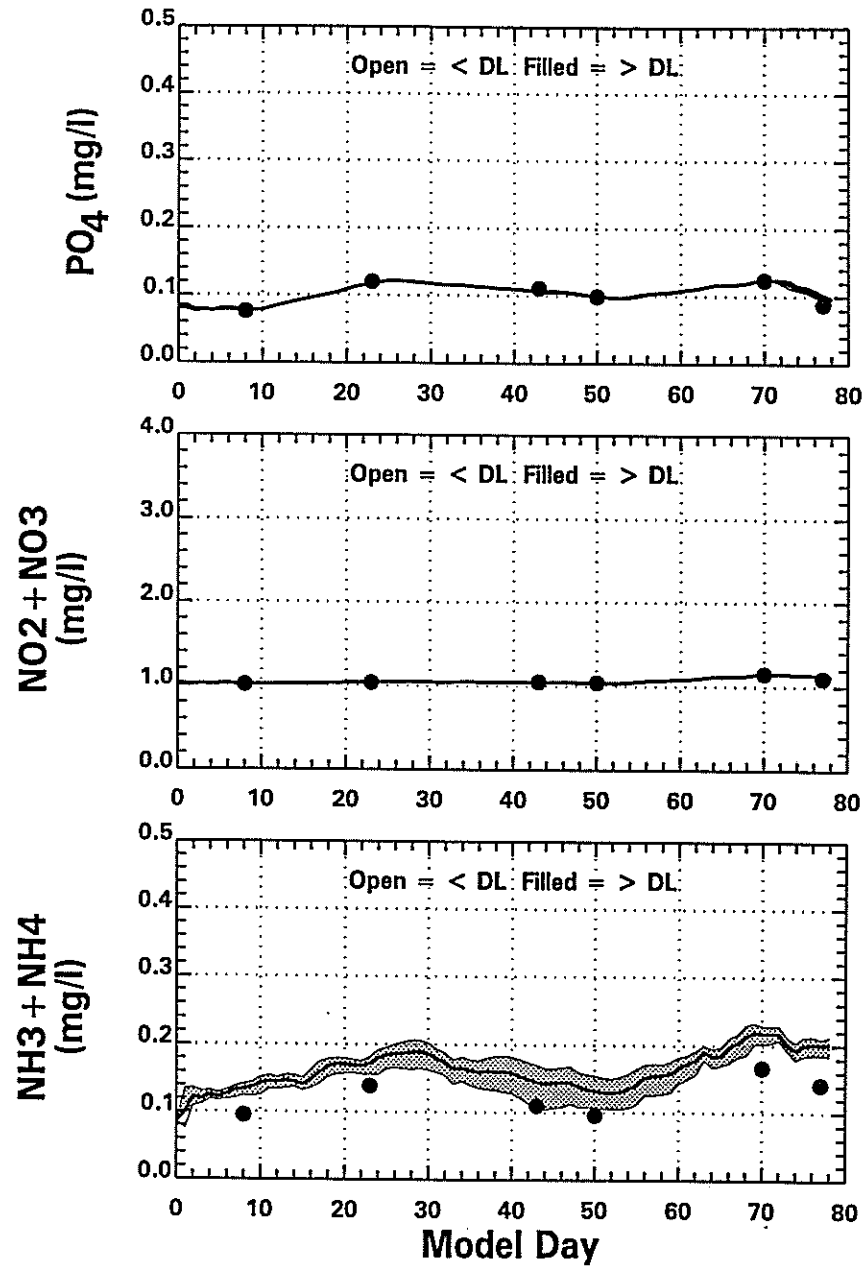
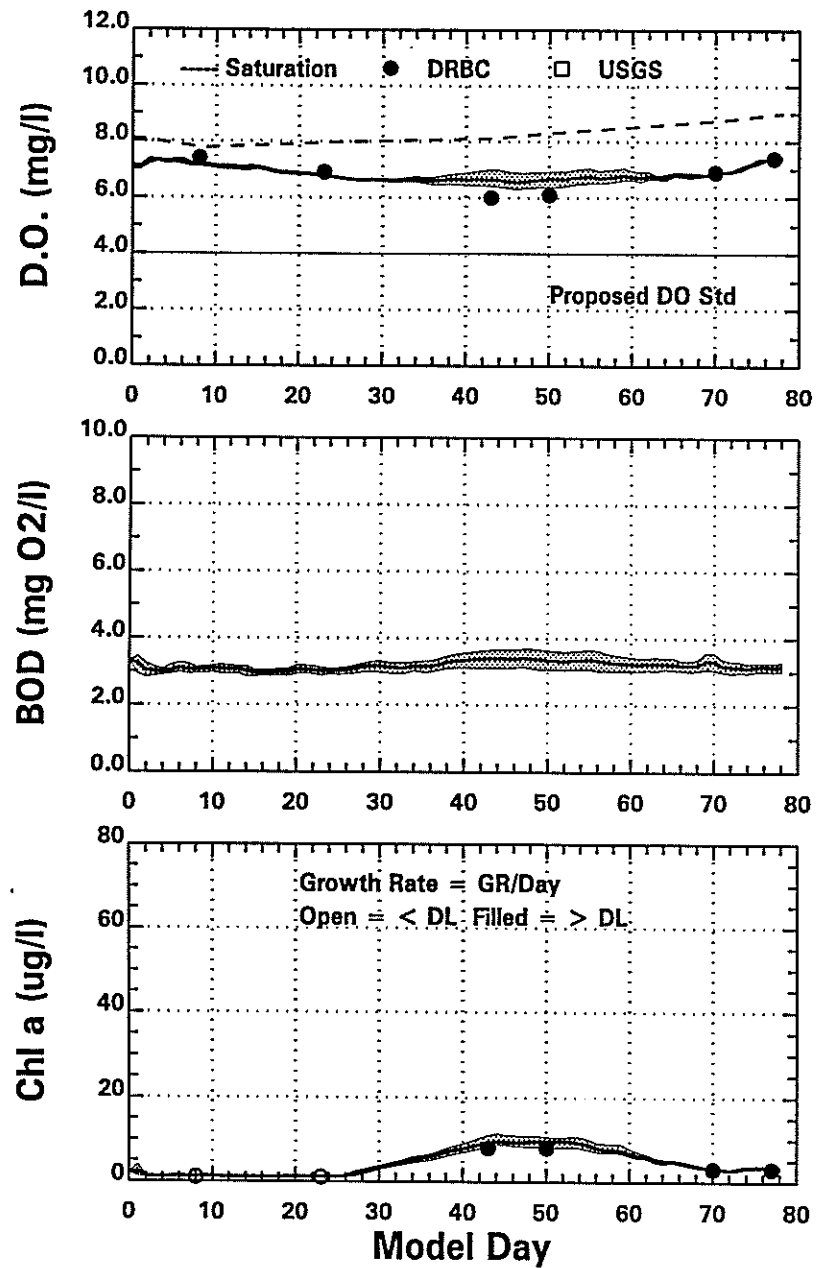


Delaware River Data (●) & Model (—) 9/25/95 (Model Day 70)
 [Daily Average & Shaded Area = Range over the Day]

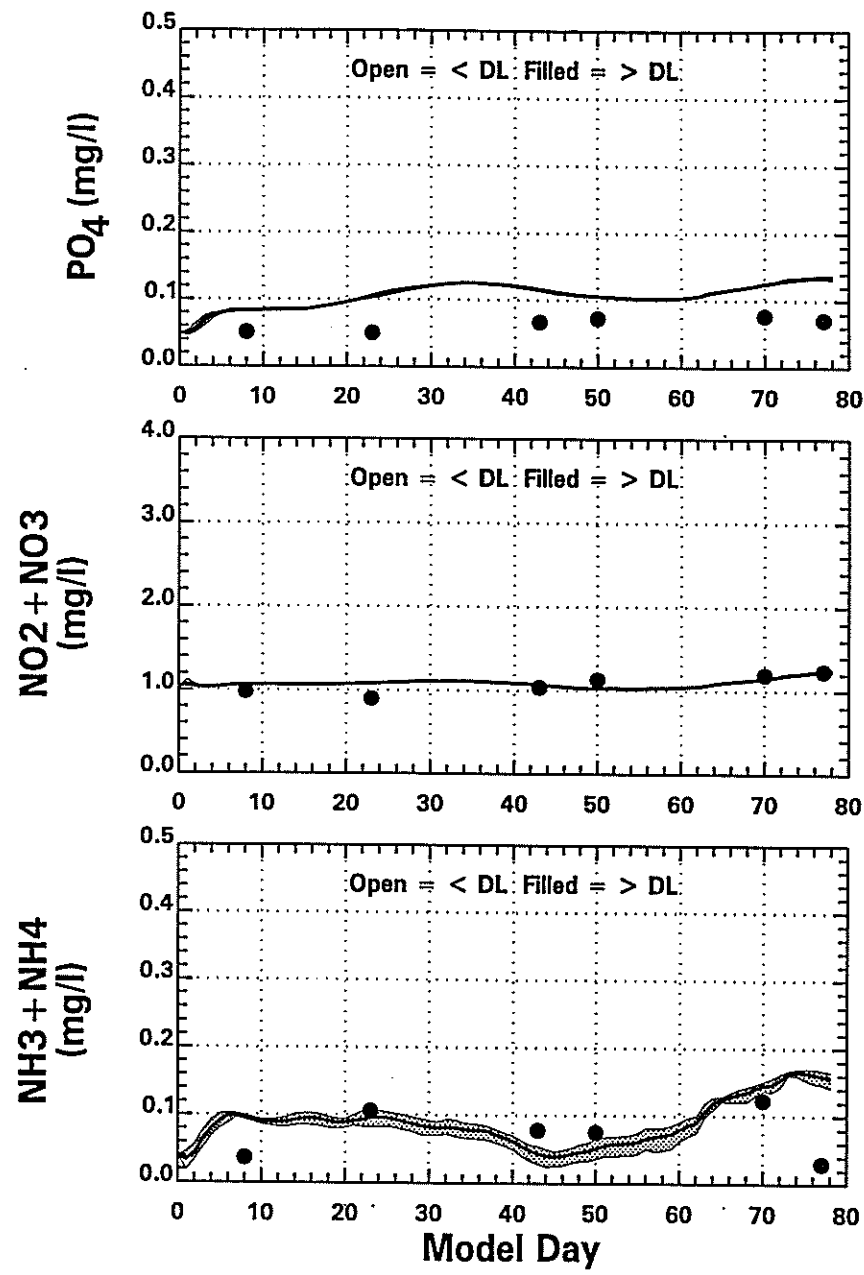
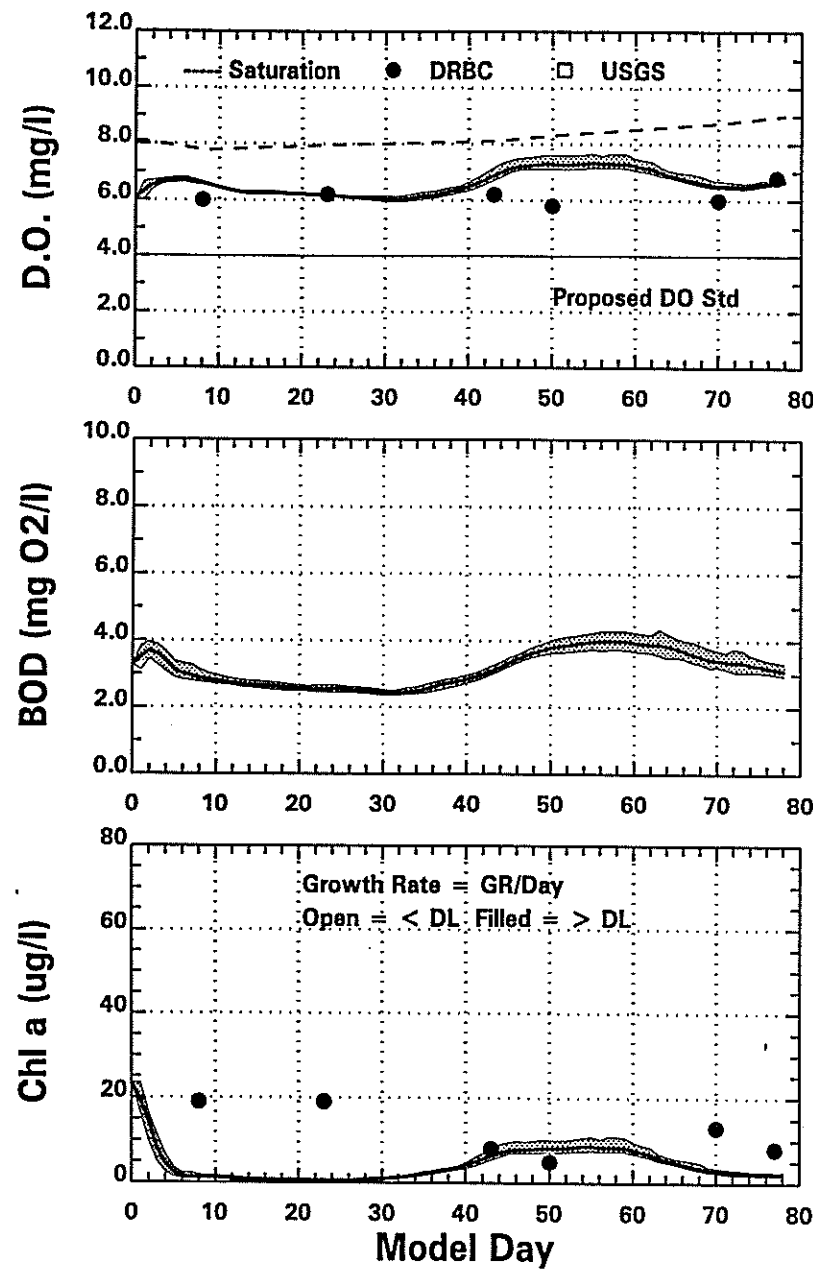




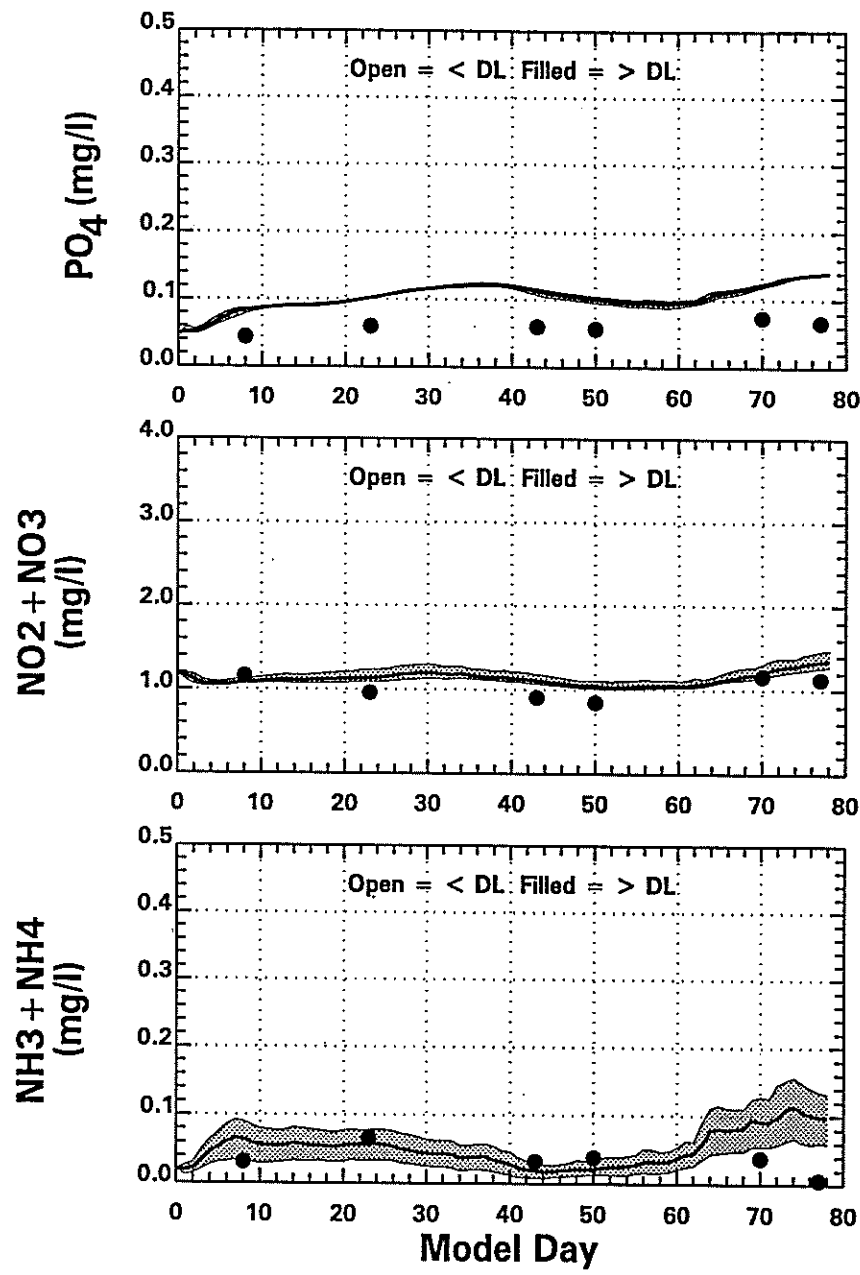
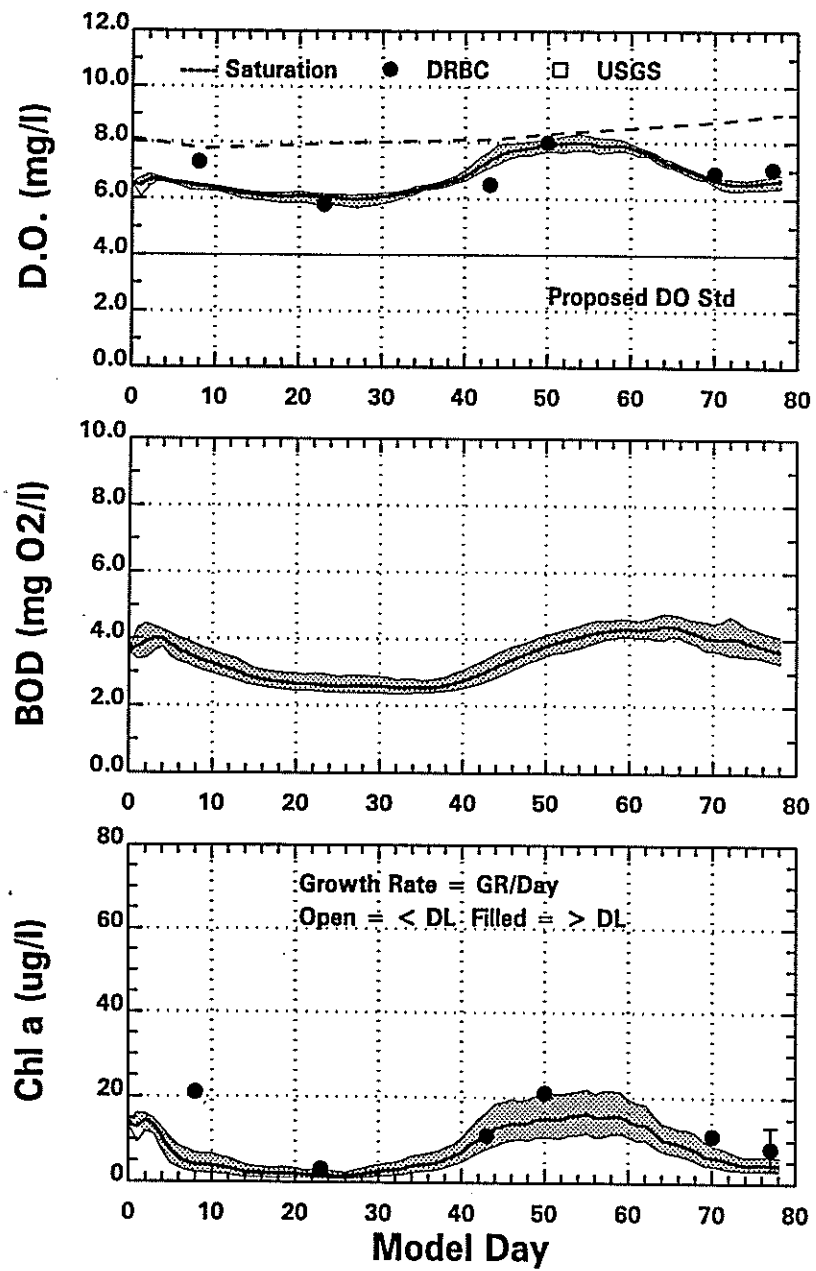
Delaware River Data (●) & Model (—) 10/2/95 (Model Day 77)
 [Daily Average & Shaded Area=Range over the Day]



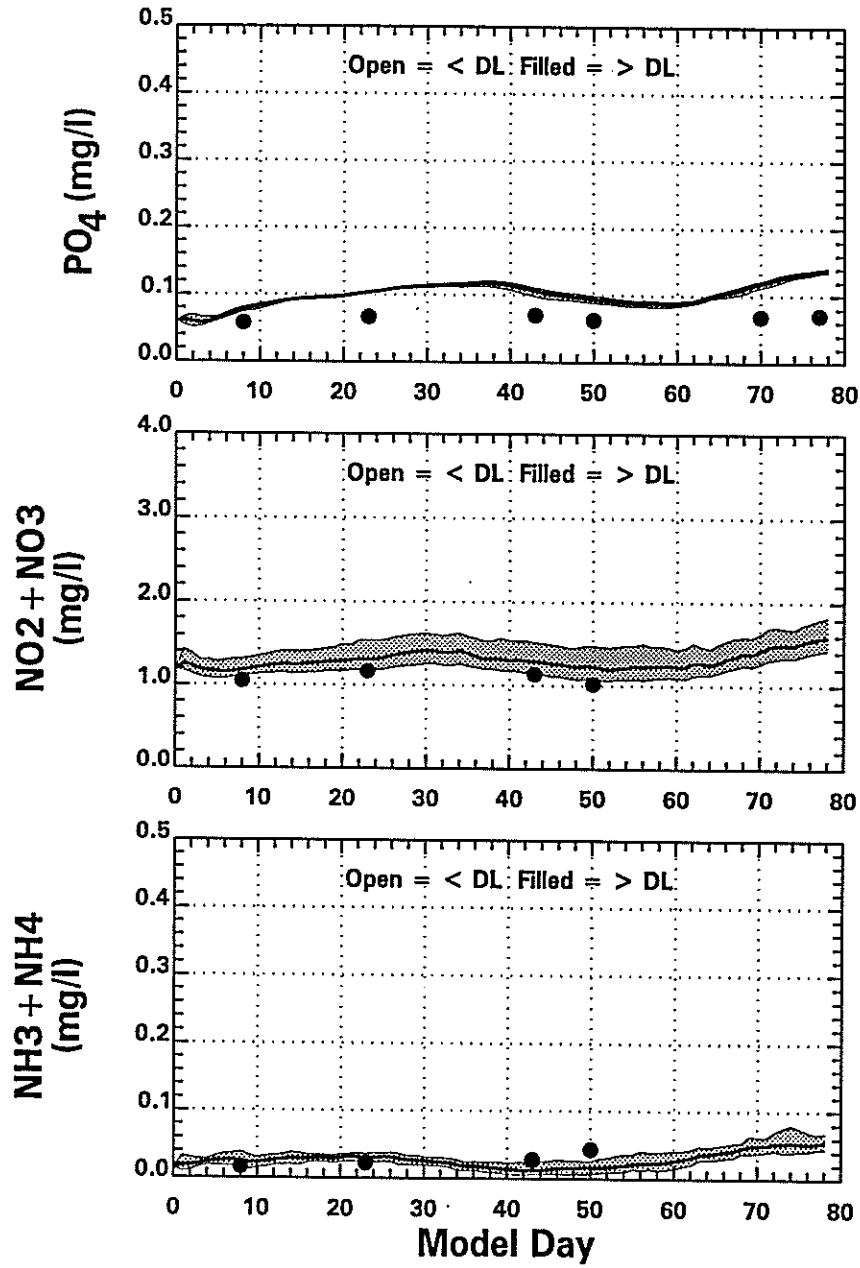
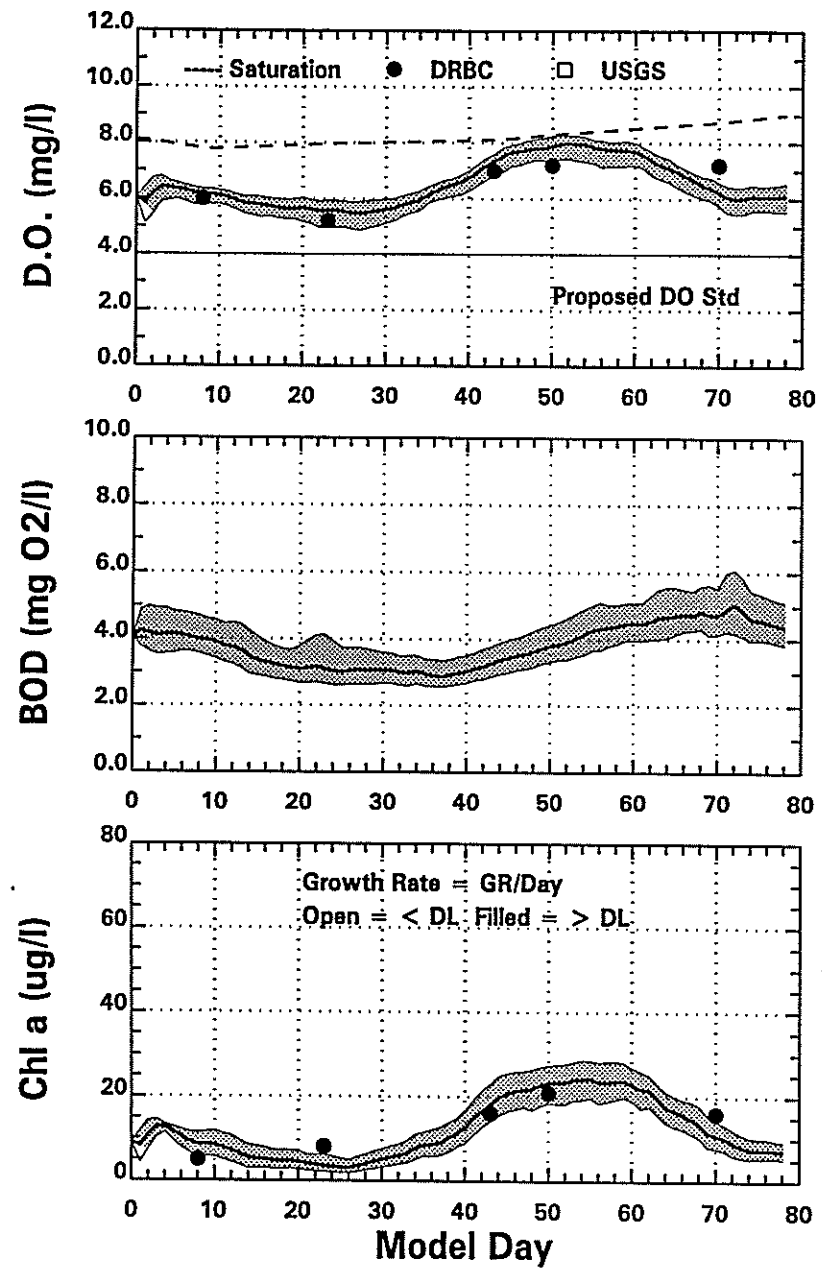
1995 Delaware River Data (●) & Model (—) (MP 127.48)
 [Daily Averages & Shaded Area = Range Over the Day]



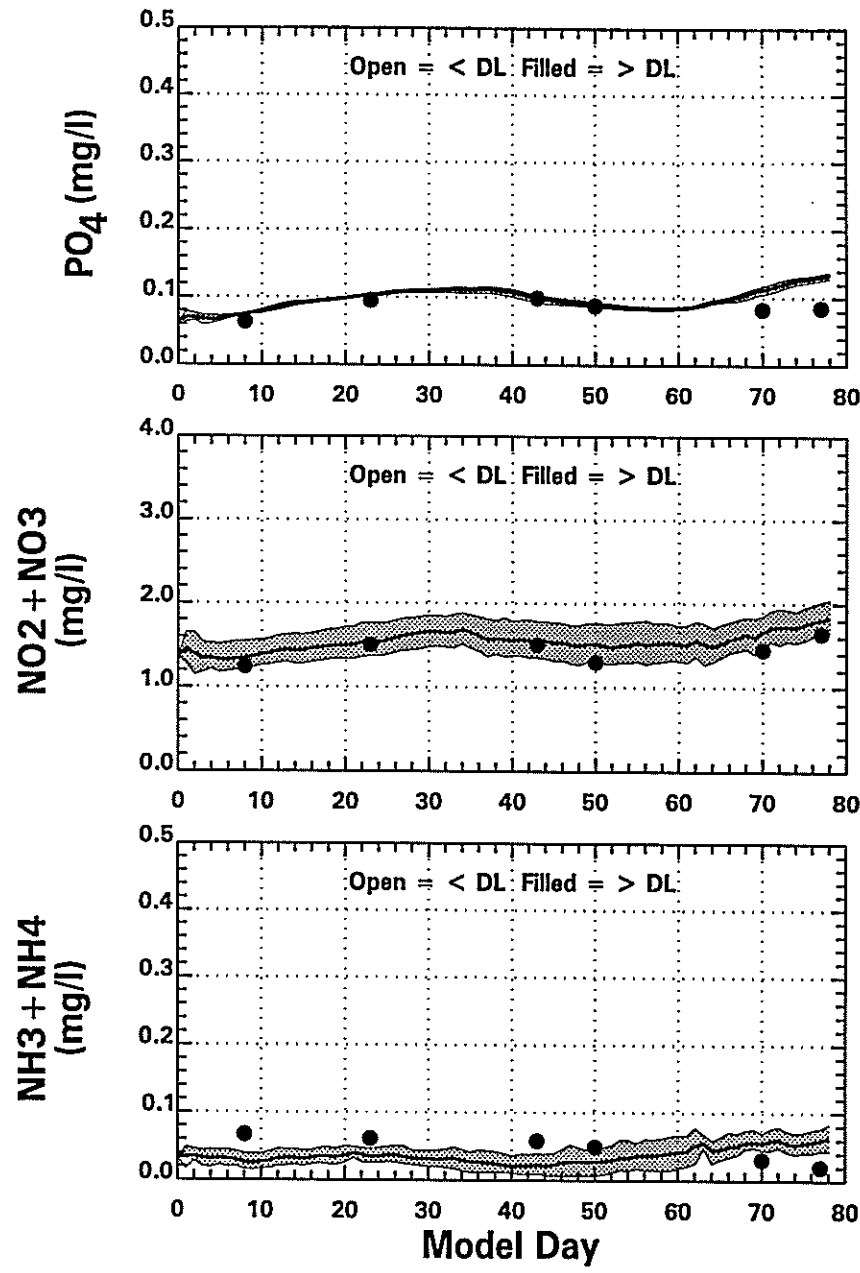
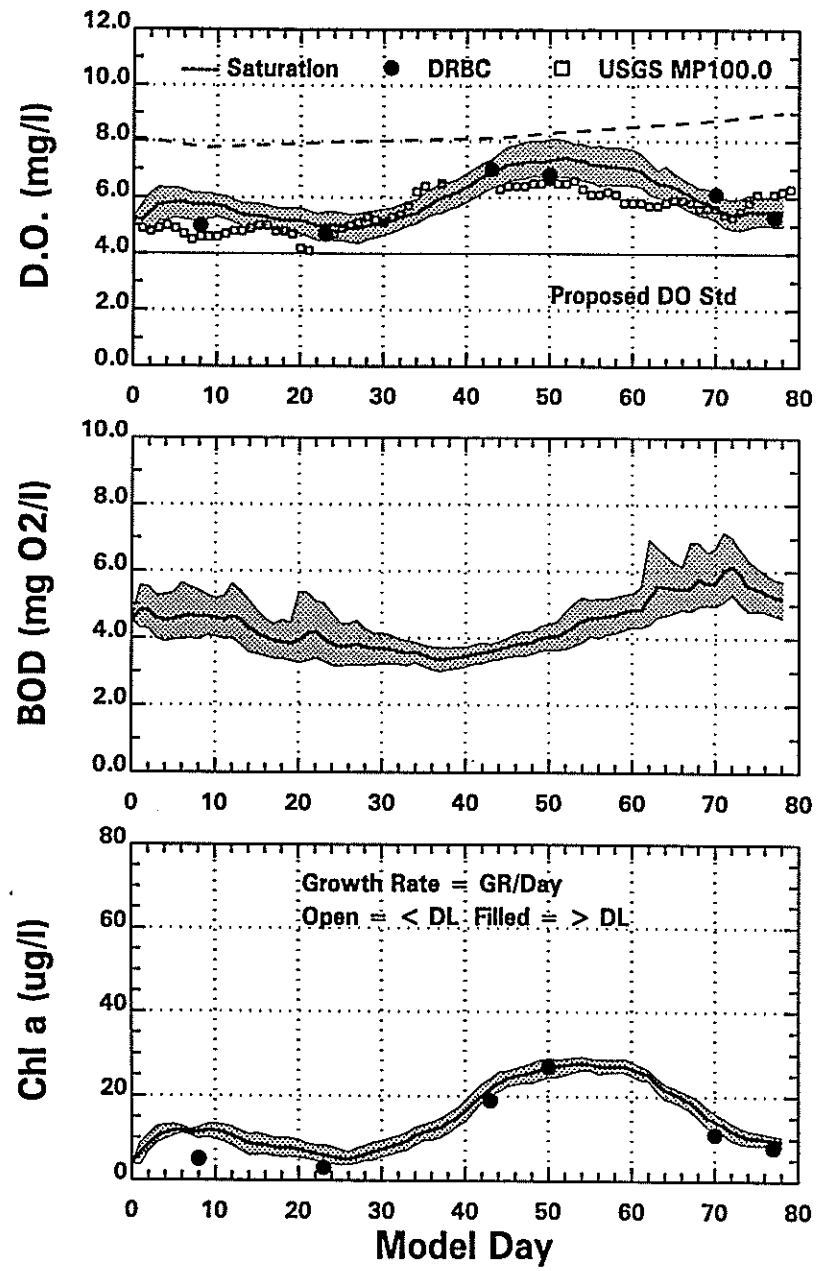
1995 Delaware River Data (●) & Model (—) (MP 117.80)
[Daily Averages & Shaded Area = Range Over the Day]



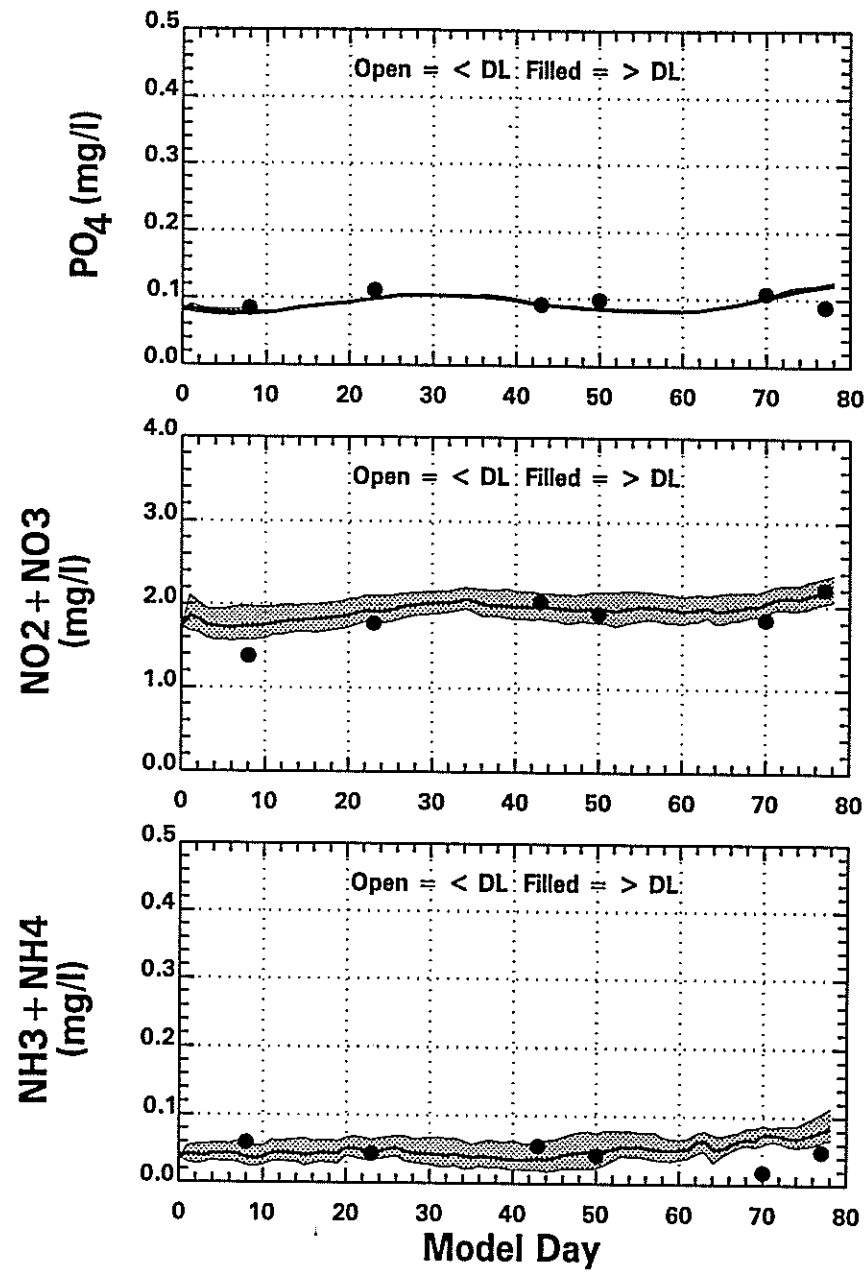
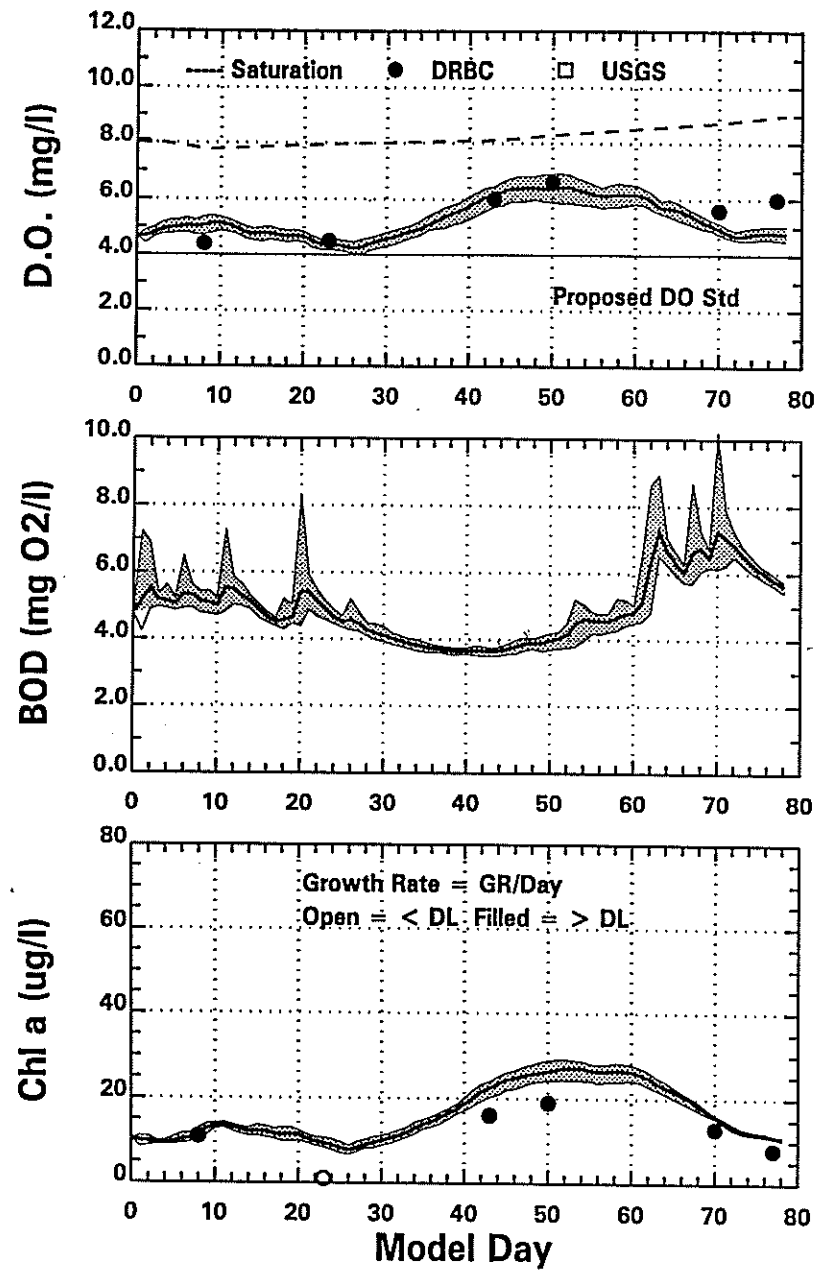
1995 Delaware River Data (●) & Model (—) (MP 110.70)
 [Daily Averages & Shaded Area = Range Over the Day]



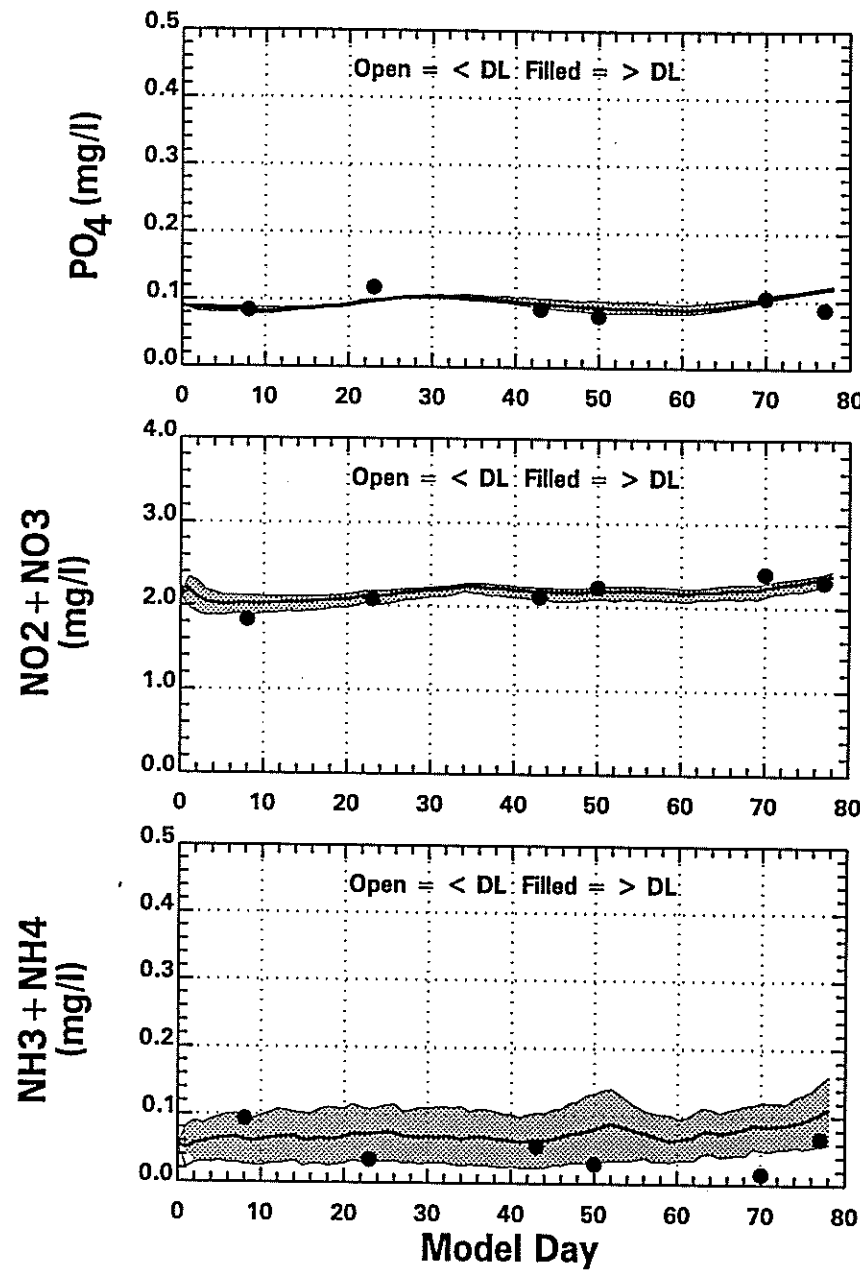
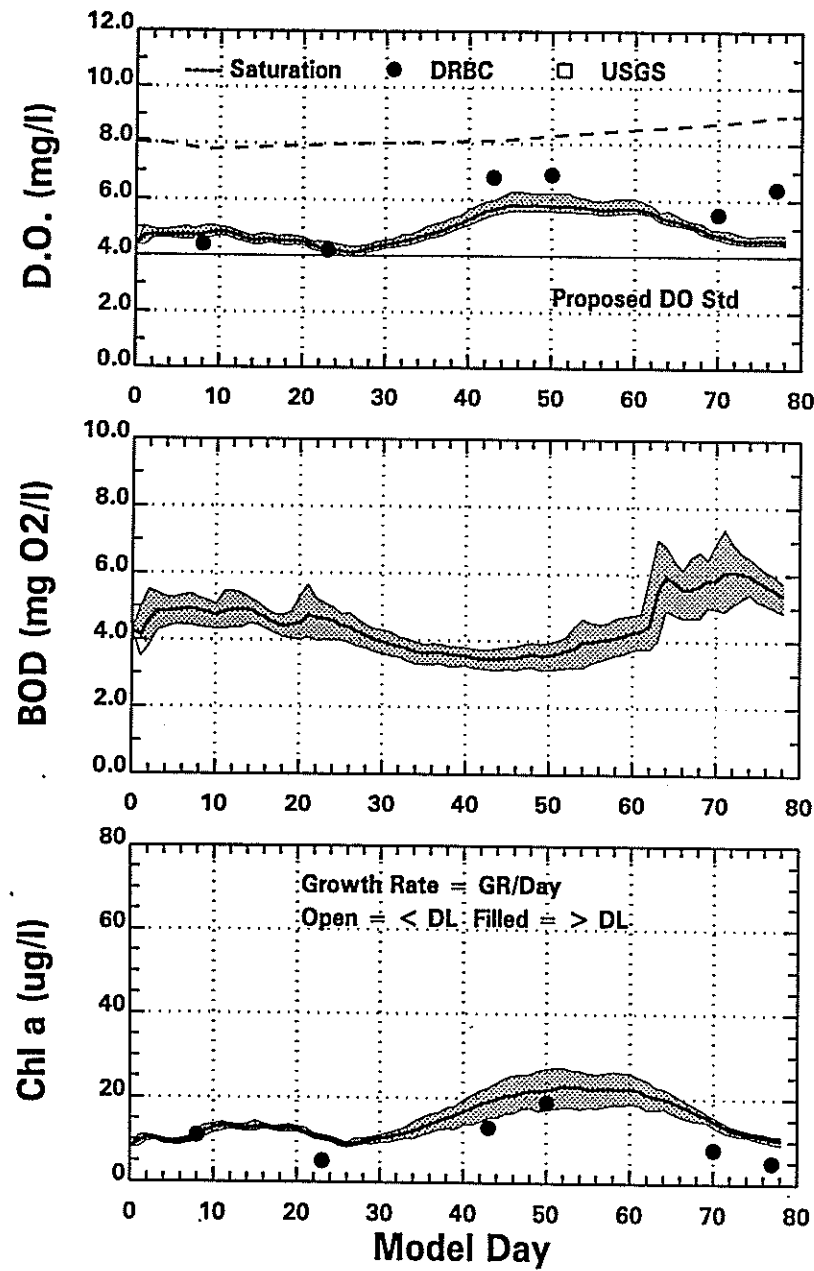
1995 Delaware River Data (●) & Model (—) (MP 104.90)
[Daily Averages & Shaded Area = Range Over the Day]



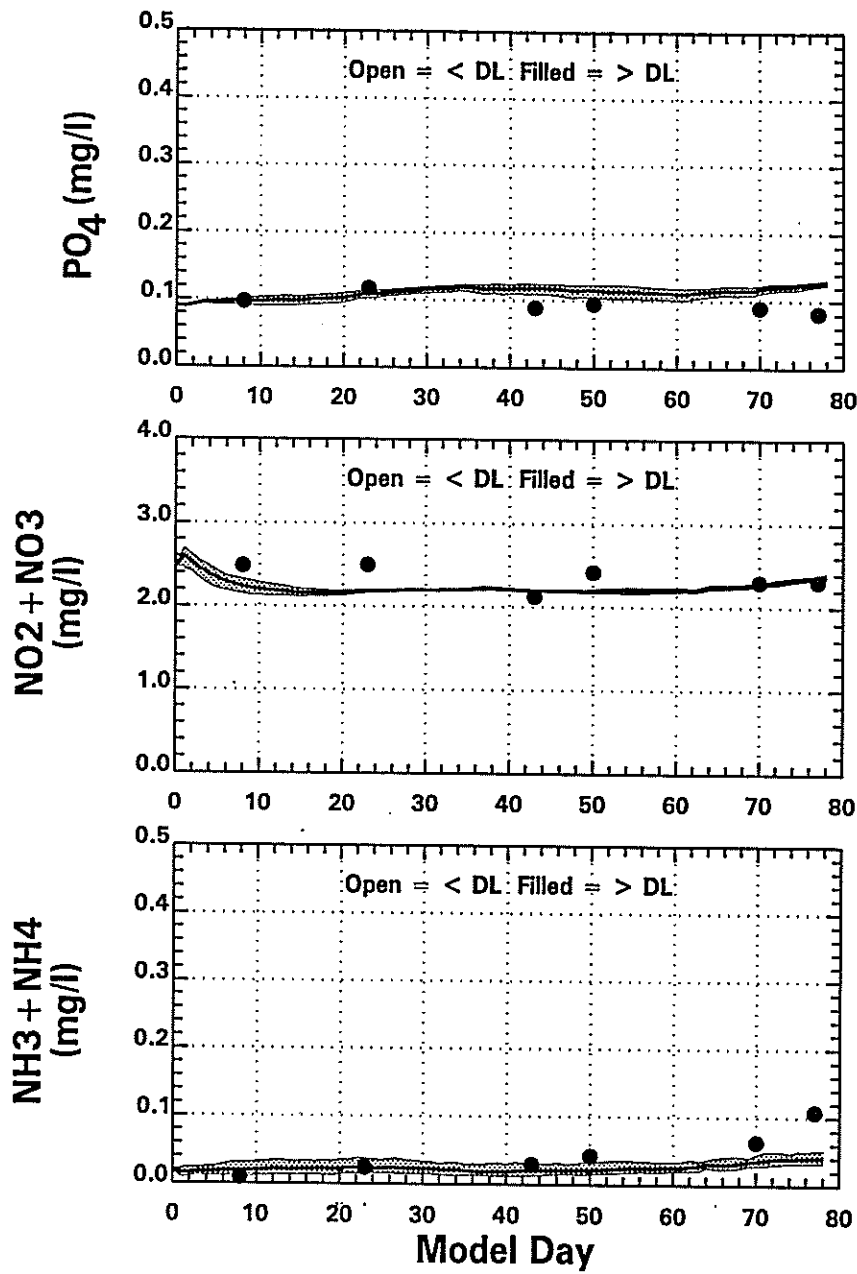
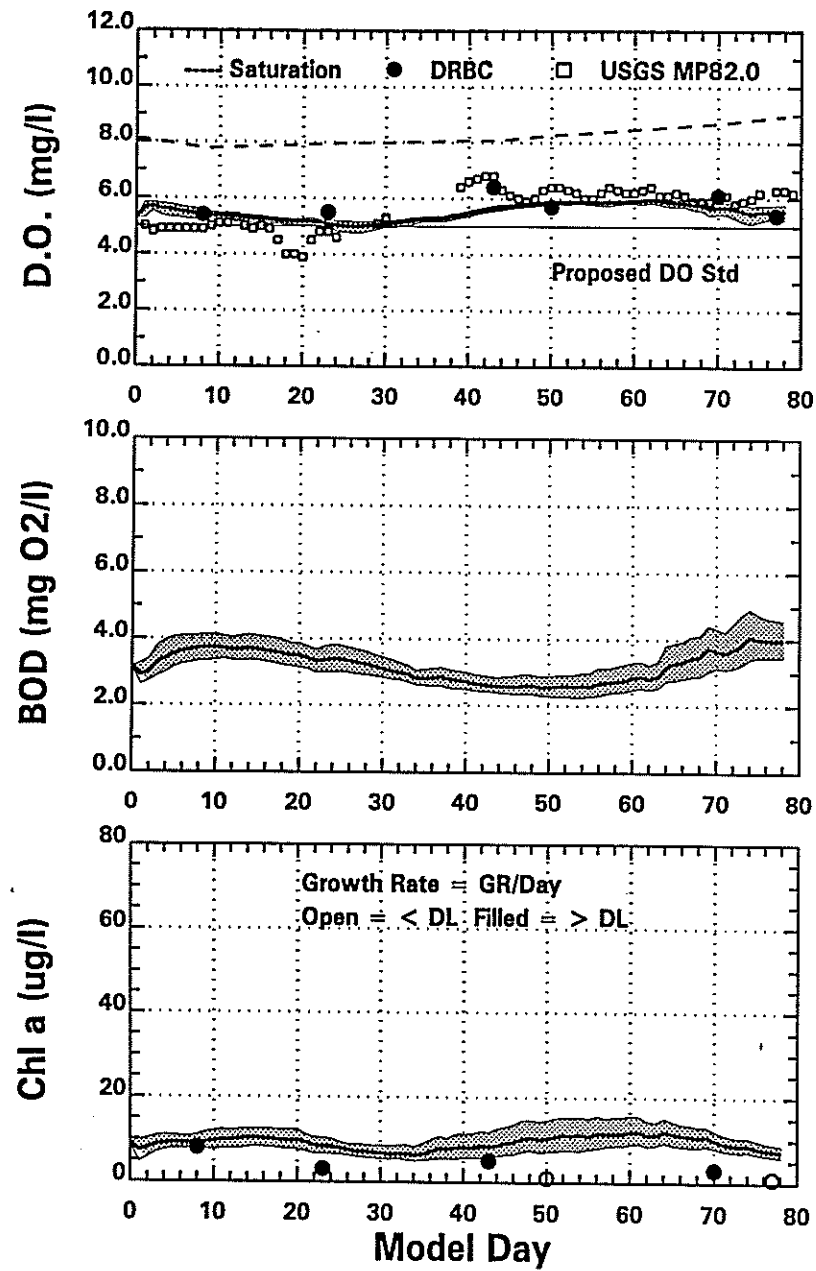
1995 Delaware River Data (●) & Model (—) (MP 100.15)
 [Daily Averages & Shaded Area = Range Over the Day]



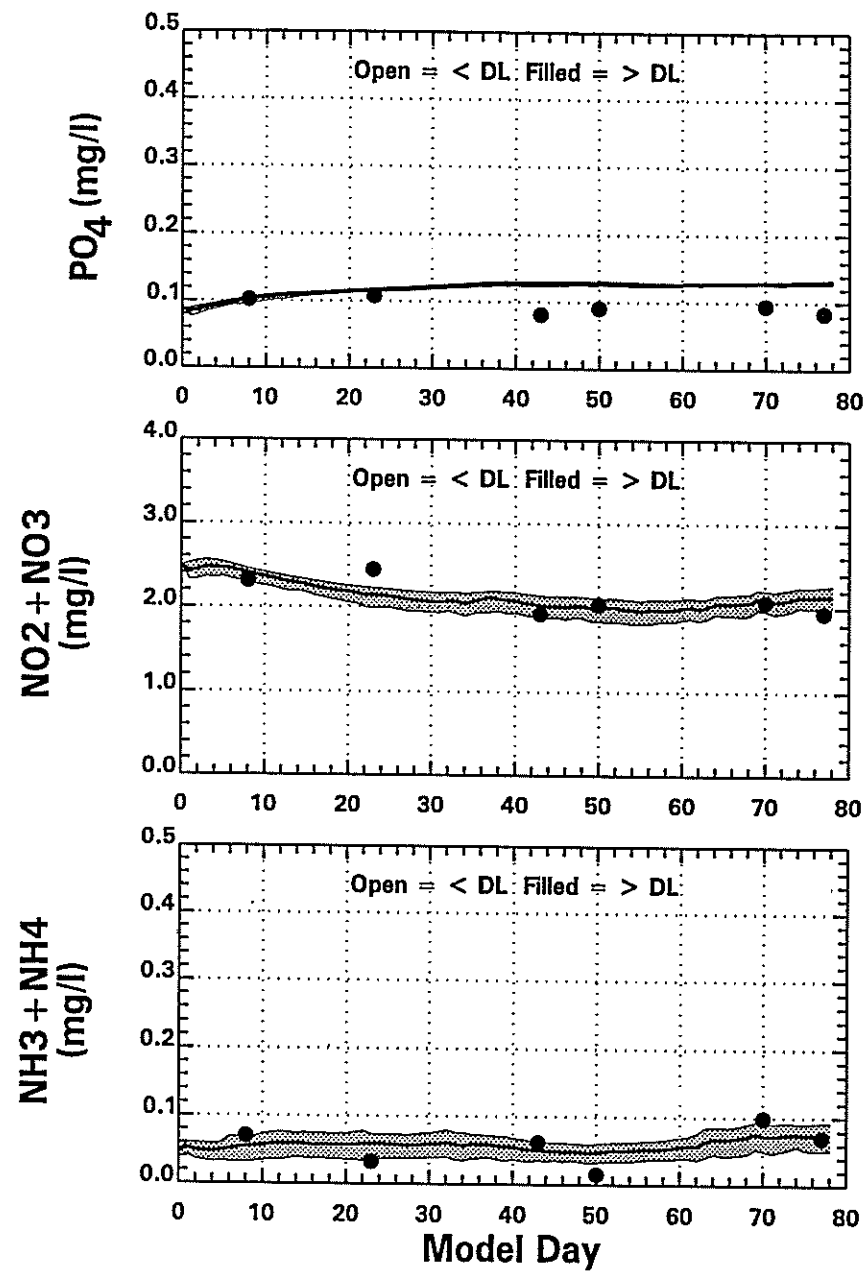
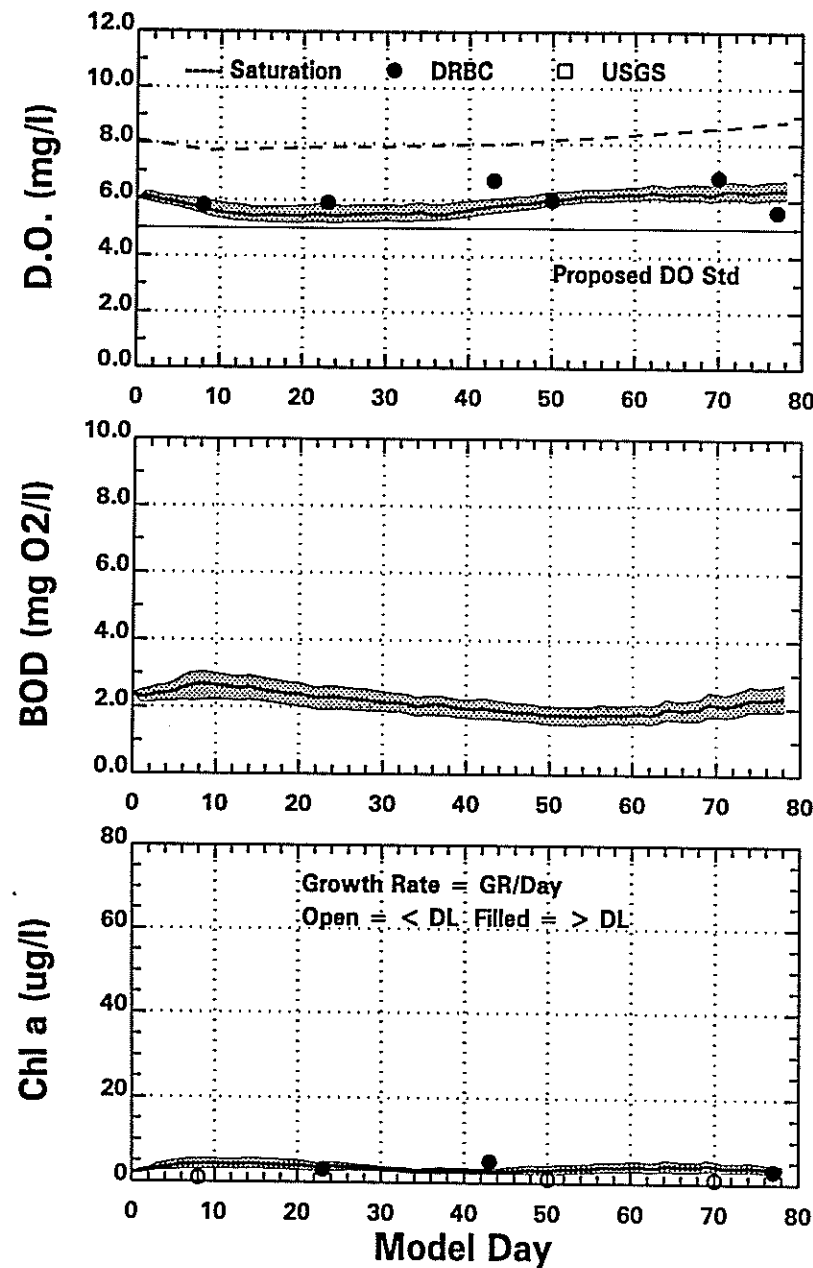
1995 Delaware River Data (●) & Model (—) (MP 93.18)
 [Daily Averages & Shaded Area = Range Over the Day]



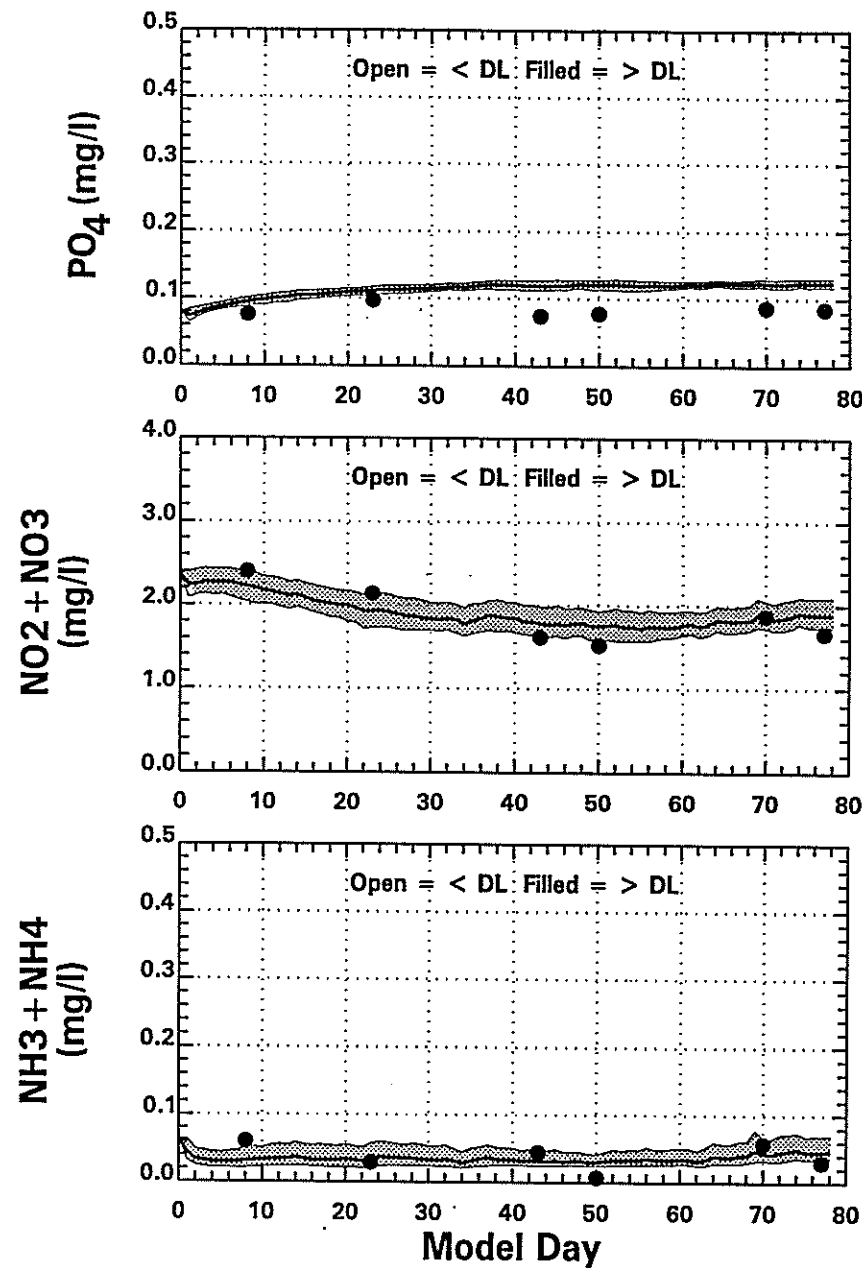
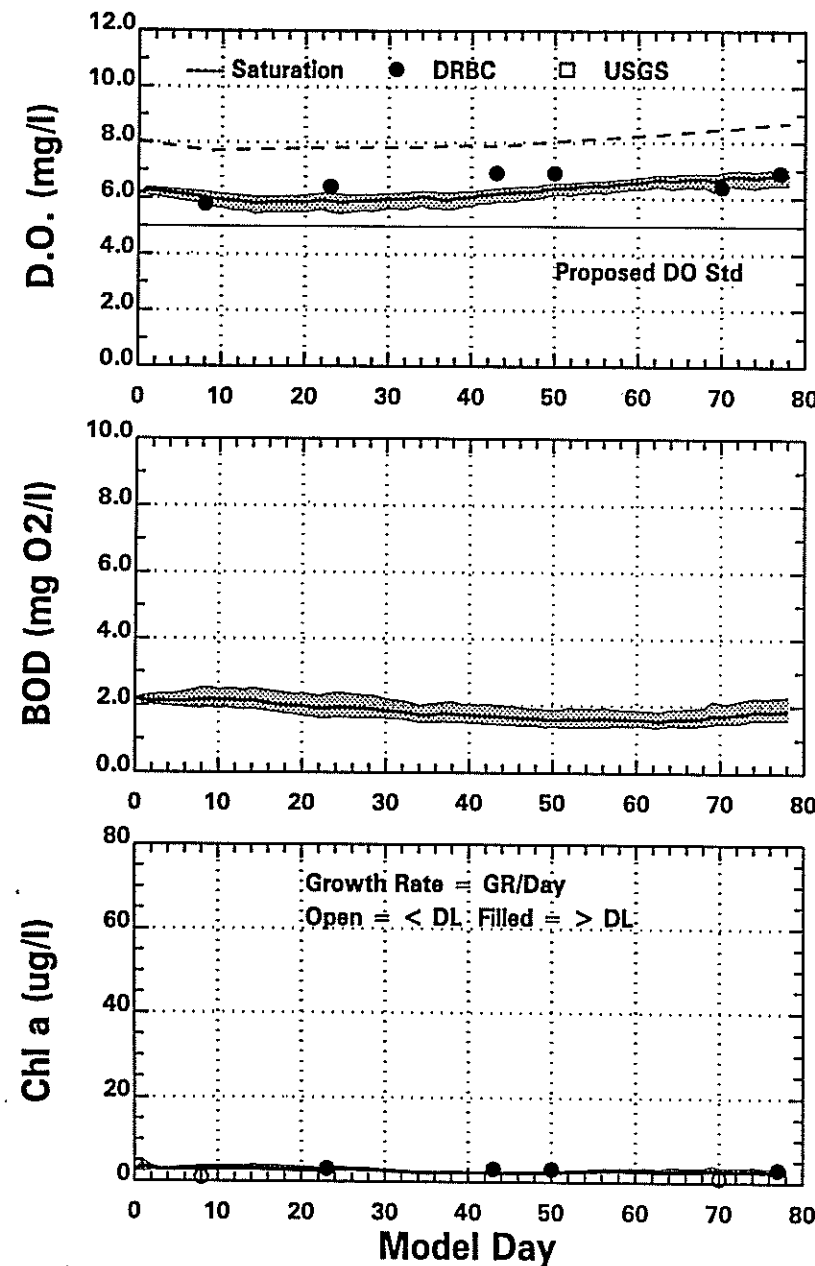
1995 Delaware River Data (●) & Model (—) (MP 87.90)
 [Daily Averages & Shaded Area = Range Over the Day]



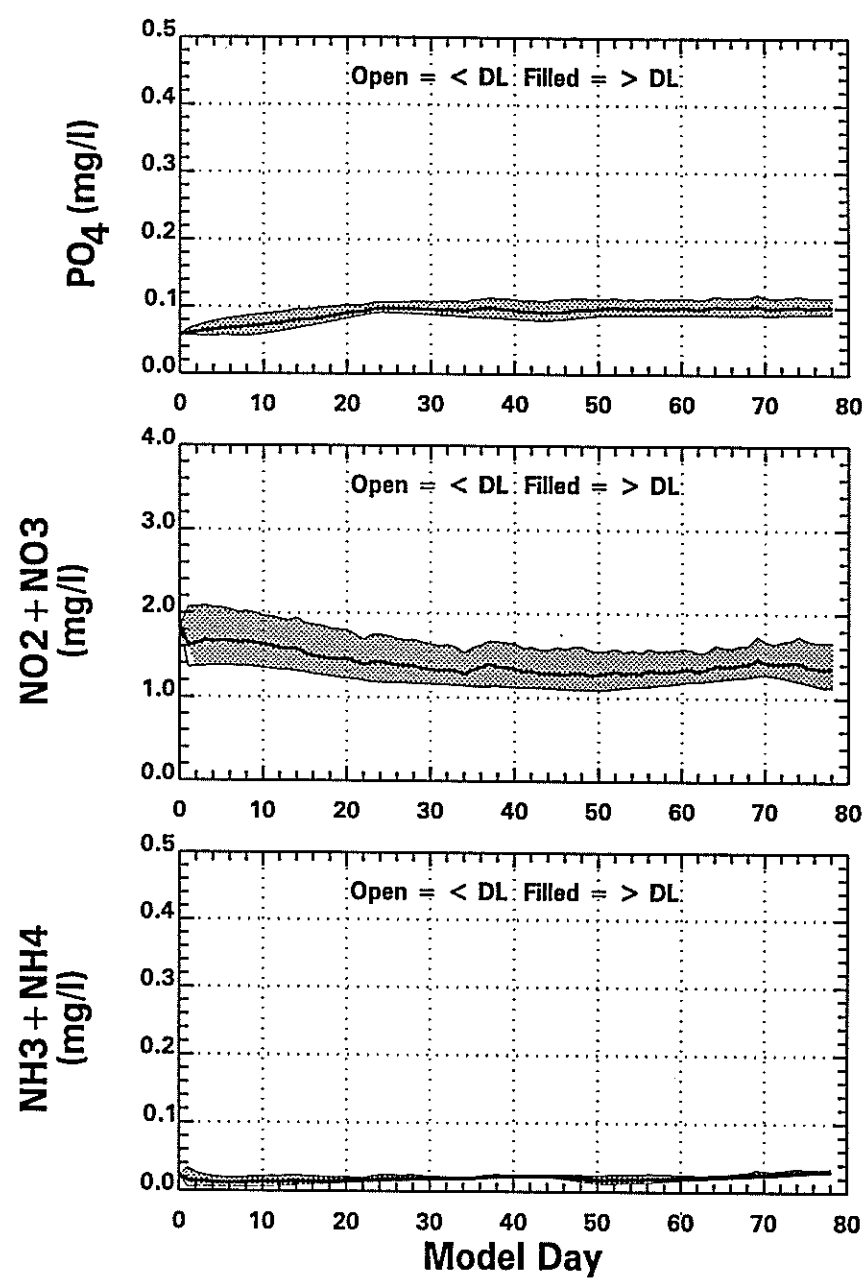
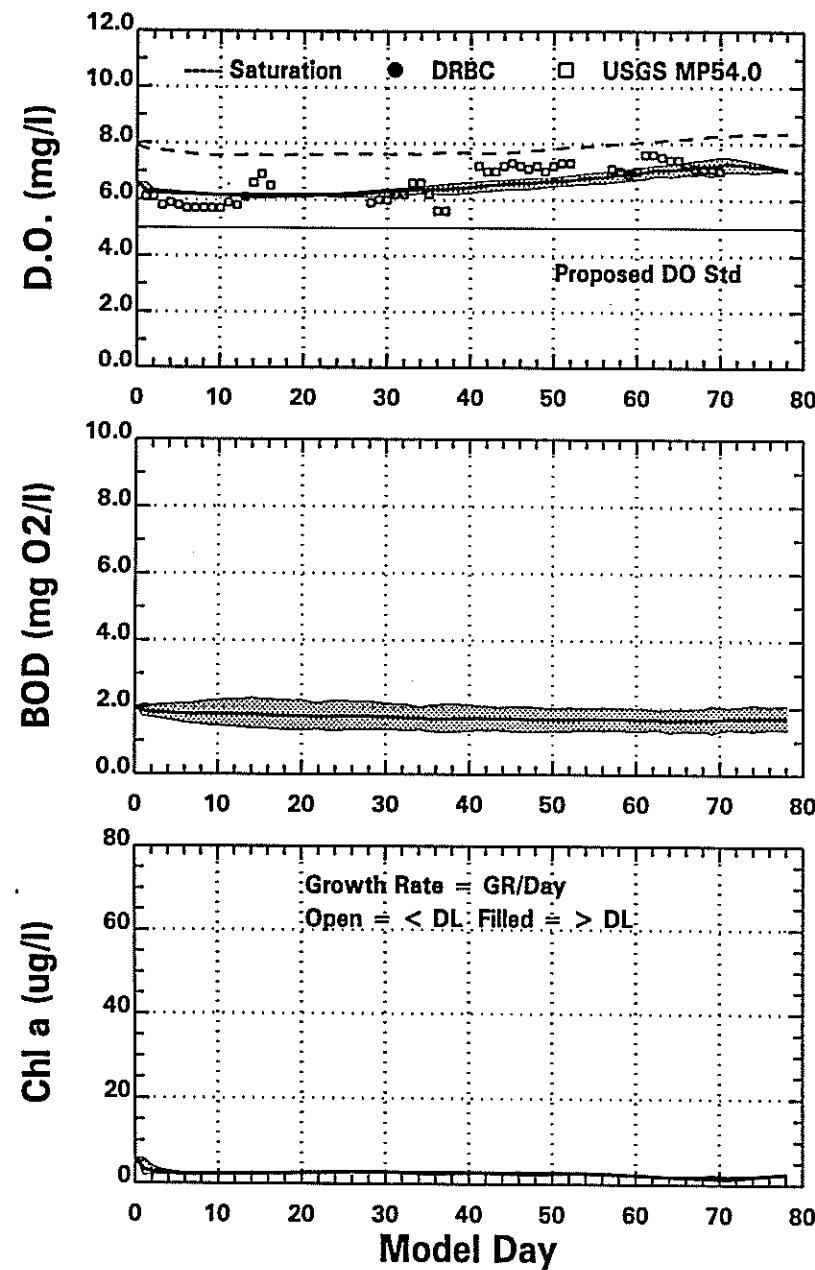
1995 Delaware River Data (●) & Model (—) (MP 78.07)
 [Daily Averages & Shaded Area = Range Over the Day]



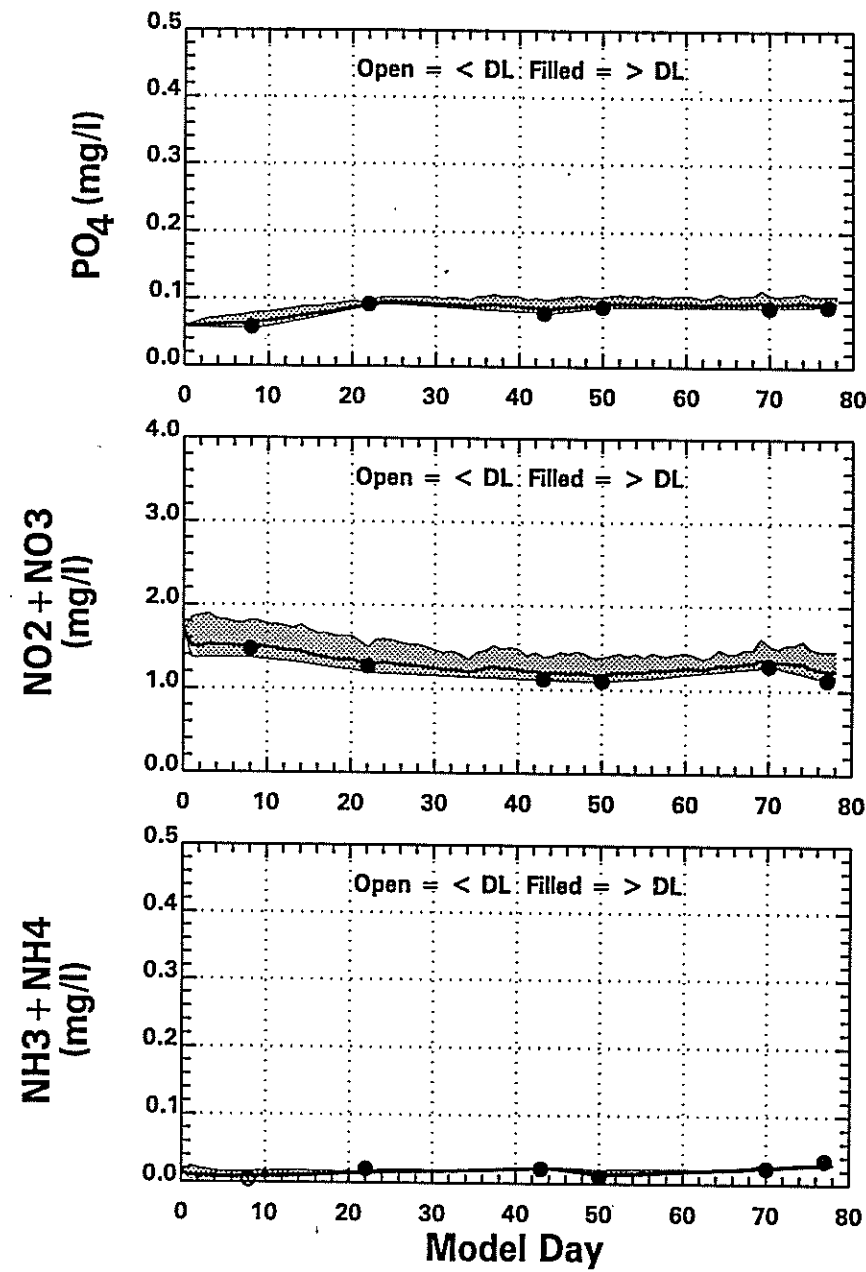
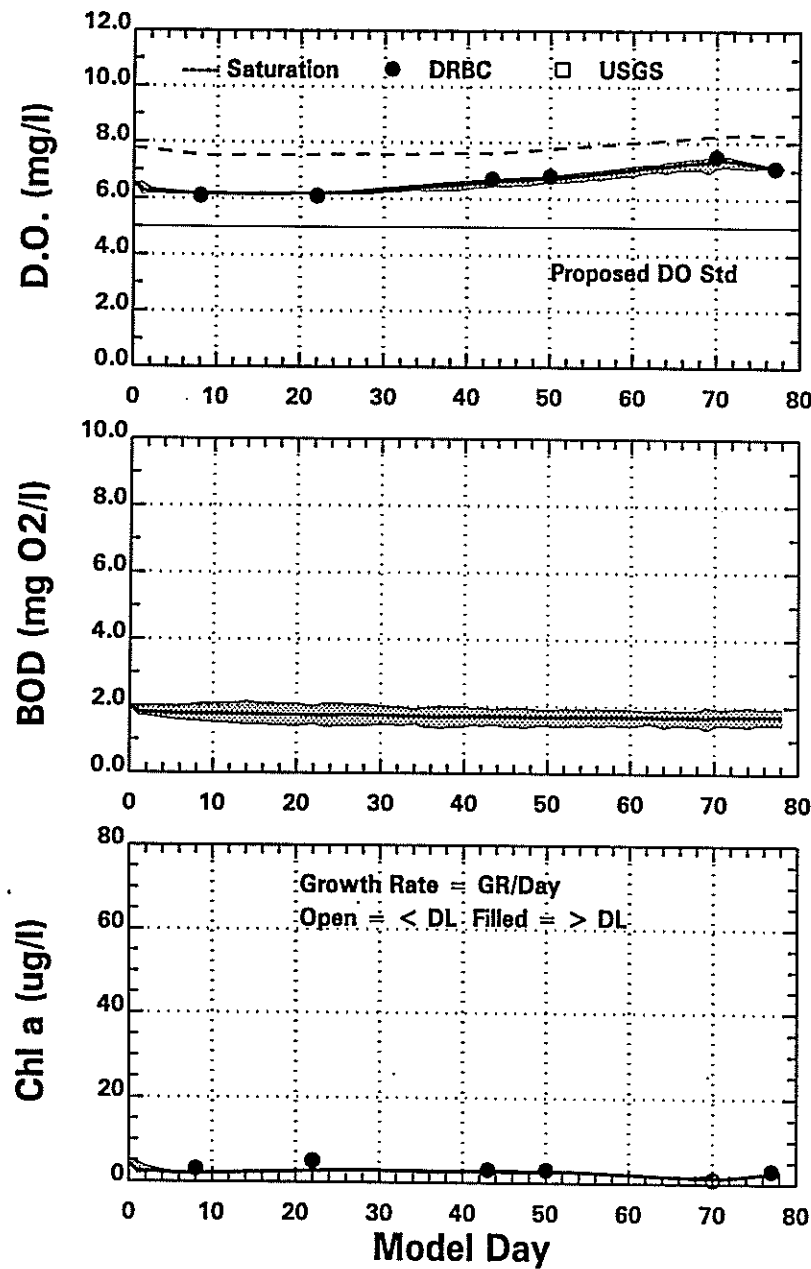
1995 Delaware River Data (●) & Model (—) (MP 65.96)
 [Daily Averages & Shaded Area = Range Over the Day]



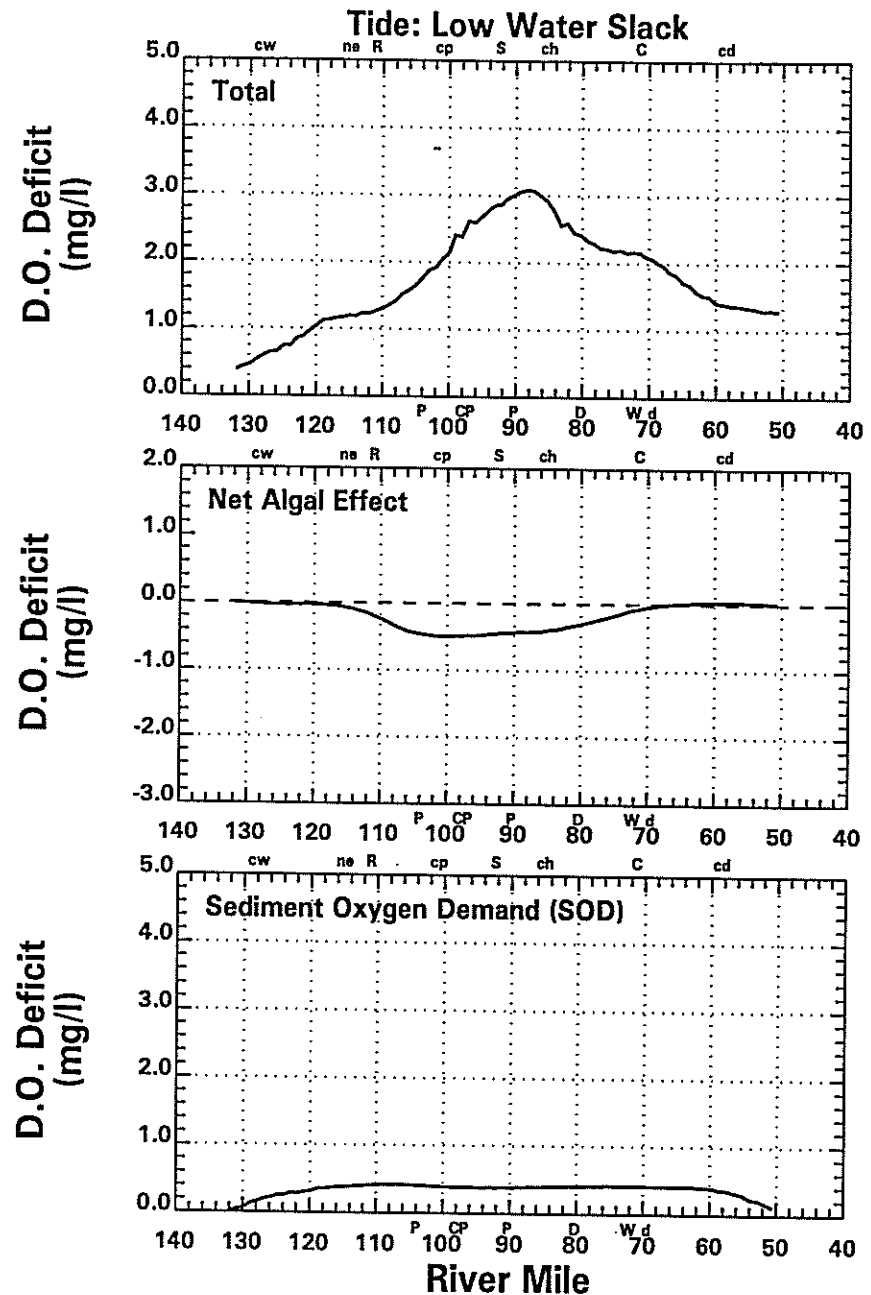
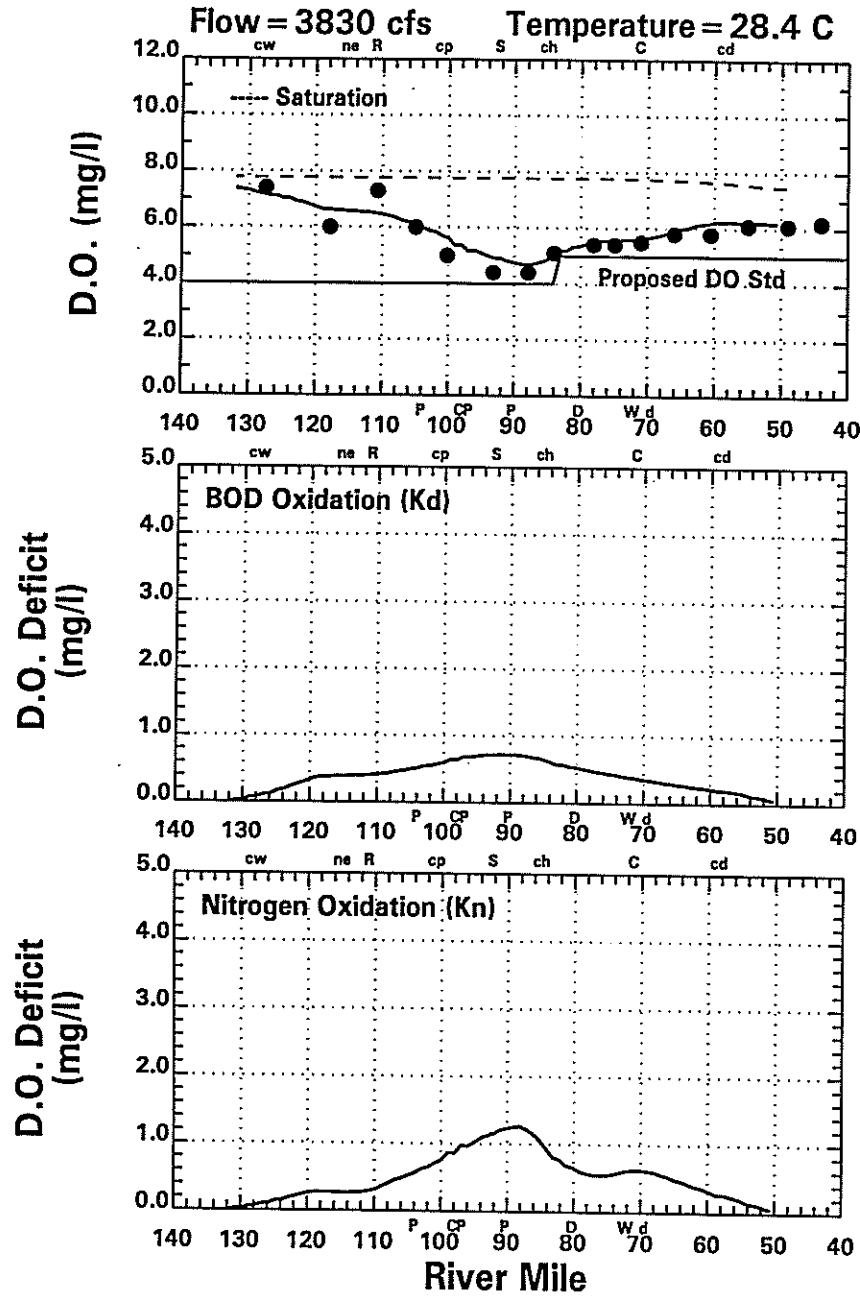
1995 Delaware River Data (●) & Model (—) (MP 60.55)
 [Daily Averages & Shaded Area = Range Over the Day]



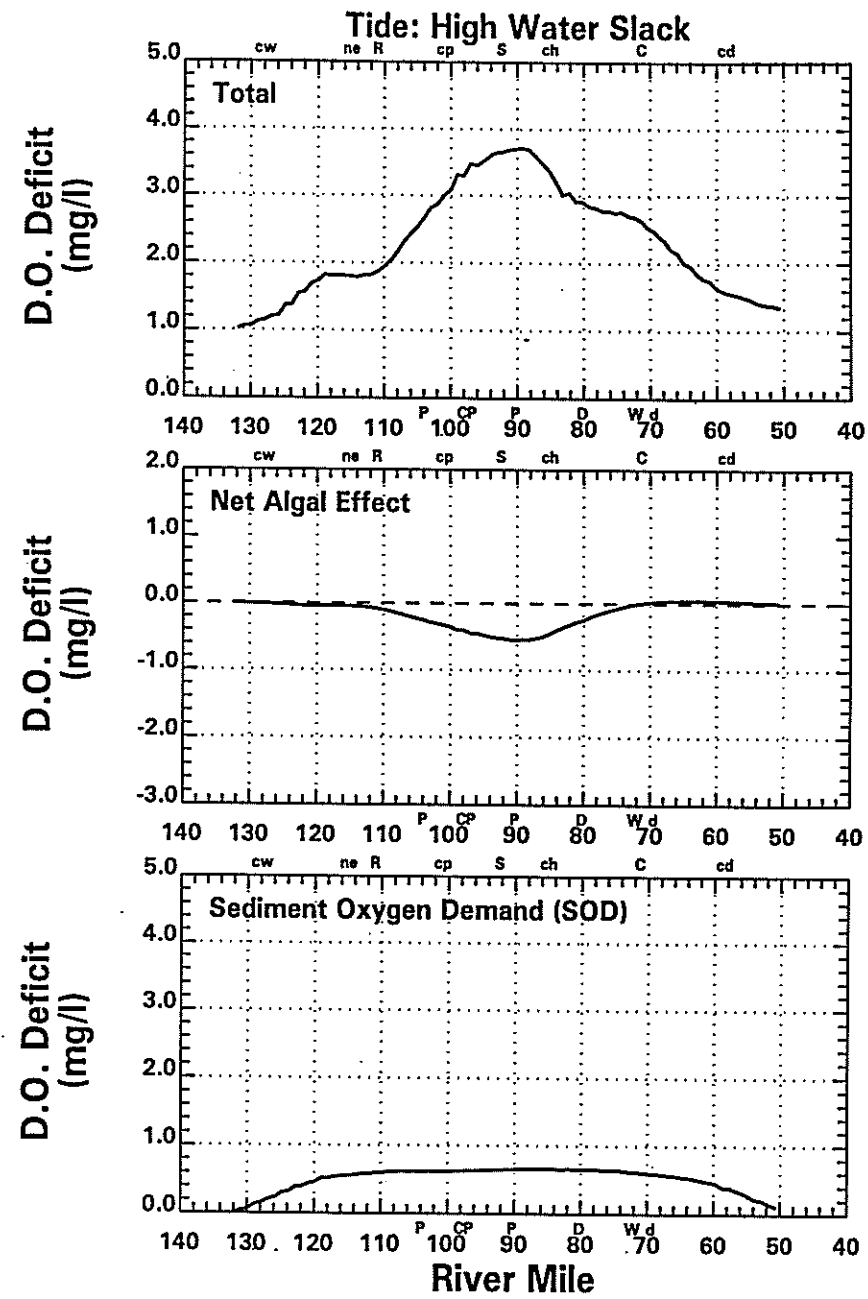
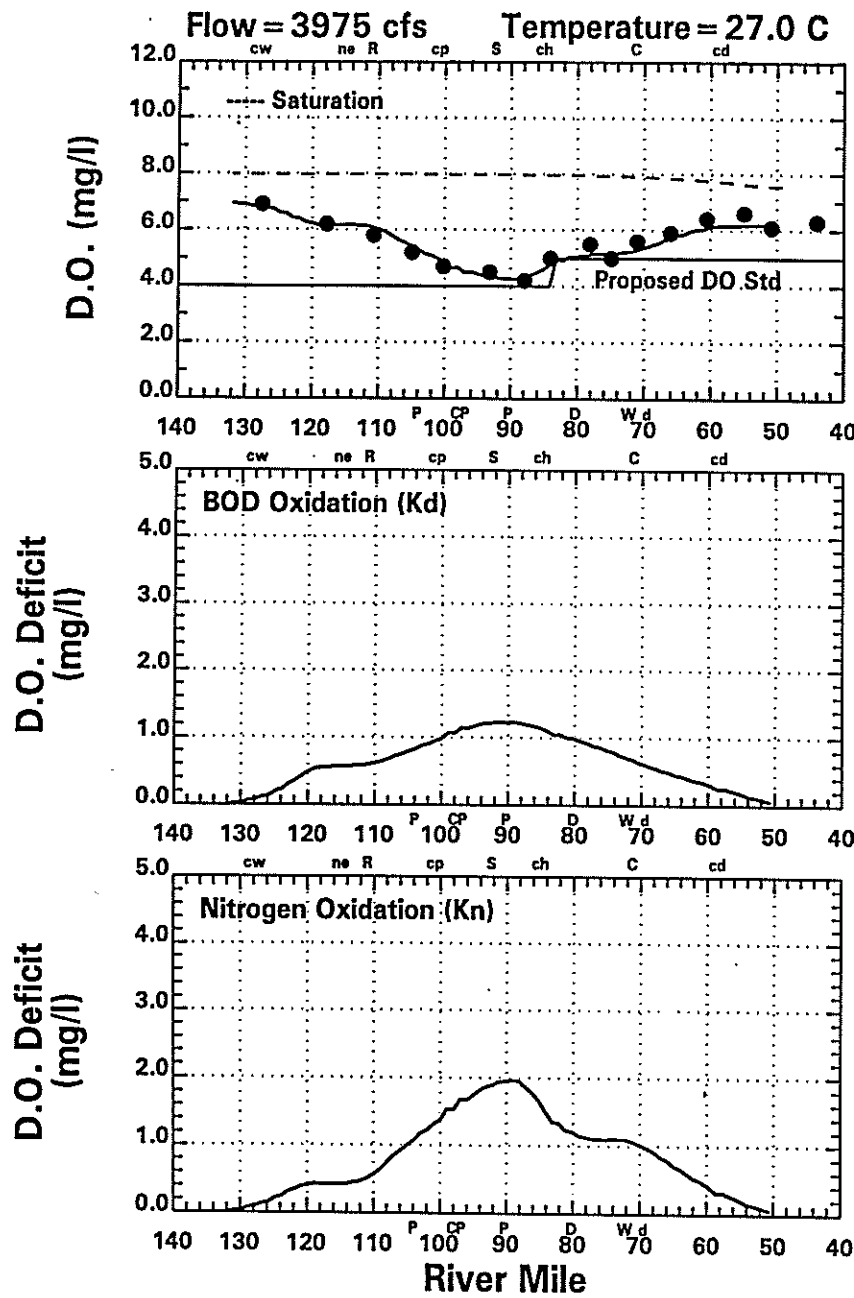
1995 Delaware River Data (●) & Model (—) (MP 50.80)
 [Daily Averages & Shaded Area = Range Over the Day]



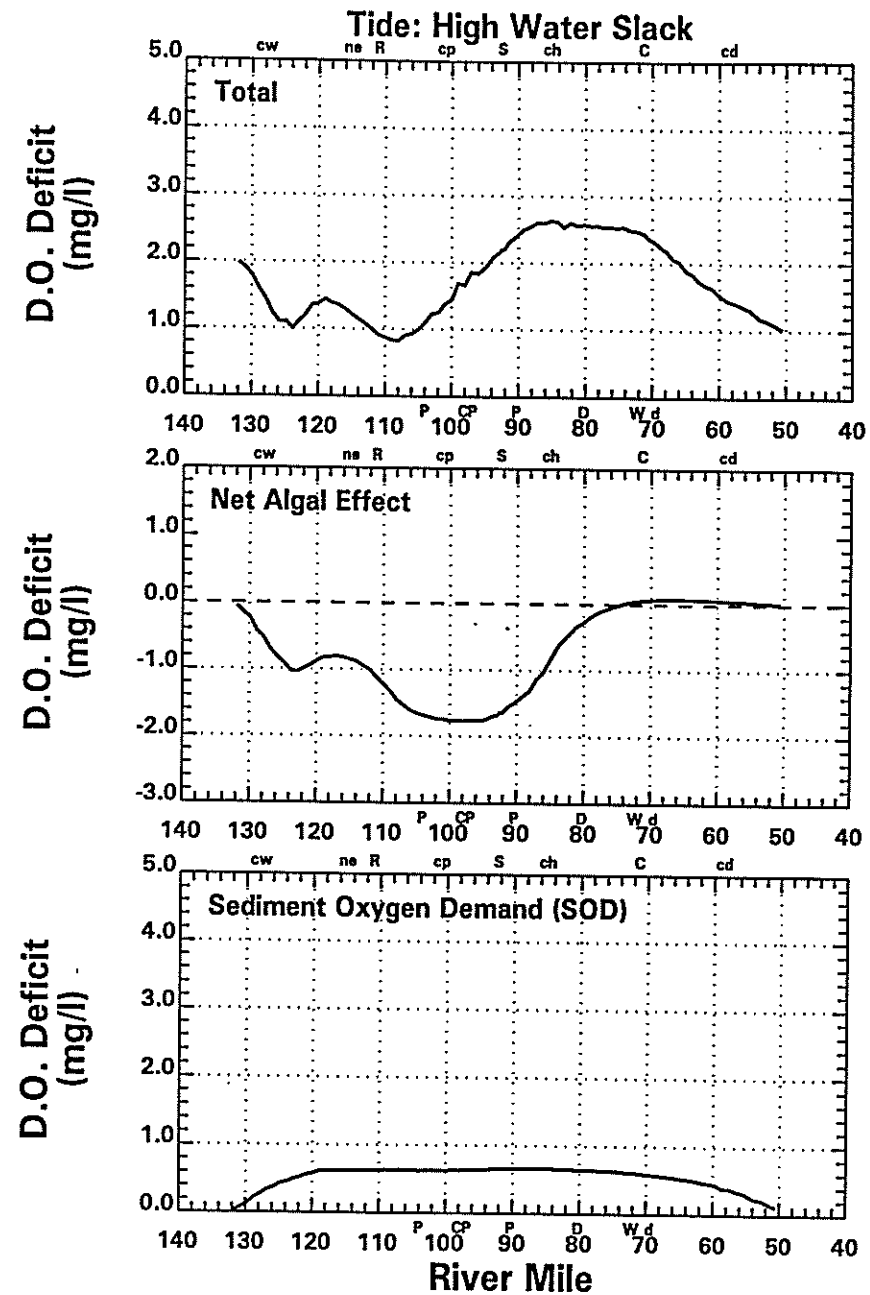
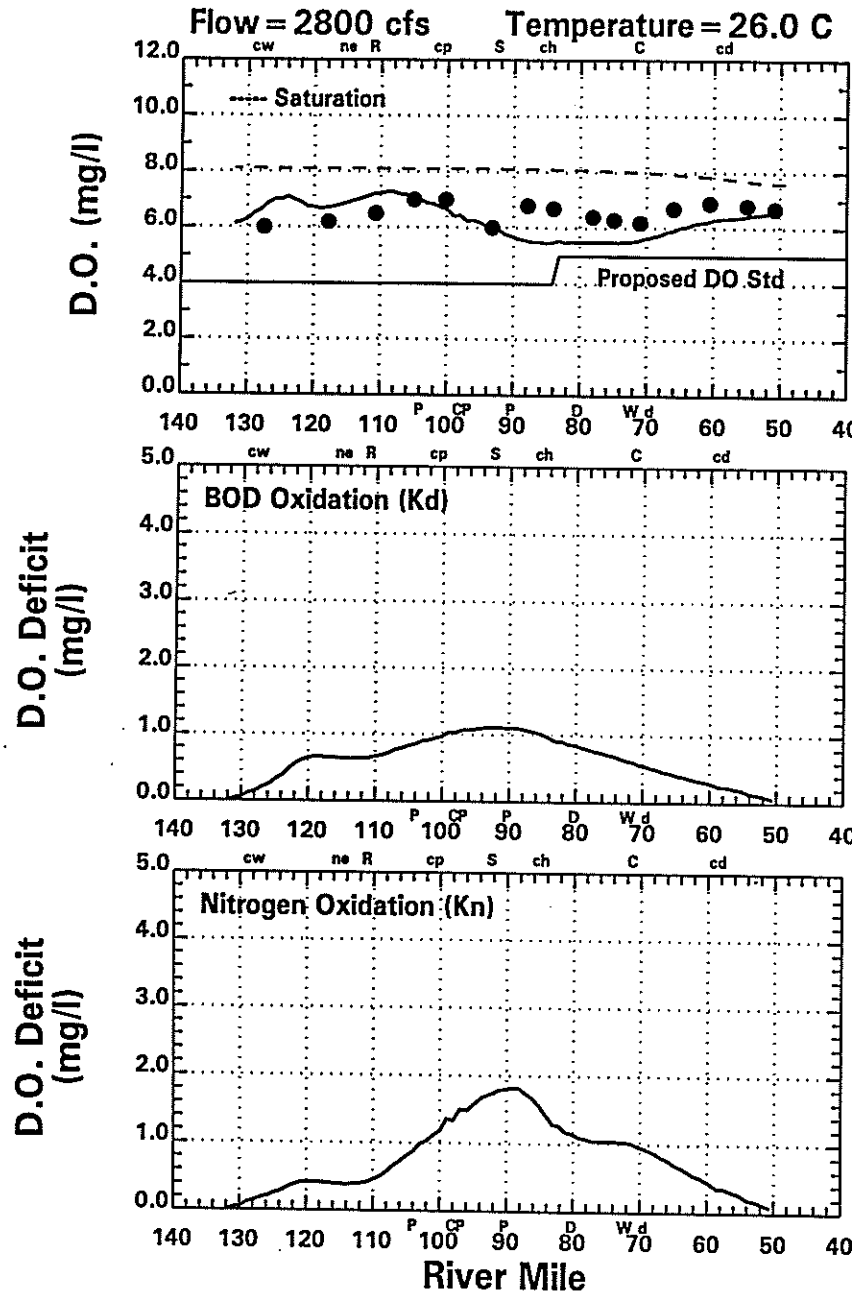
1995 Delaware River Data (●) & Model (—) (MP 48.2)
 [Daily Averages & Shaded Area = Range Over the Day]



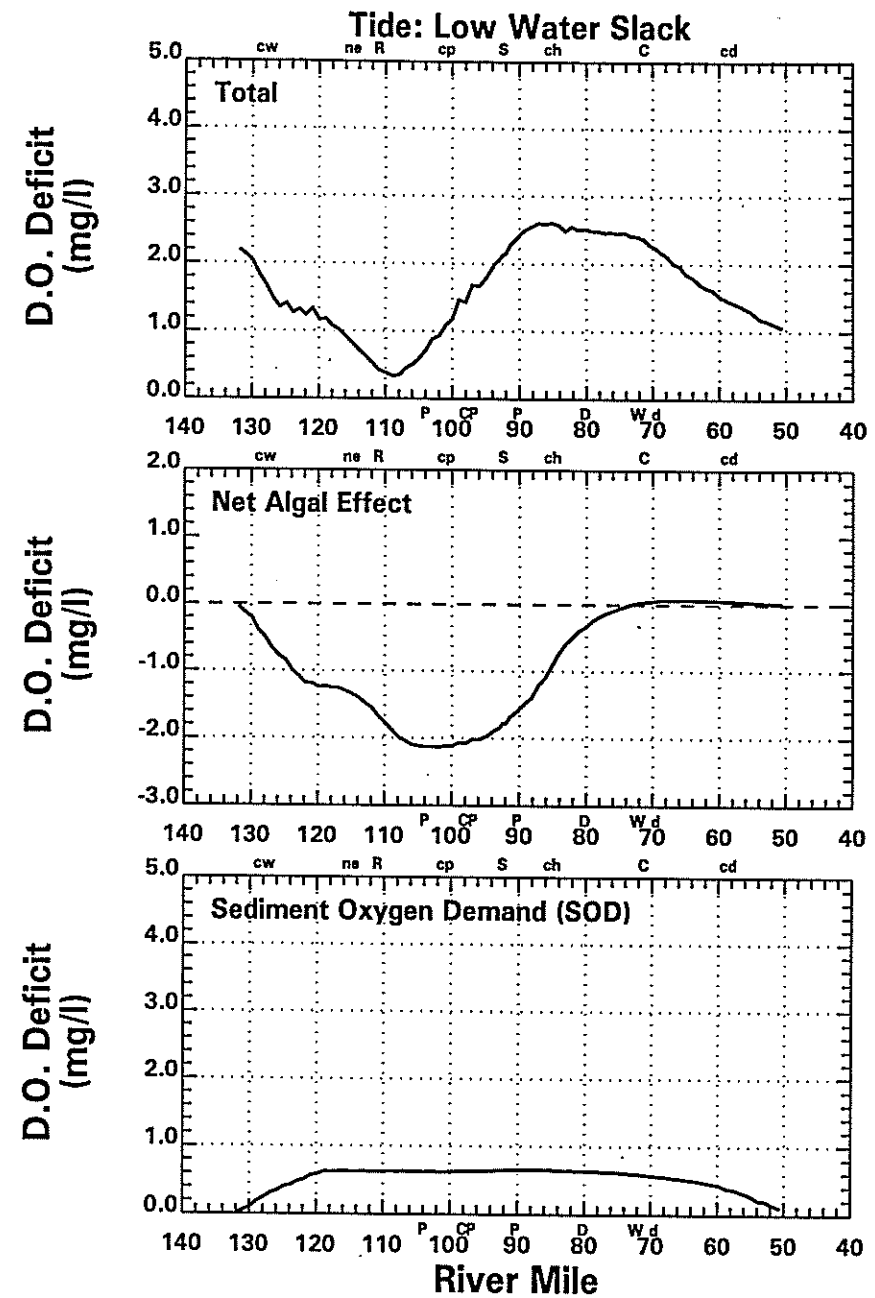
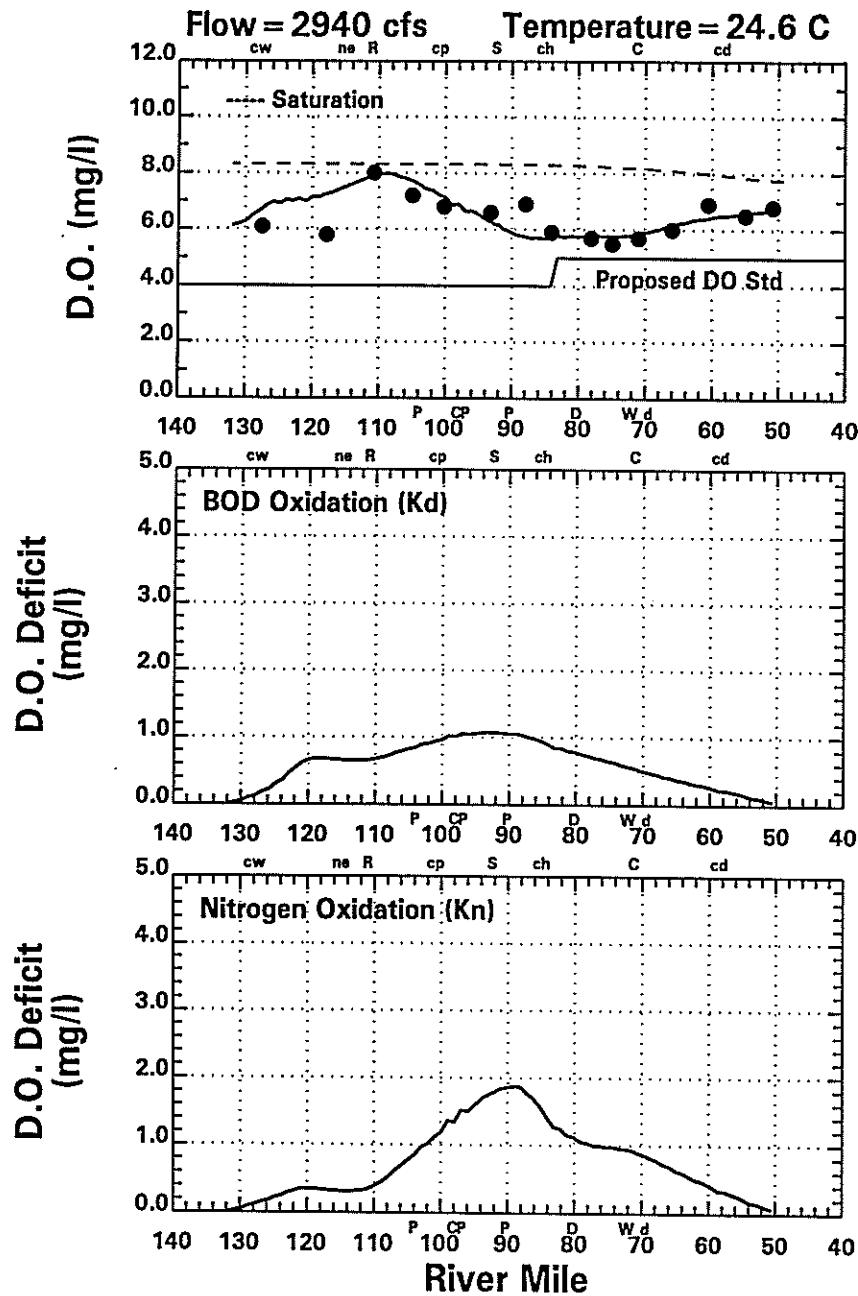
Delaware River Data (●) & Model (—) 7/25/95 (Model Day 8)
 [Temporally, Vertically and Laterally Averaged]



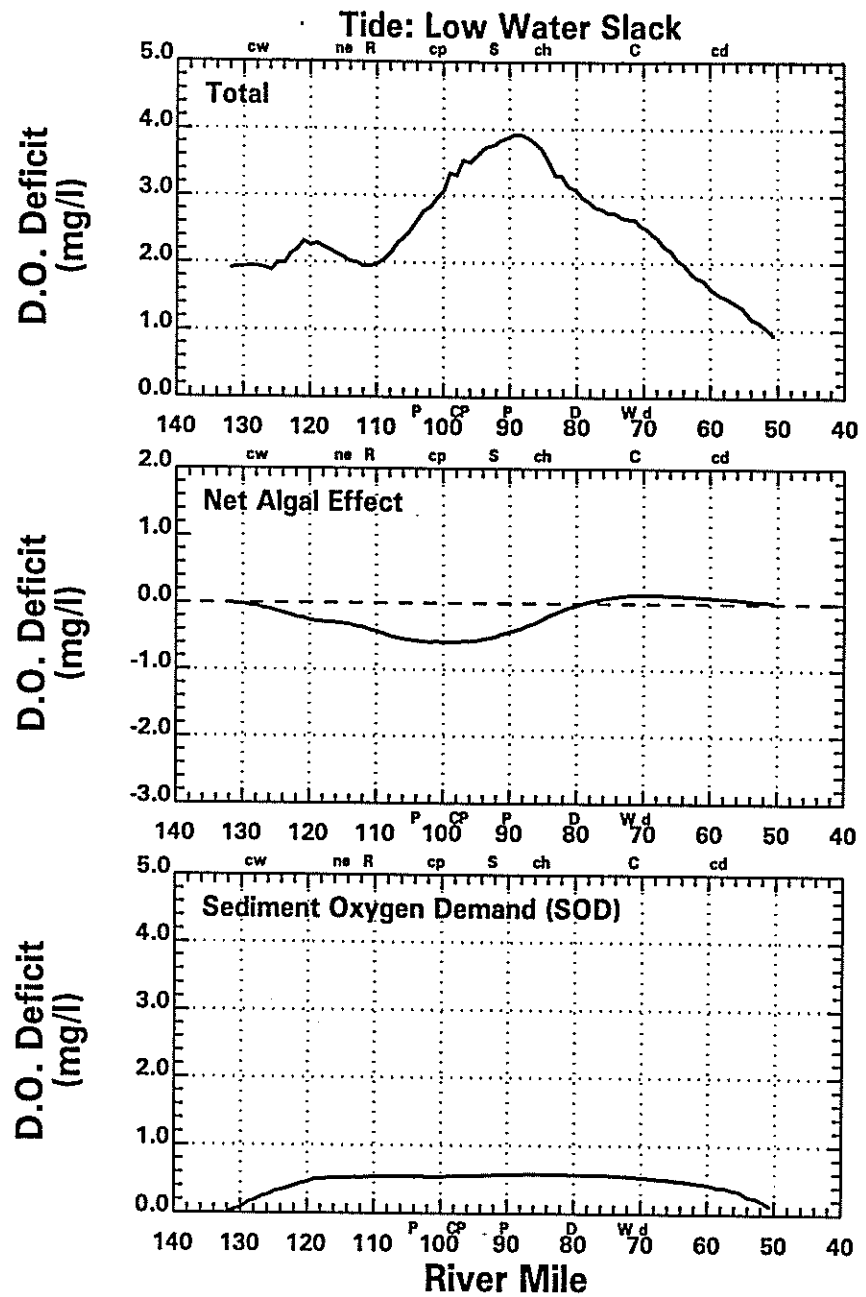
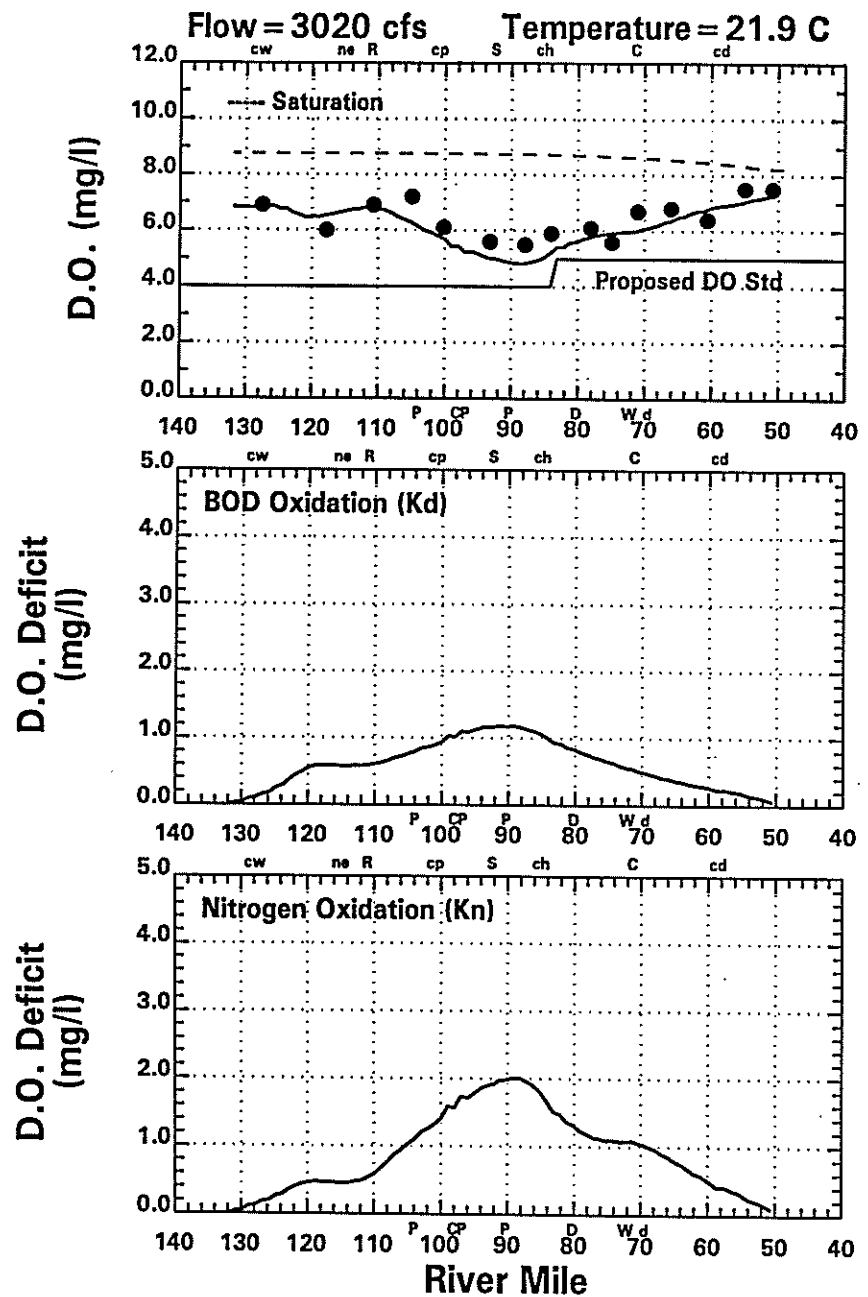
Delaware River Data (●) & Model (—) 8/8-9/95 (Model Day 23)
 [Temporally, Vertically and Laterally Averaged]



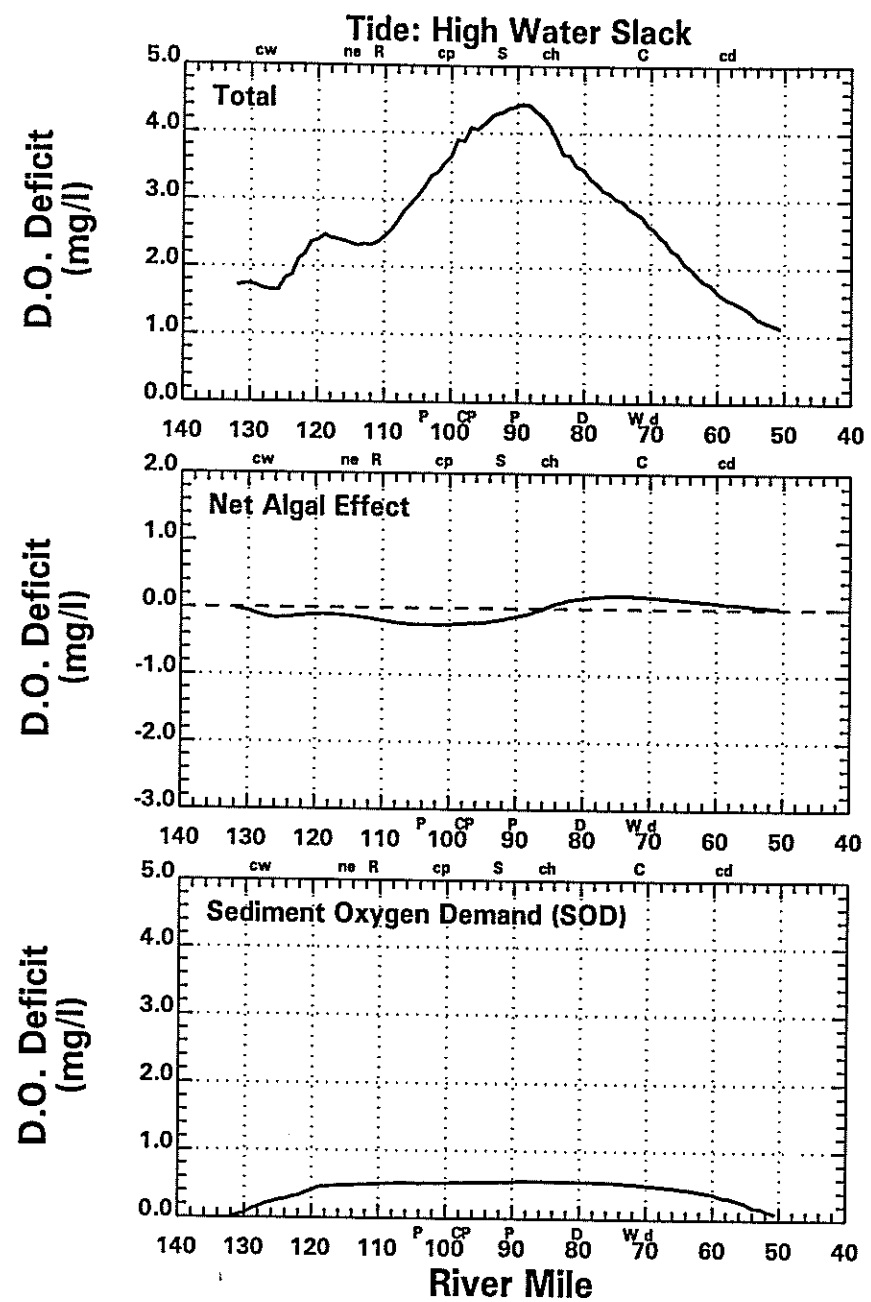
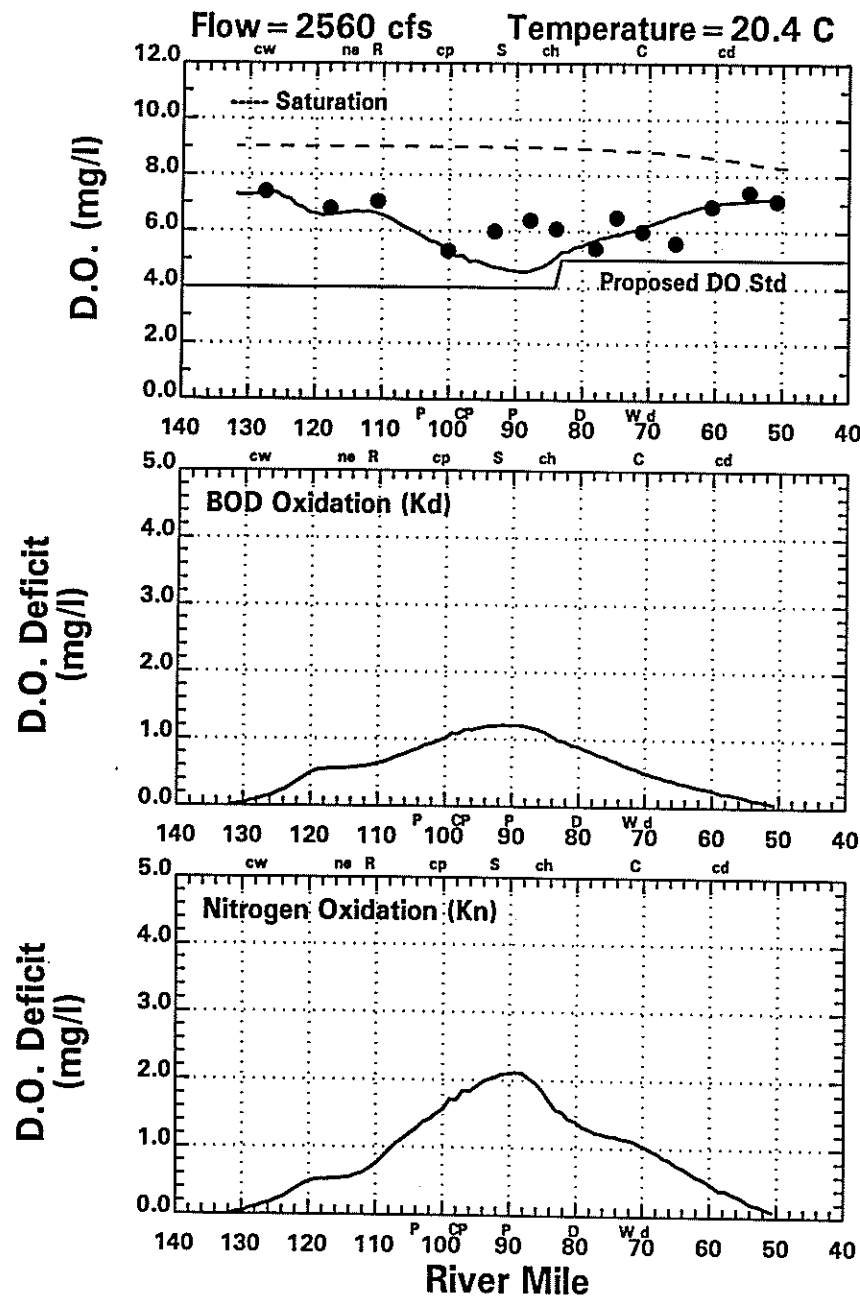
Delaware River Data (●) & Model (—) 8/29/95 (Model Day 43)
 [Temporally, Vertically and Laterally Averaged]



Delaware River Data (●) & Model (—) 9/5/95 (Model Day 50)
 [Temporally, Vertically and Laterally Averaged]

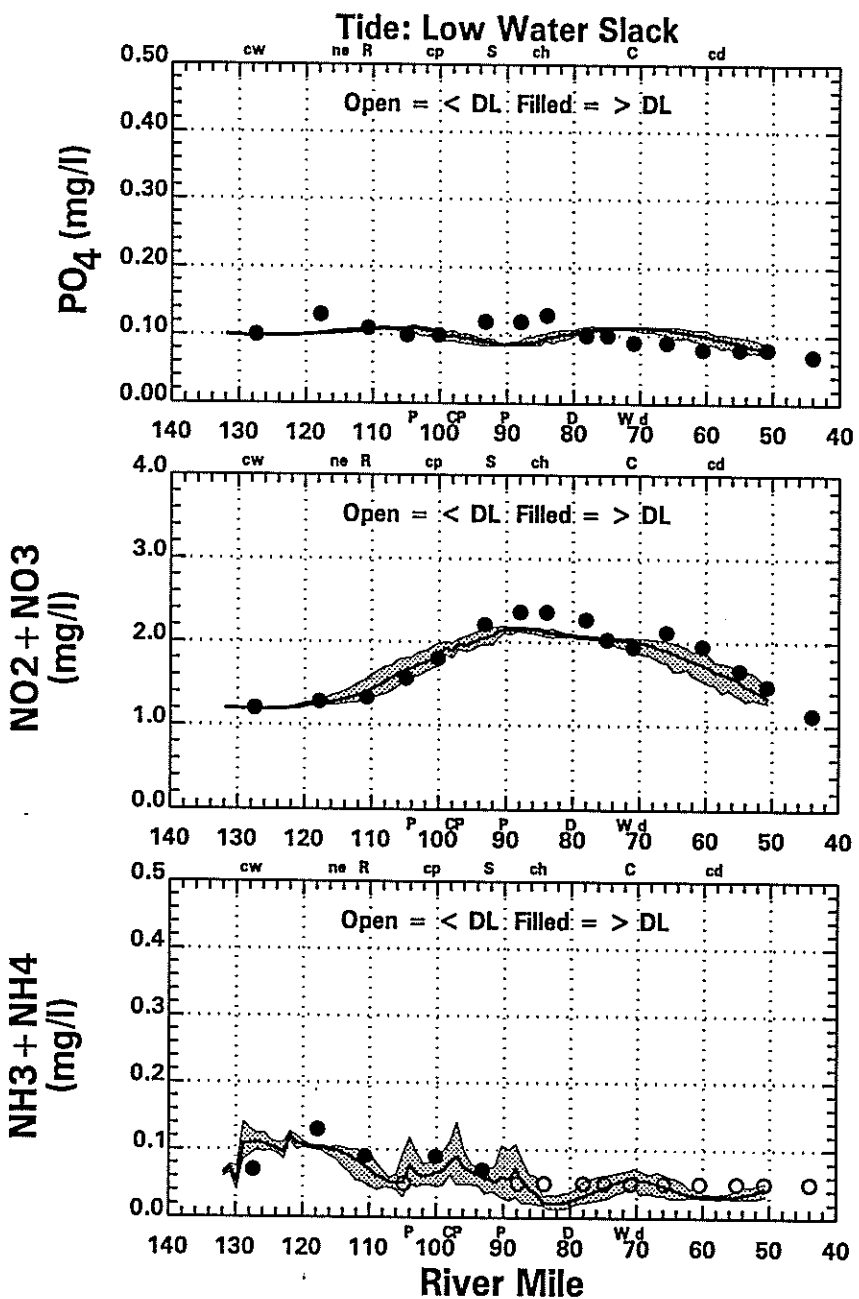
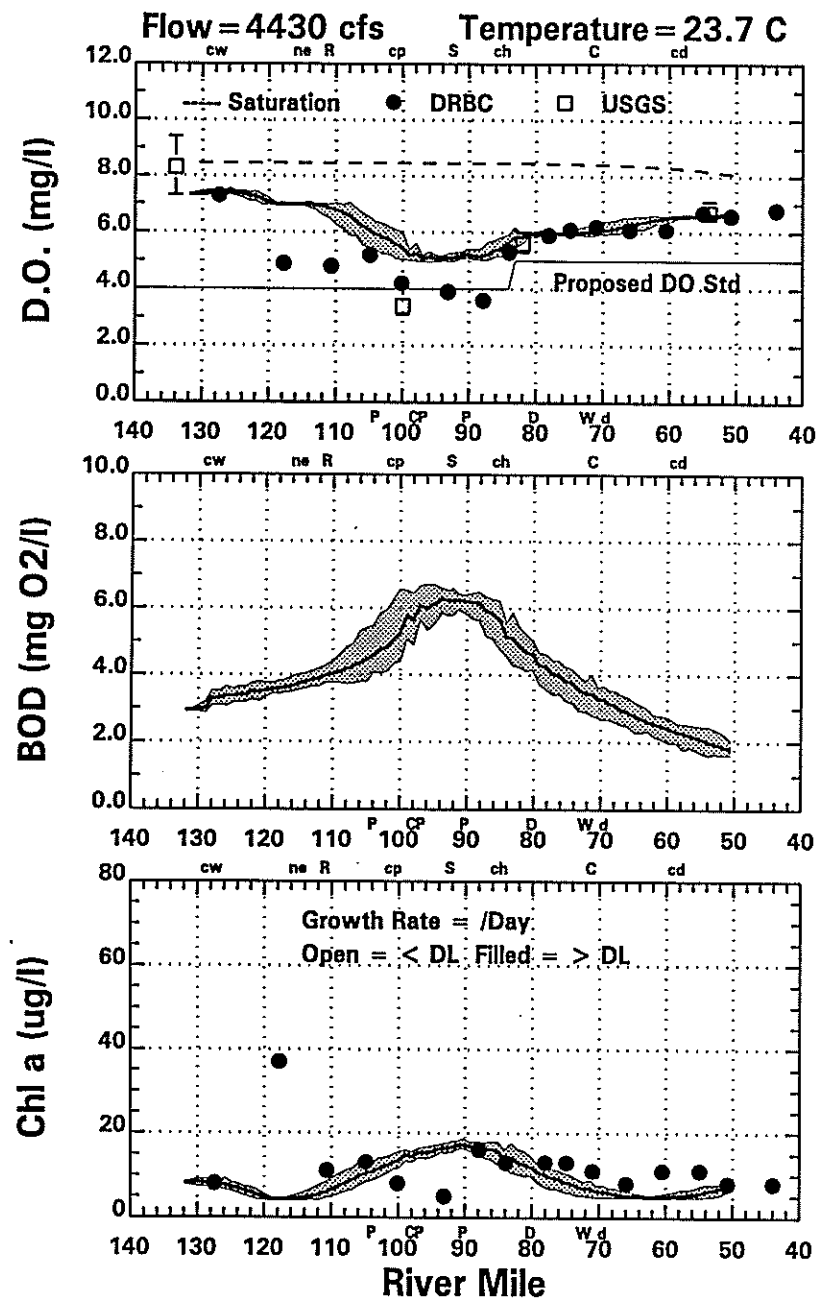


Delaware River Data (●) & Model (—) 9/25/95 (Model Day 70)
 [Temporally, Vertically and Laterally Averaged]

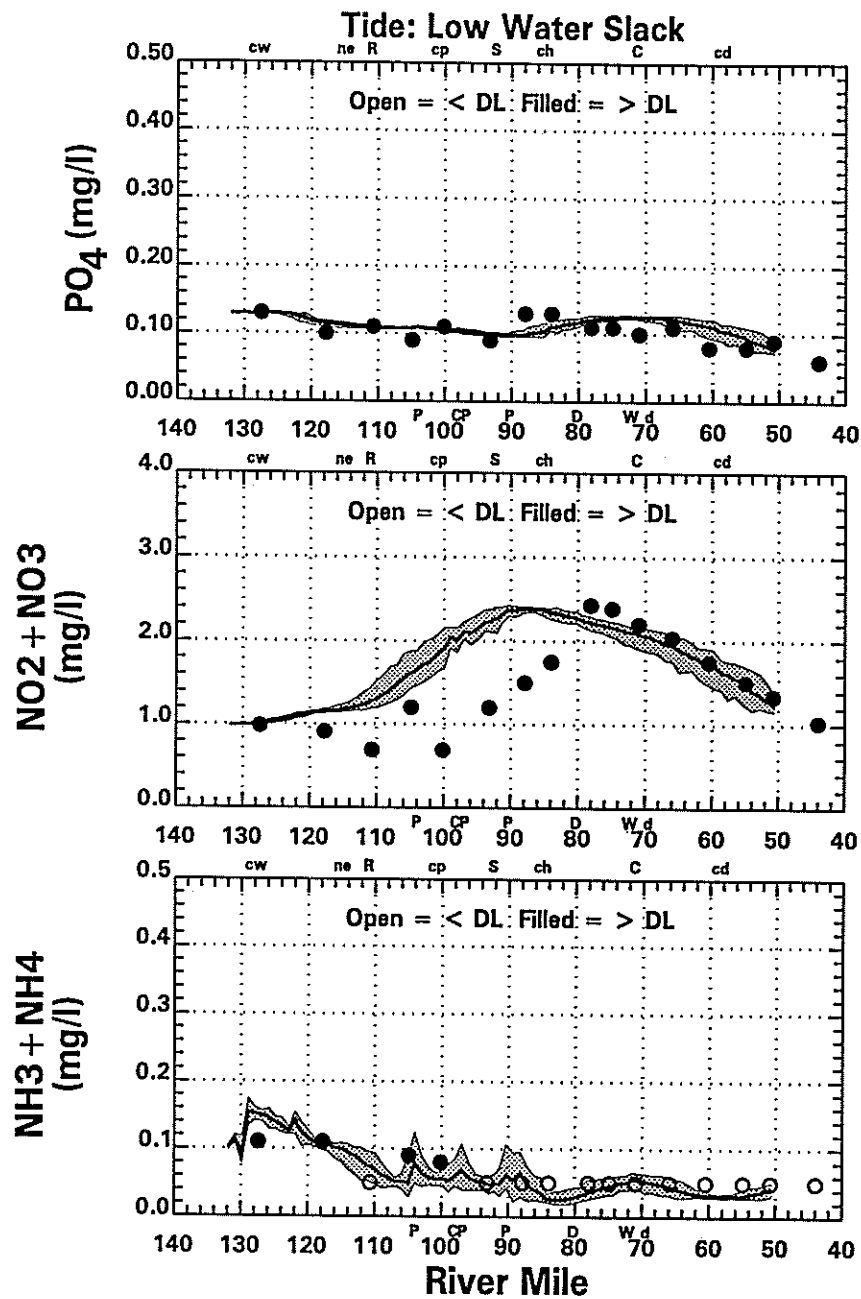
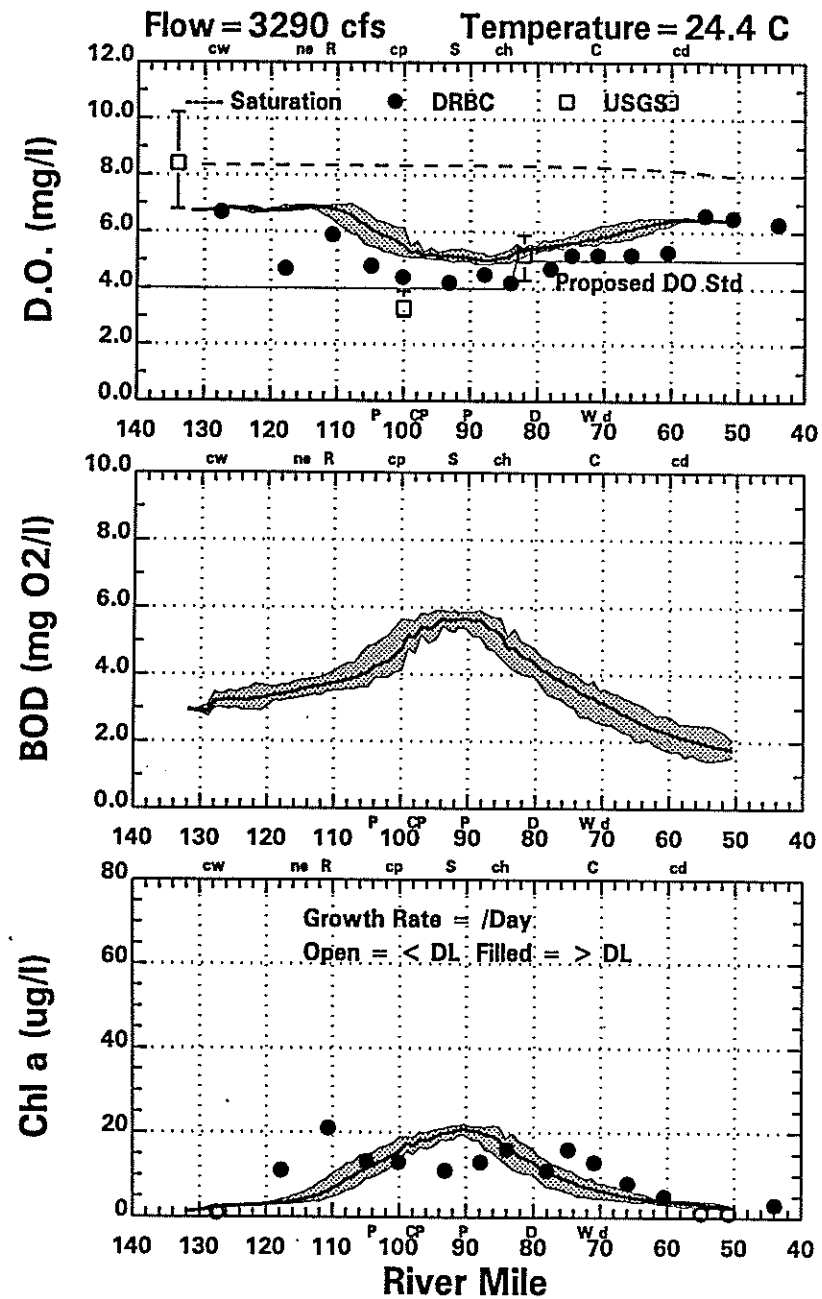


Delaware River Data (●) & Model (—) 10/2/95 (Model Day 77)
 [Temporally, Vertically and Laterally Averaged]

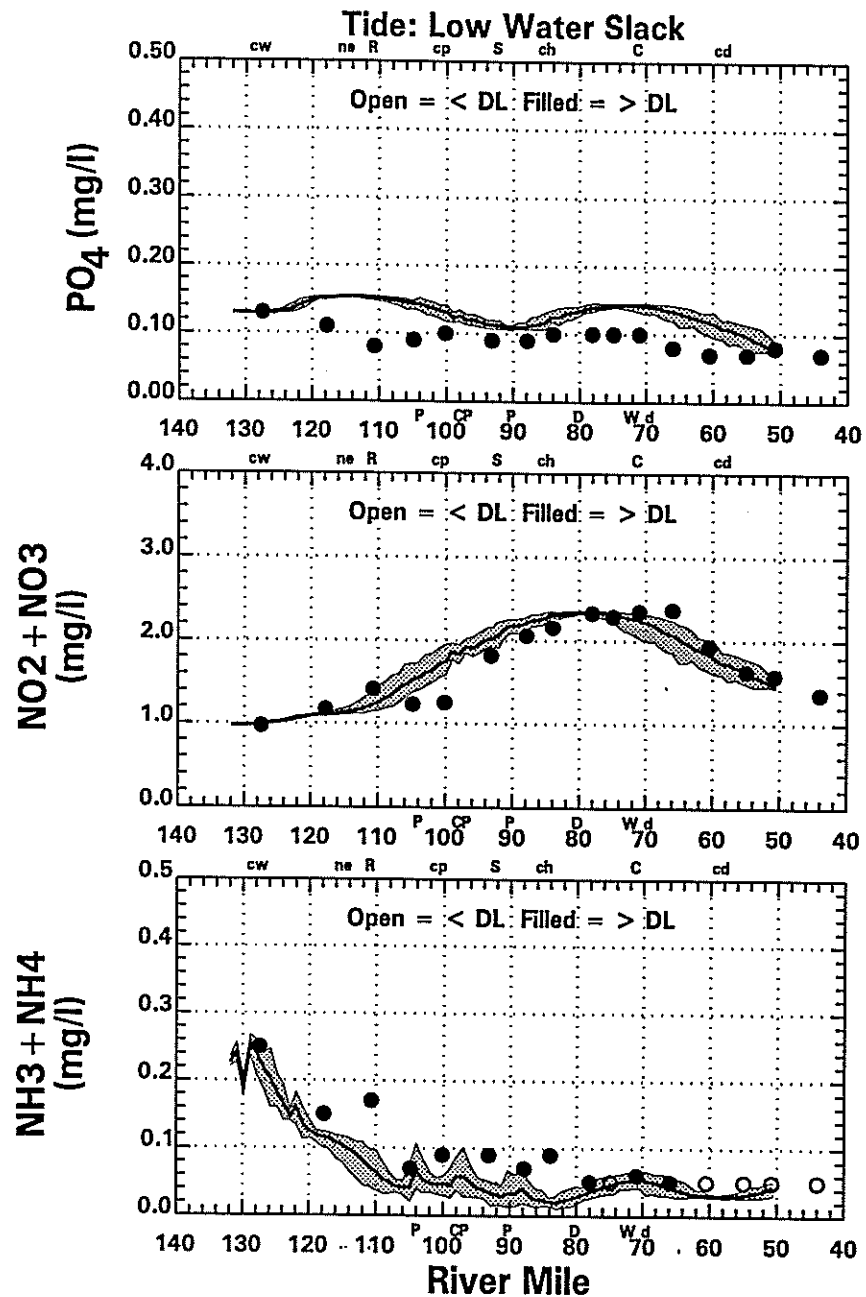
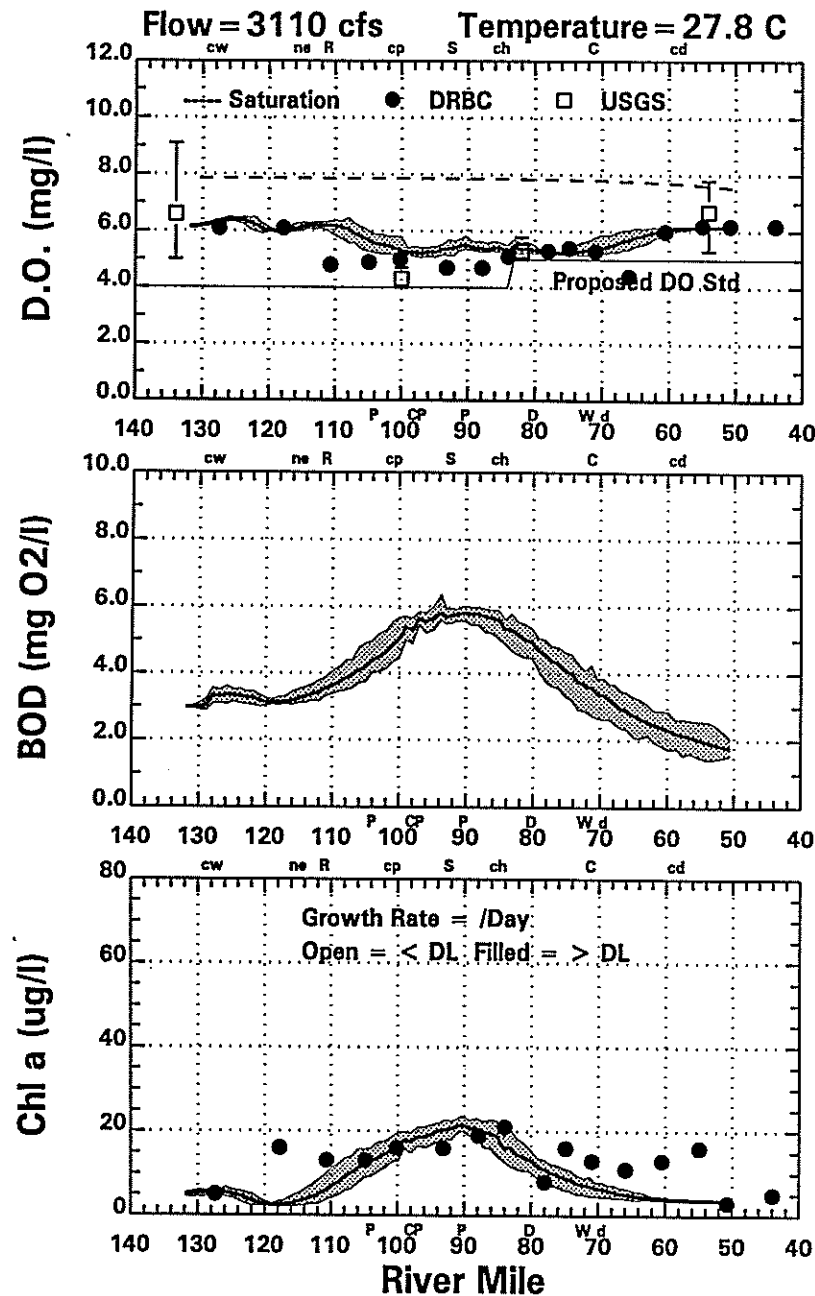
APPENDIX B-4
1991 Water Quality Model Runs



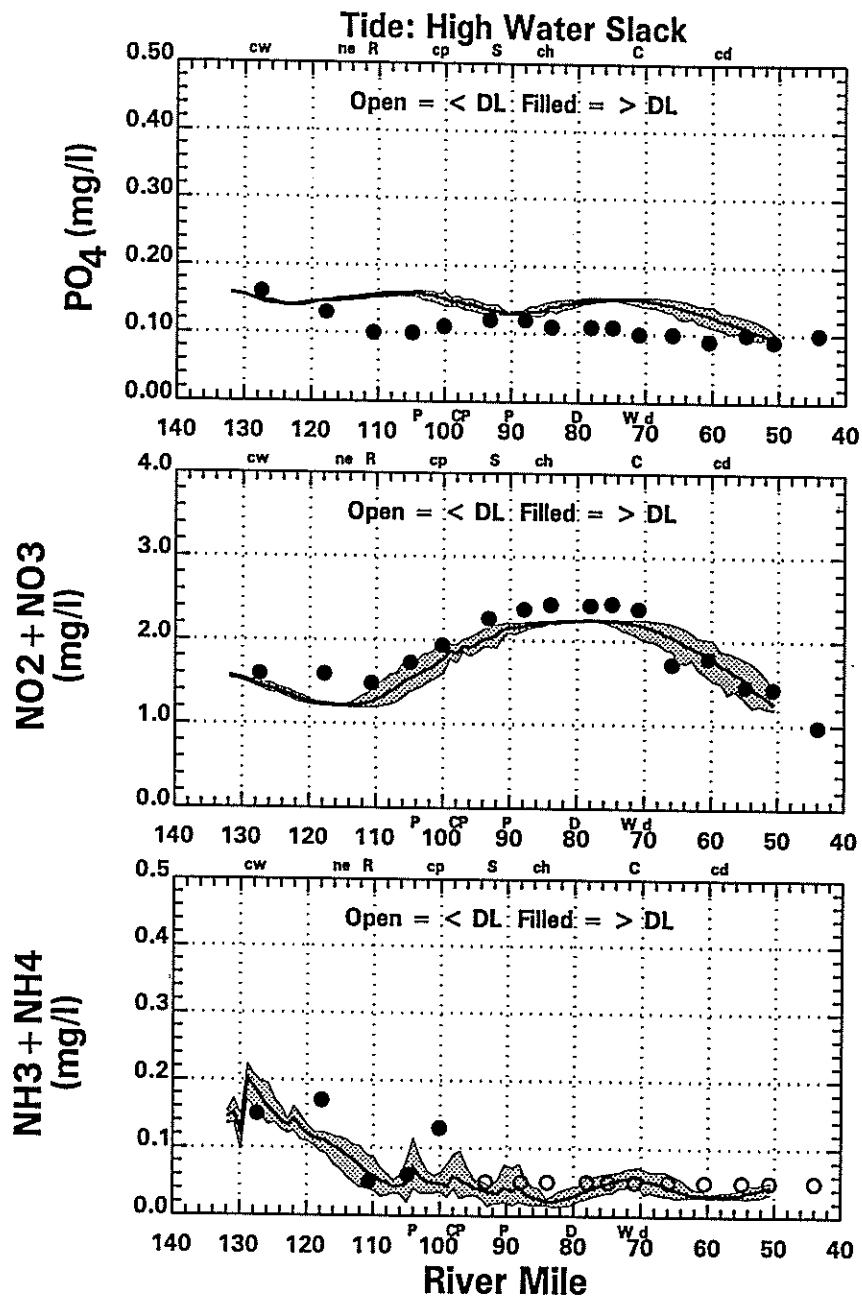
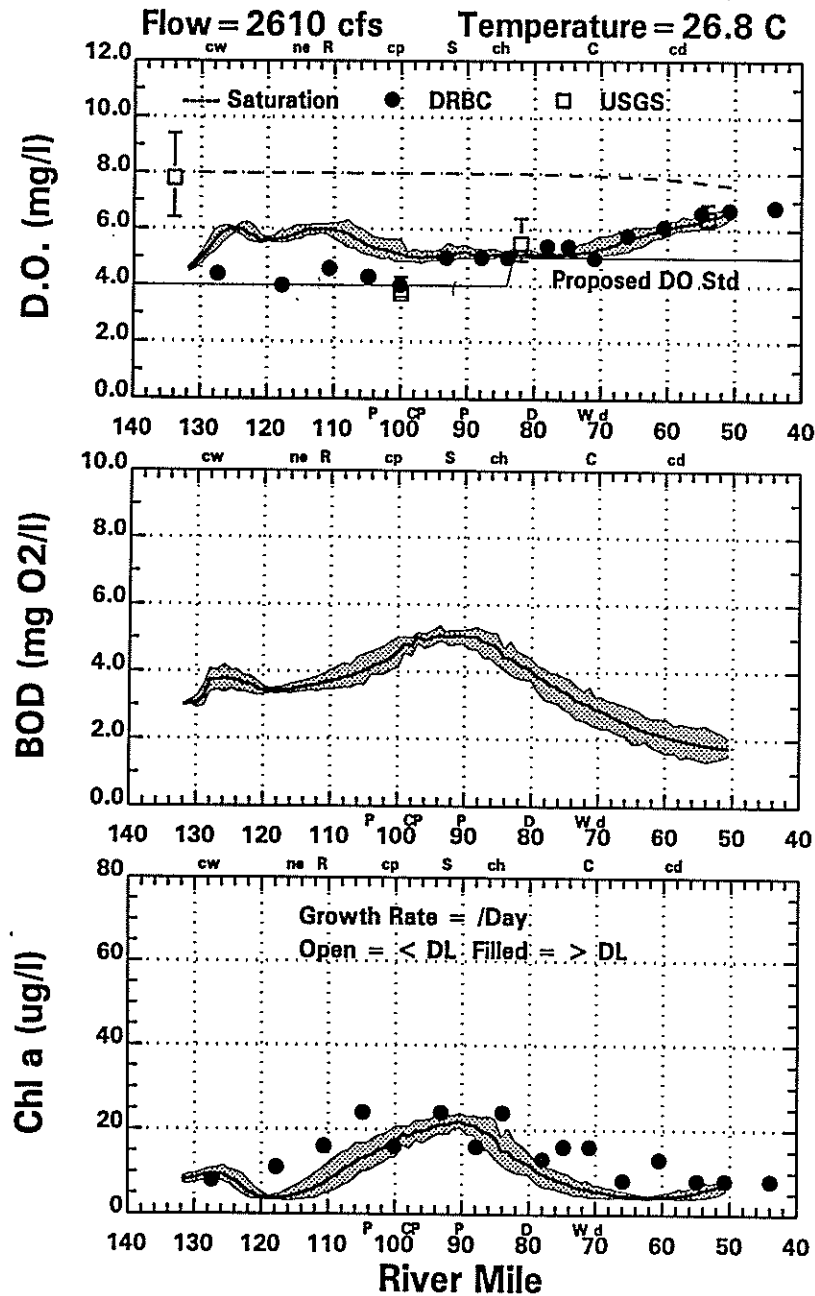
Delaware River Data (●) & Model (—) 6/25/91 (Model Day 15)
 [Daily Average & Shaded Area = Range over the Day]



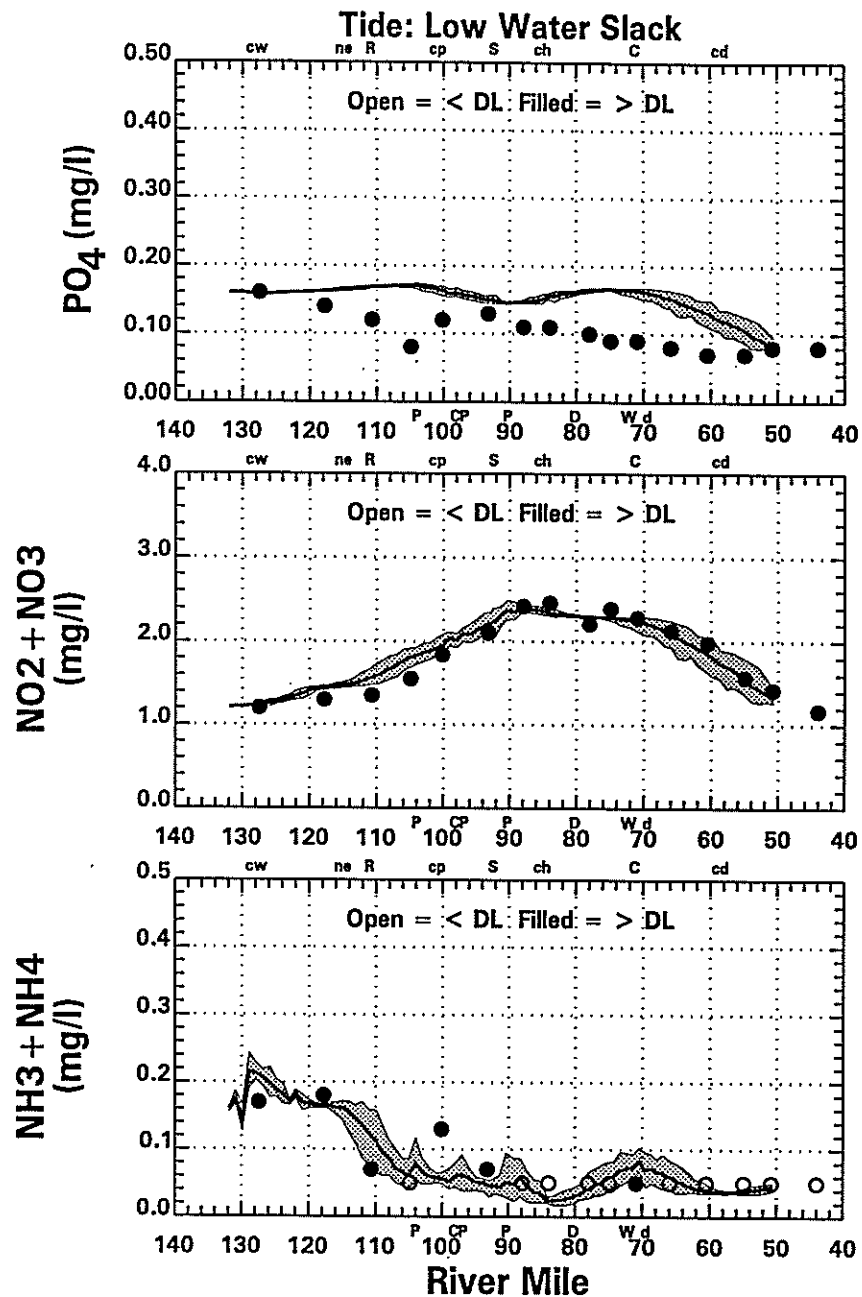
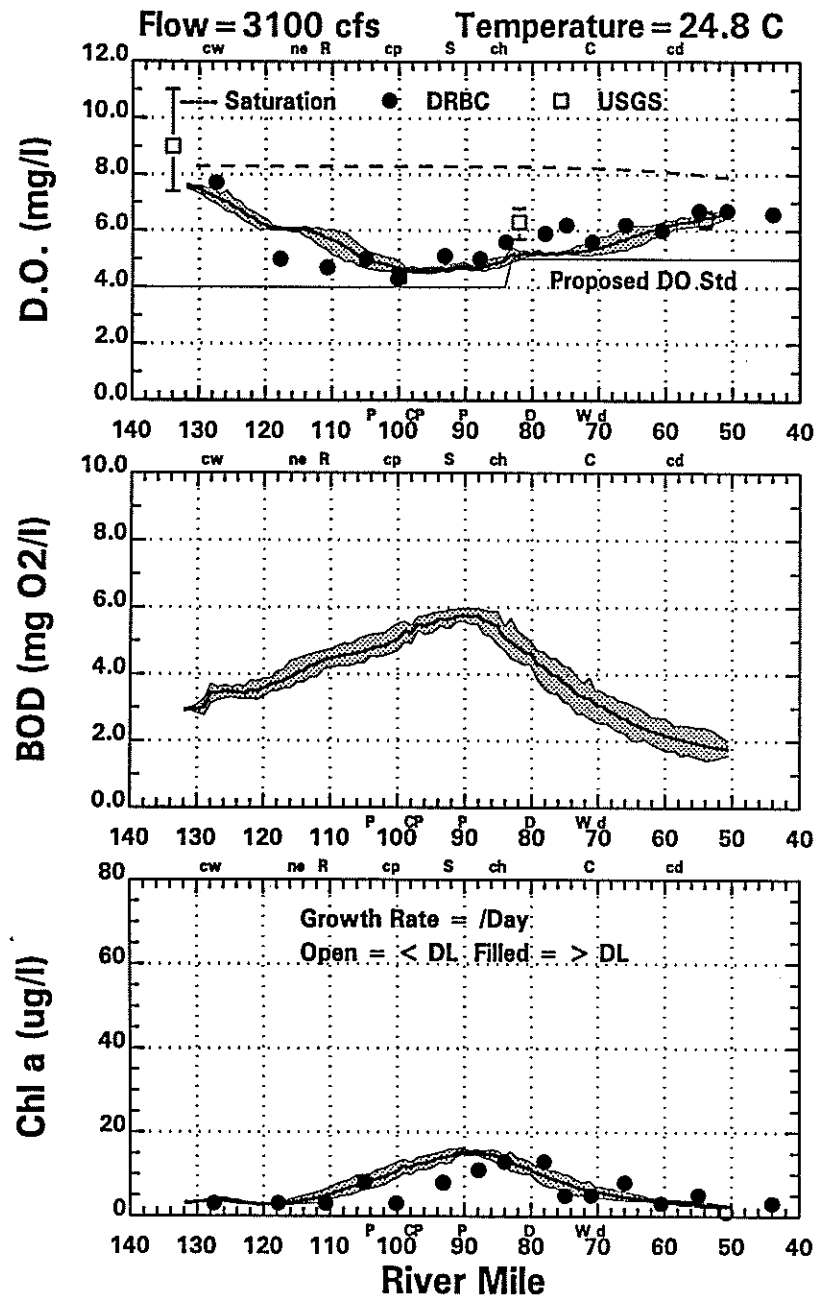
Delaware River Data (●) & Model (—) 7/10/91 (Model Day 30)
 [Daily Average & Shaded Area = Range over the Day]



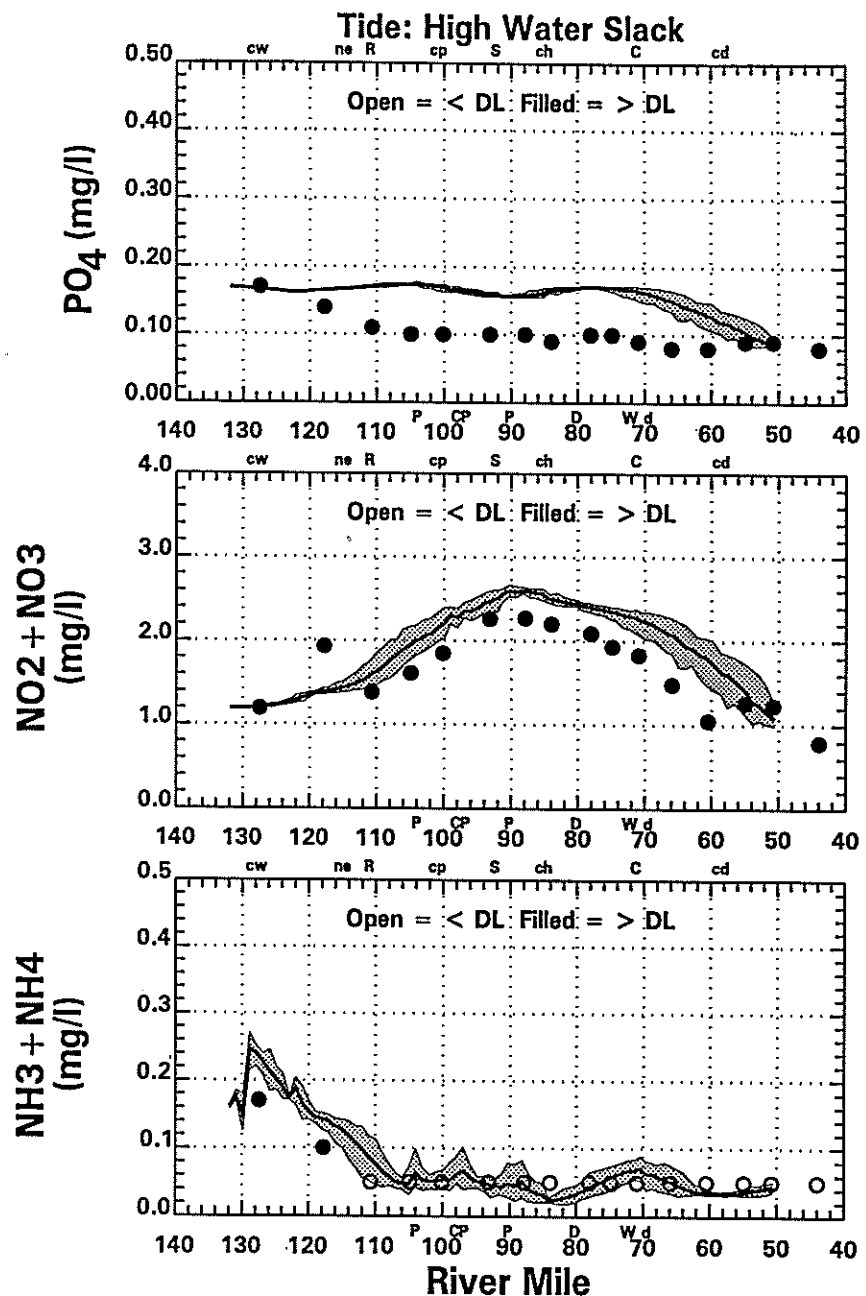
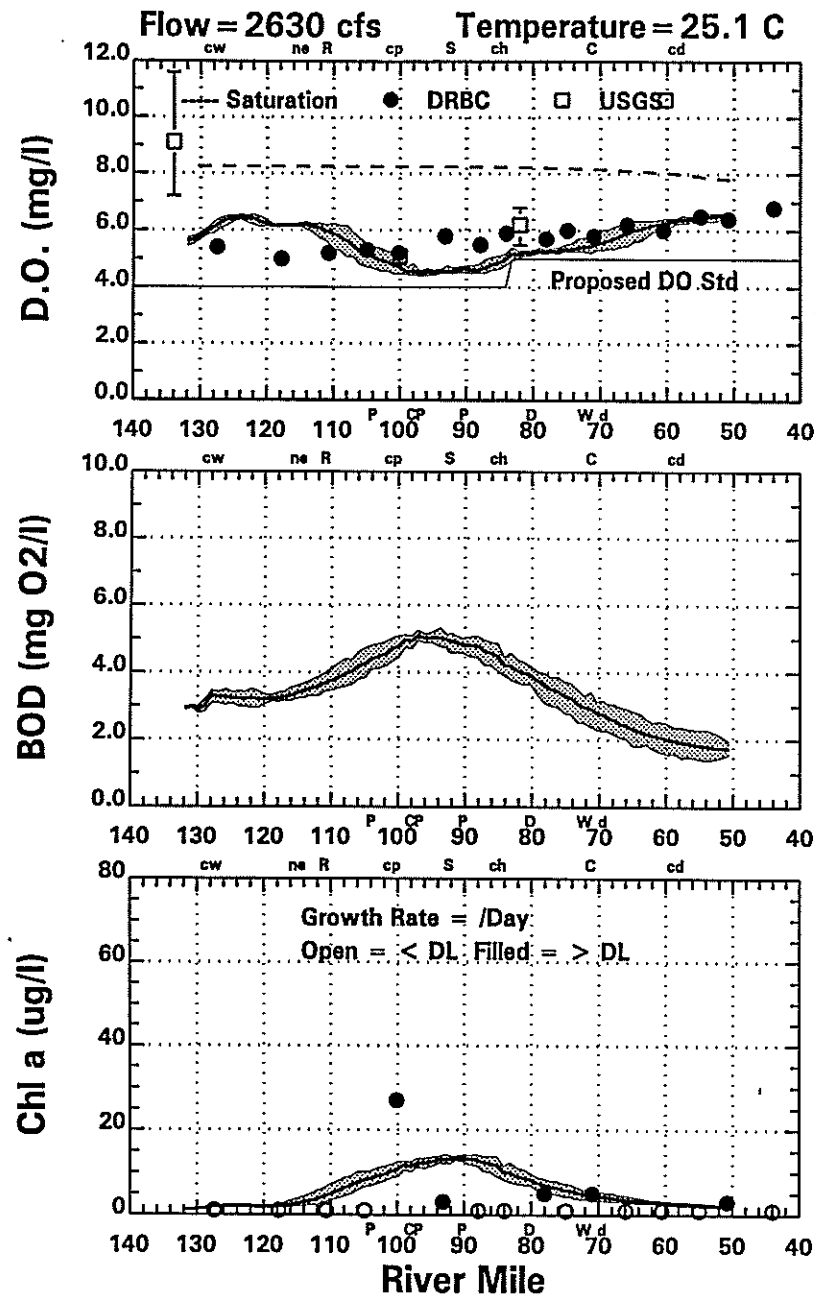
Delaware River Data (●) & Model (—) 7/23/91 (Model Day 43)
 [Daily Average & Shaded Area=Range over the Day]



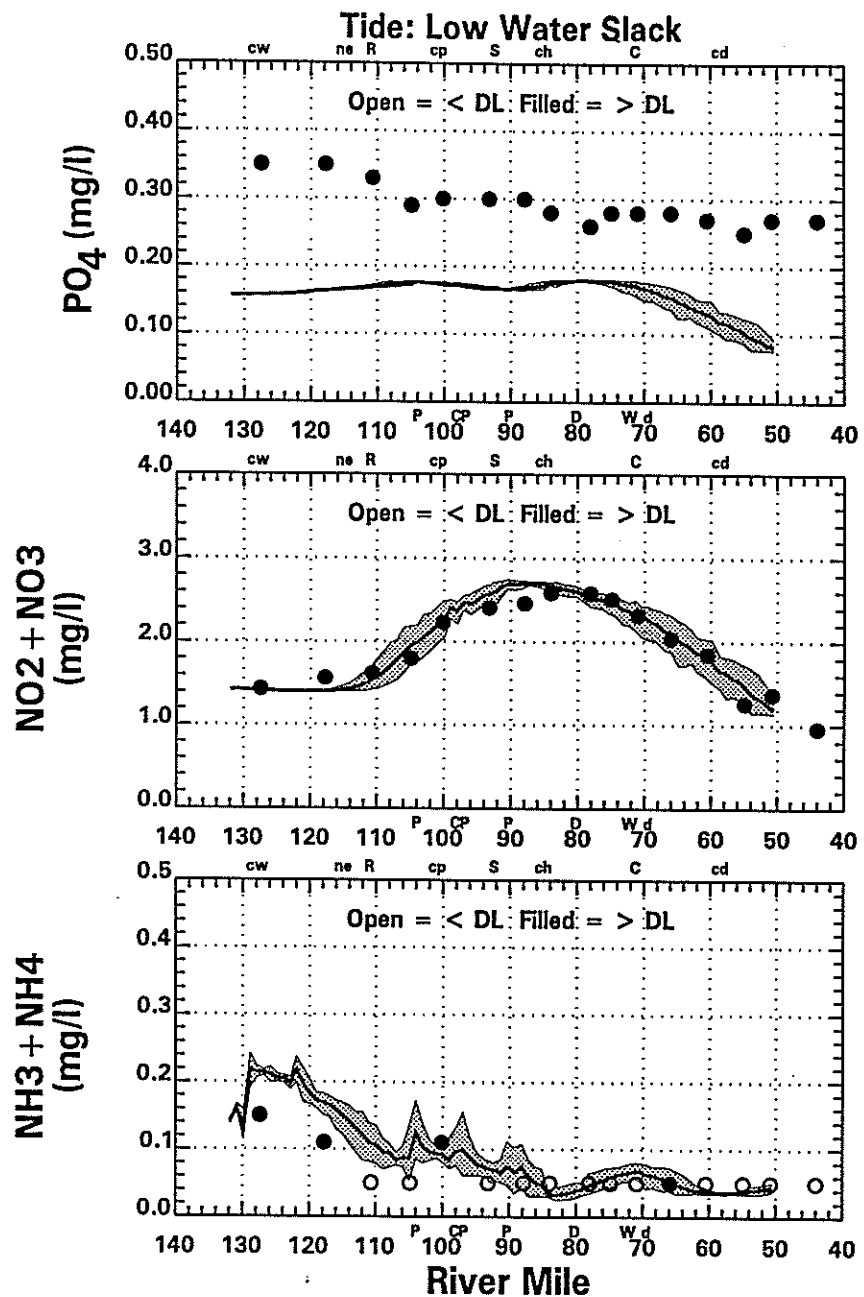
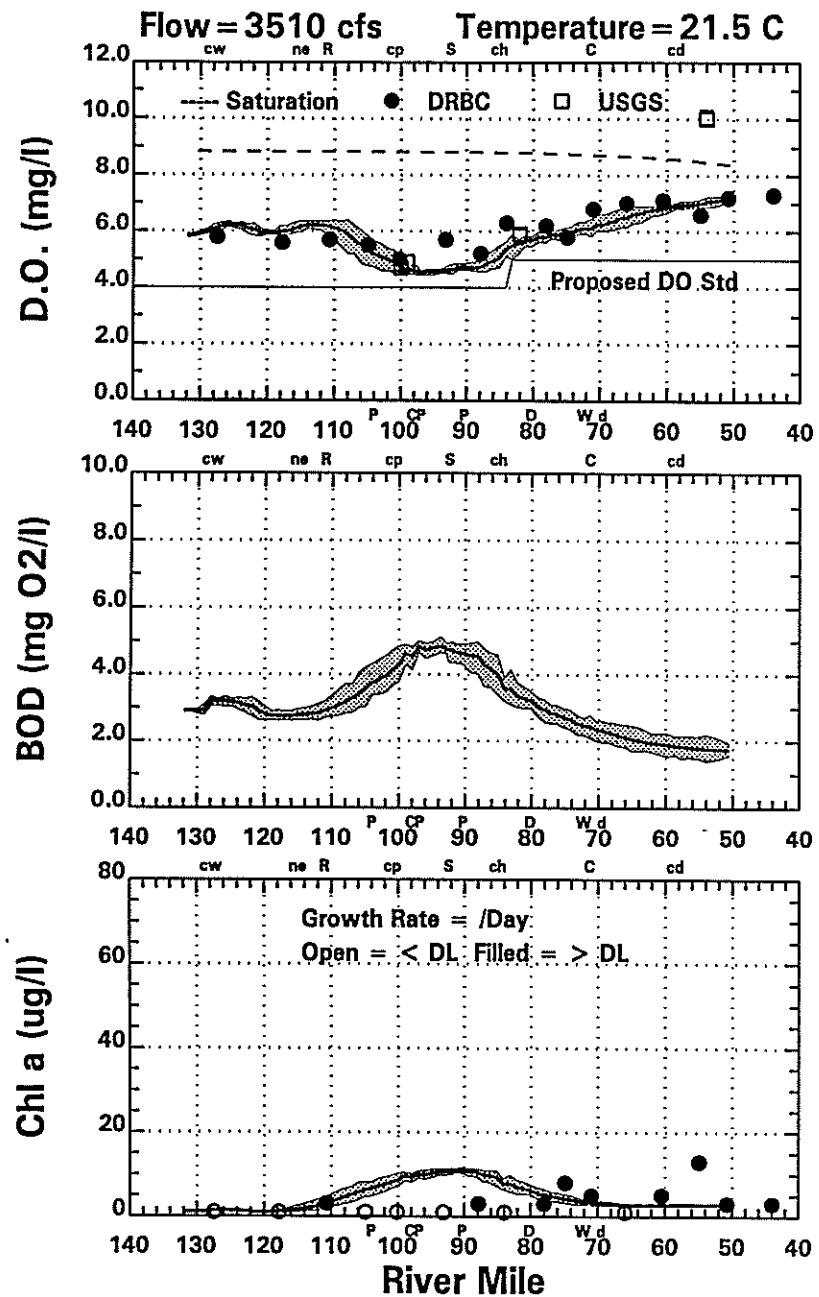
Delaware River Data (●) & Model (—) 8/5/91 (Model Day 56)
 [Daily Average & Shaded Area=Range over the Day]



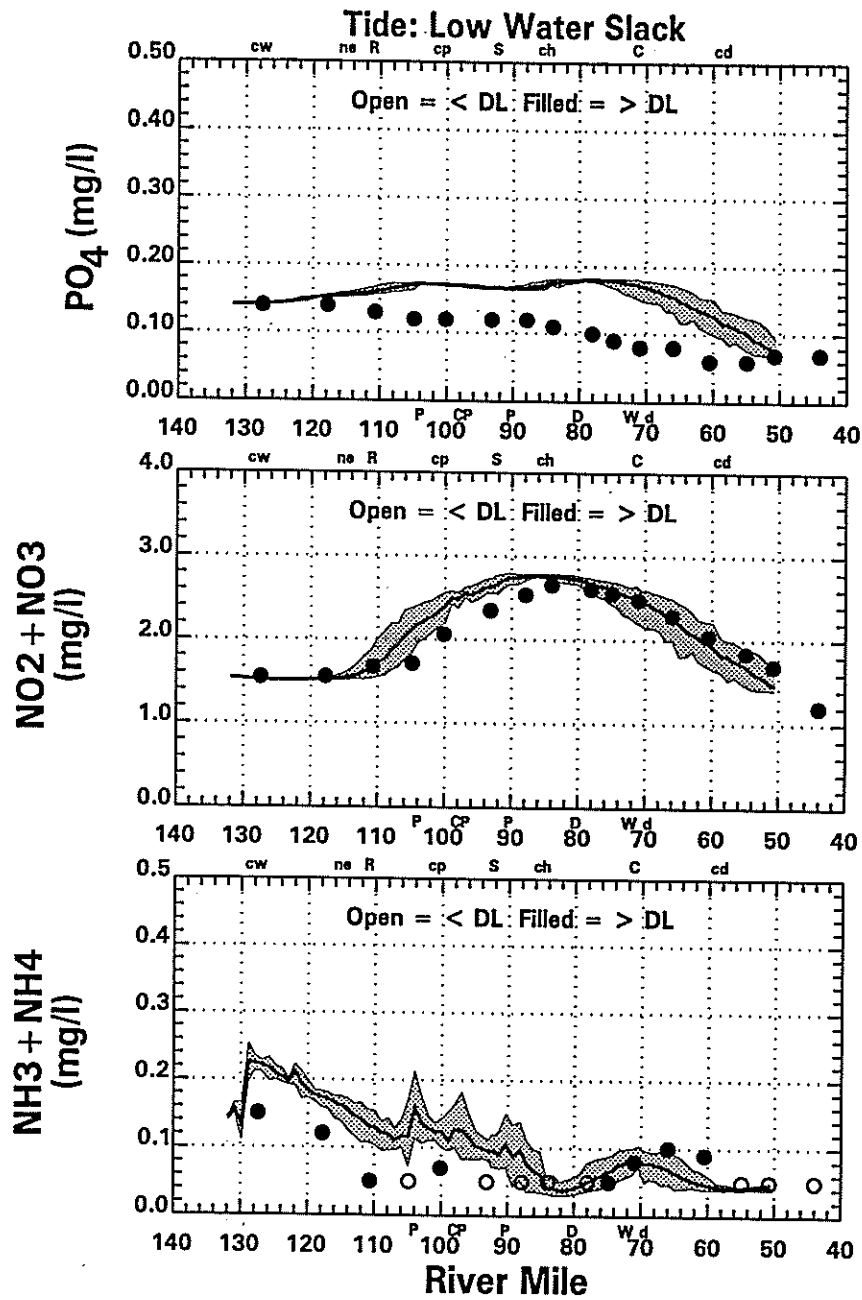
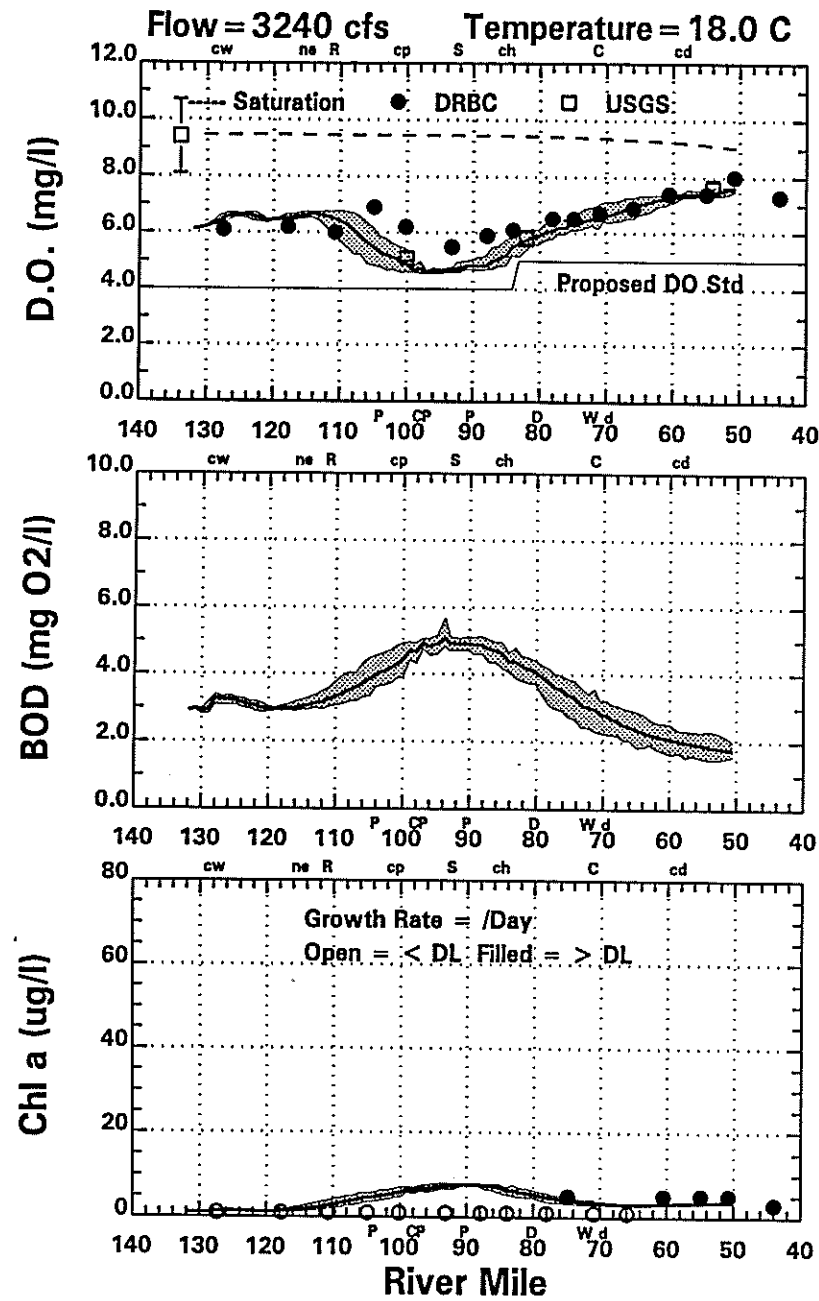
Delaware River Data (●) & Model (—) 8/26/91 (Model Day 77)
[Daily Average & Shaded Area=Range over the Day]



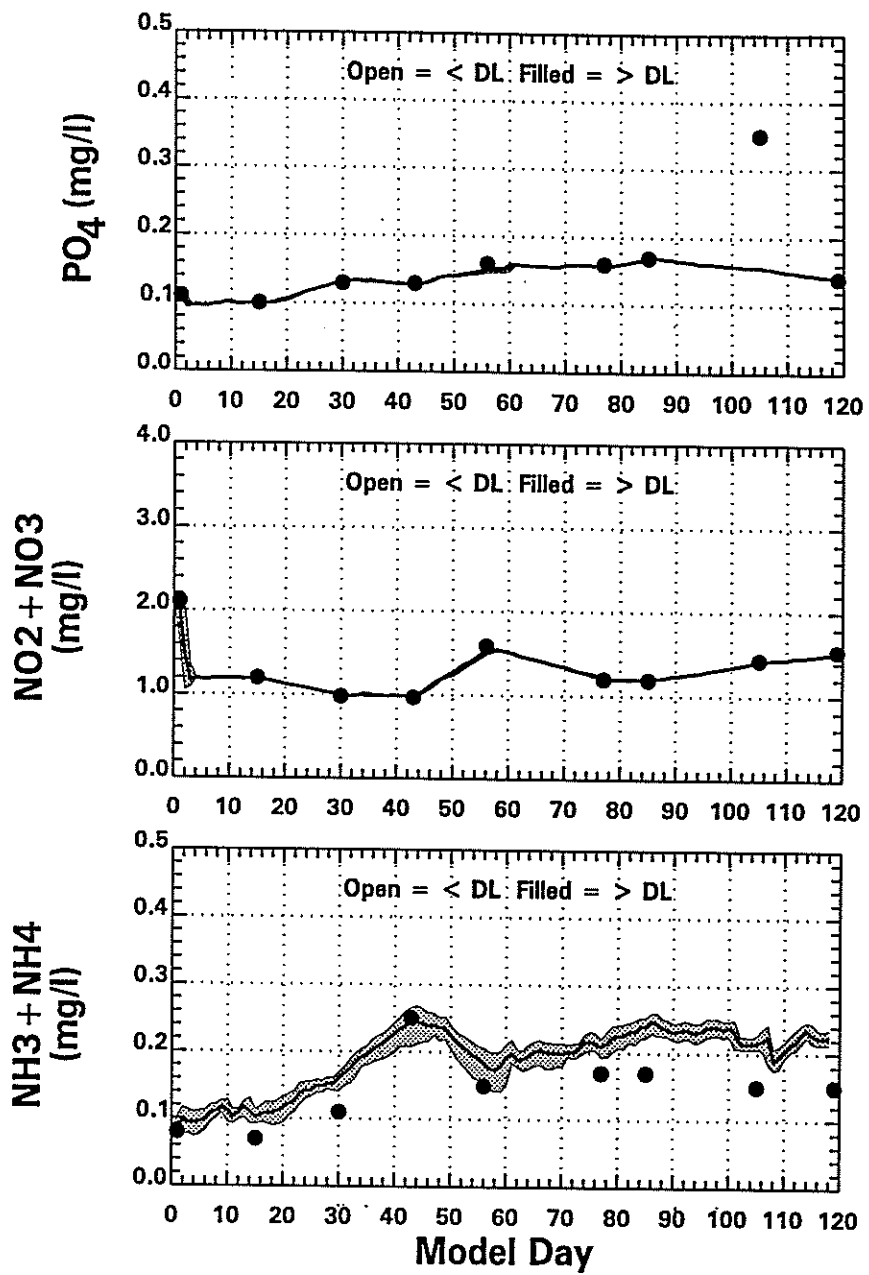
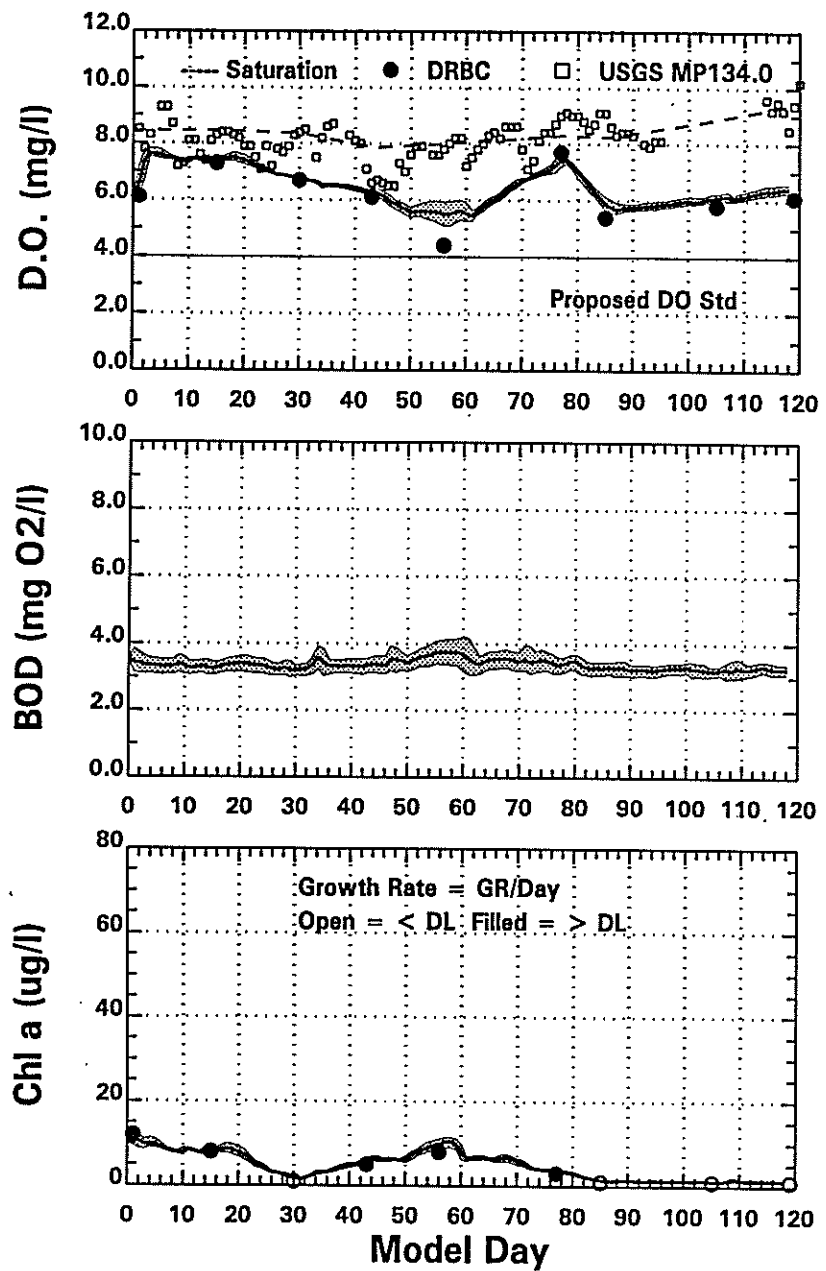
Delaware River Data (●) & Model (—) 9/3/91 (Model Day 85)
 [Daily Average & Shaded Area = Range over the Day]



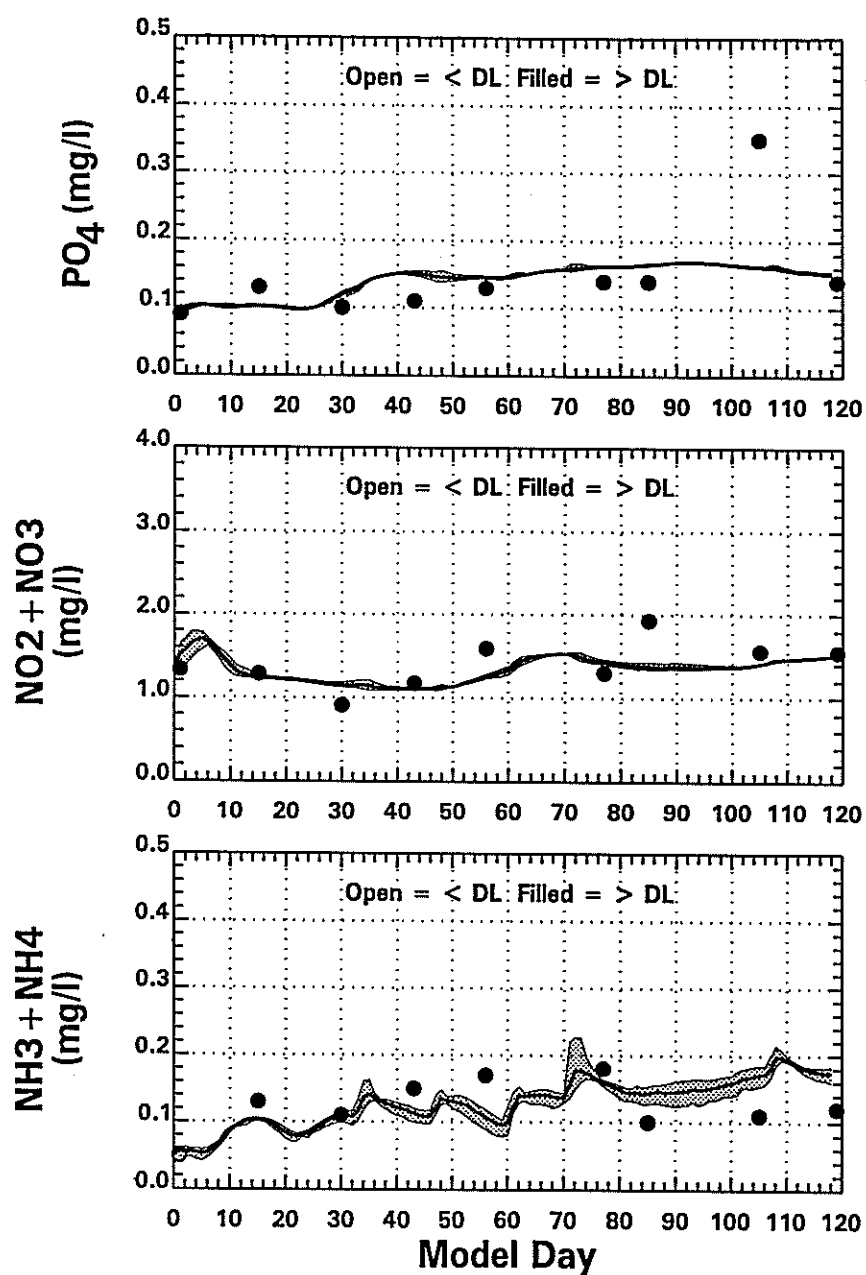
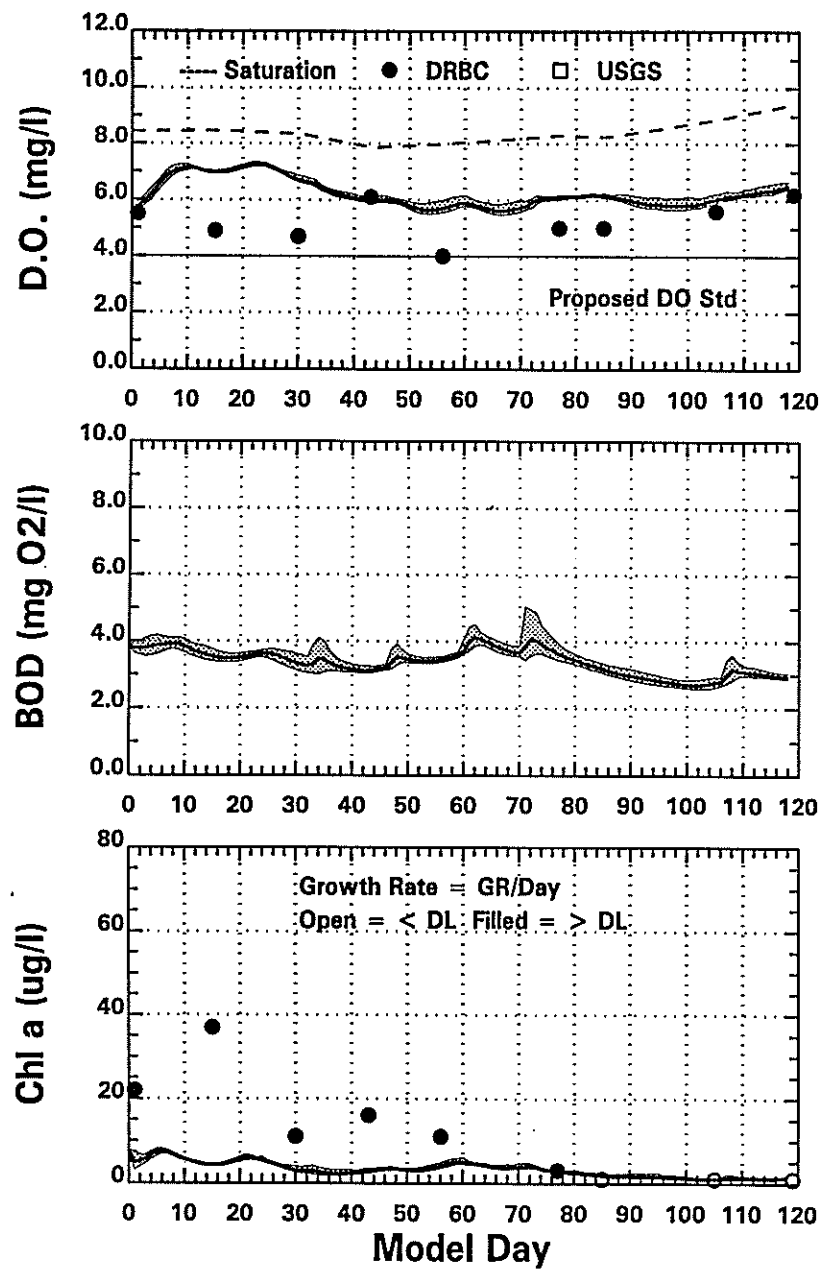
Delaware River Data (●) & Model (—) 9/23/91 (Model Day 105)
 [Daily Average & Shaded Area = Range over the Day]



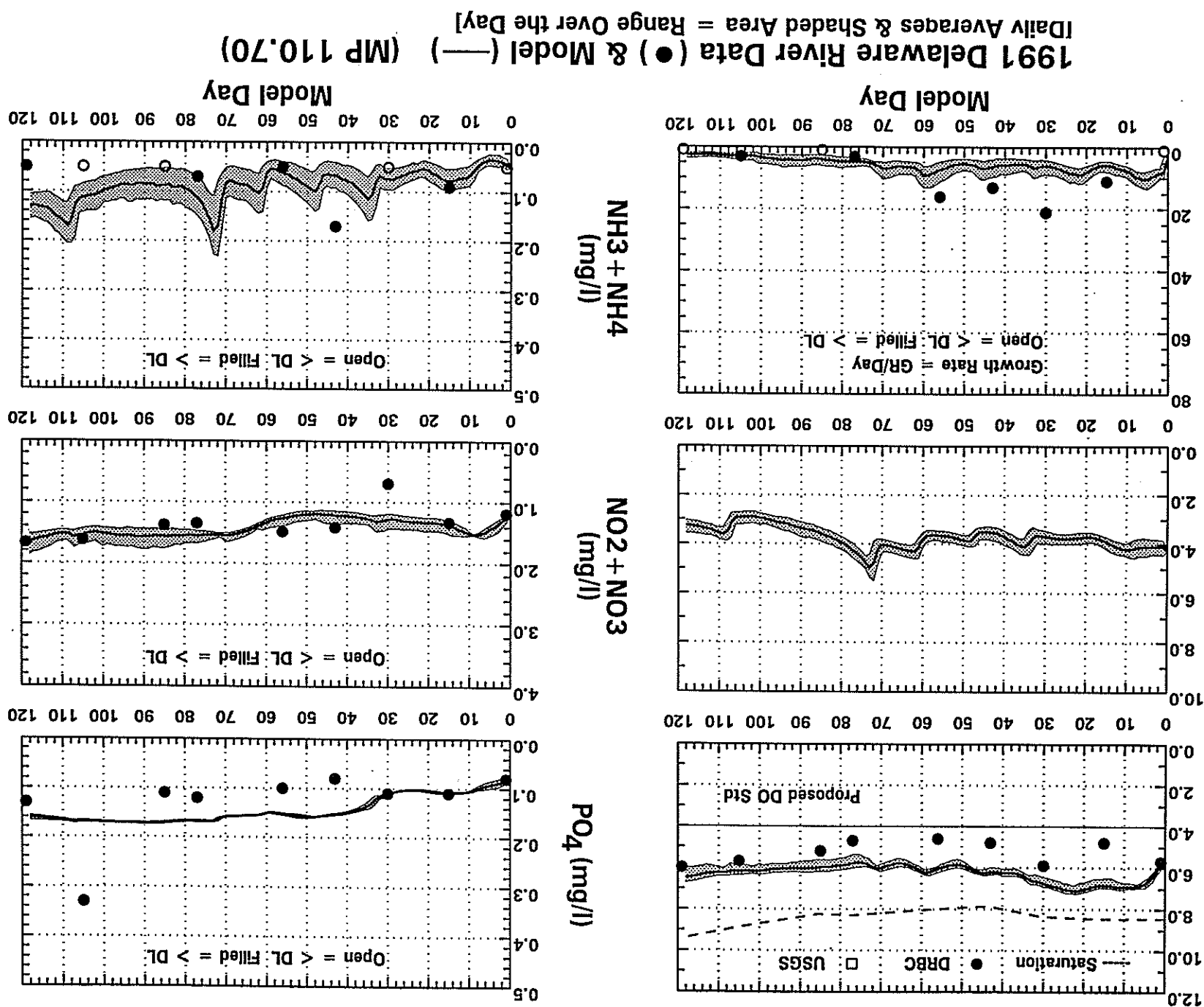
Delaware River Data (●) & Model (—) 10/7/91 (Model Day 119)
[Daily Average & Shaded Area = Range over the Day]

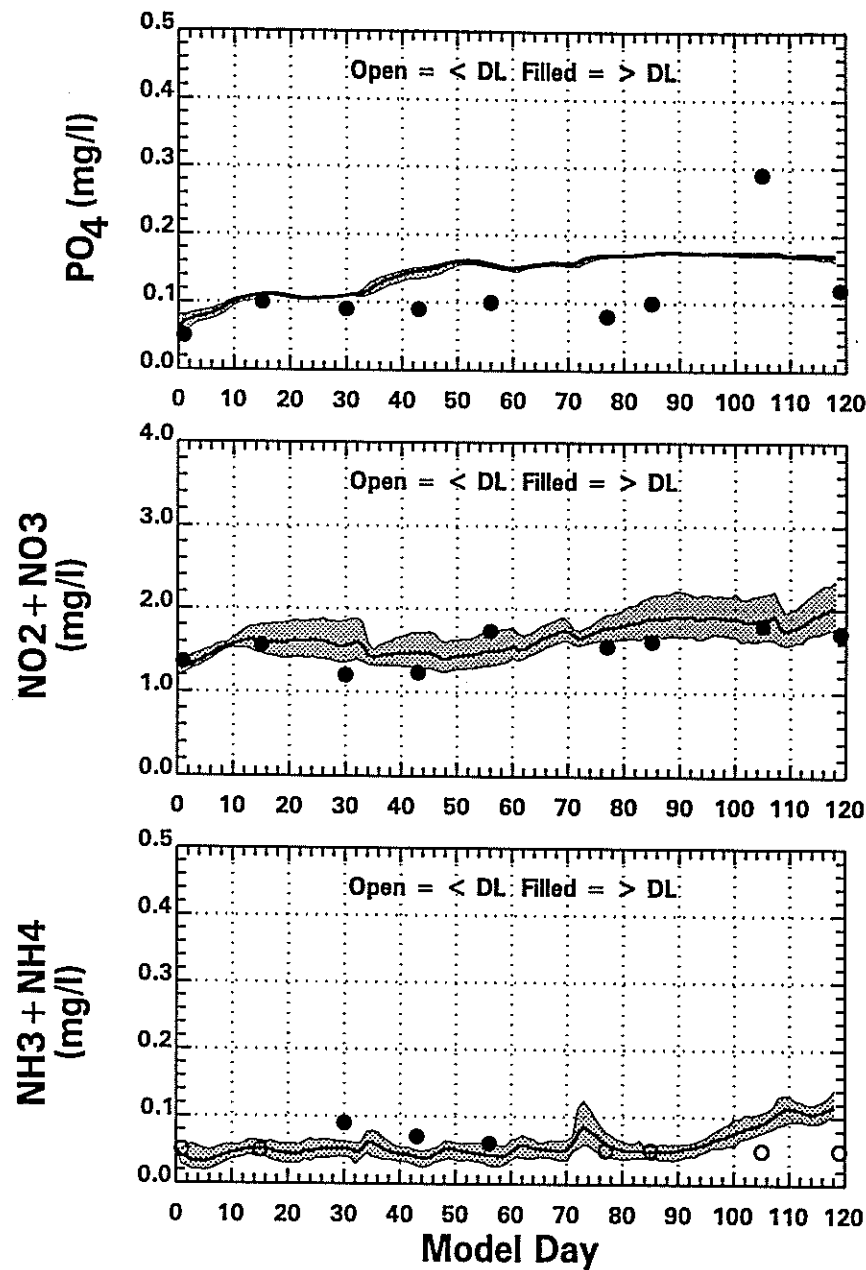
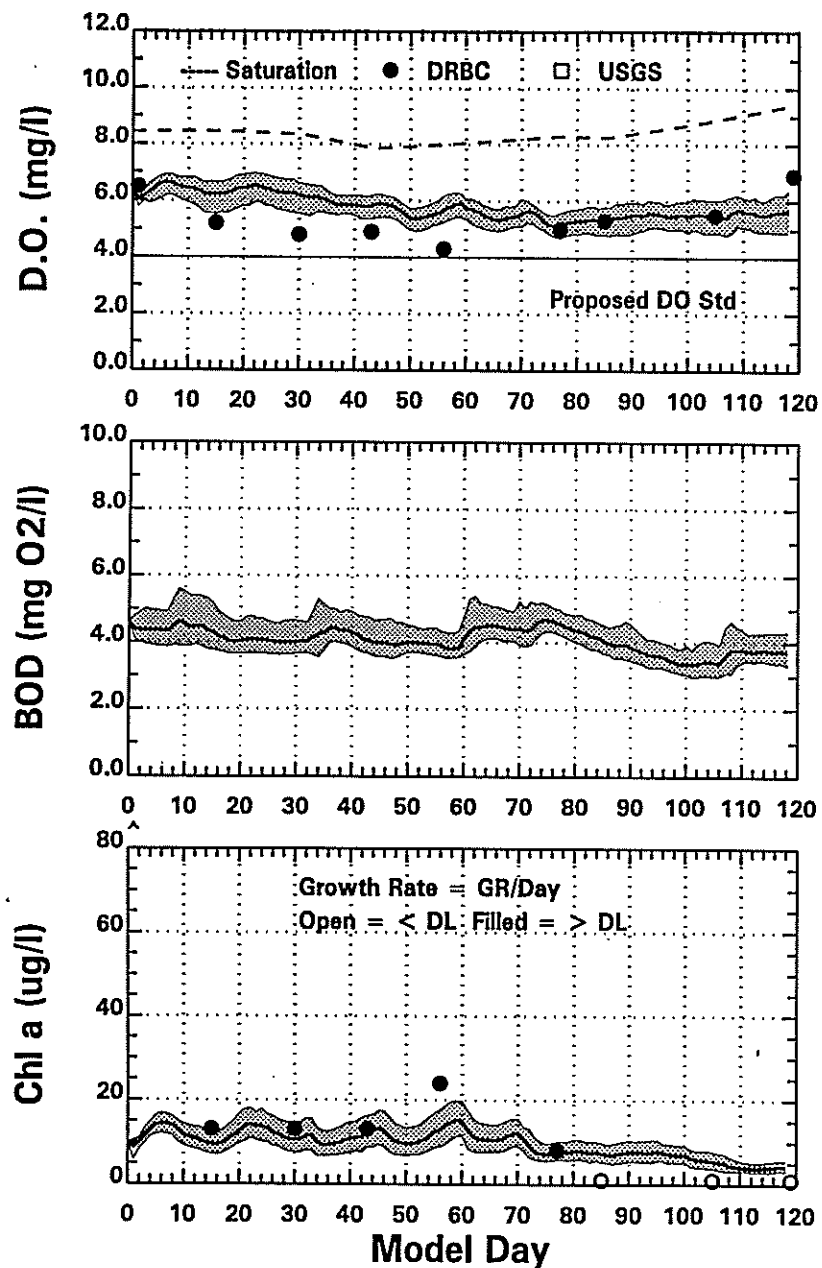


1991 Delaware River Data (●) & Model (—) (MP 127.48)
[Daily Averages & Shaded Area = Range Over the Day]

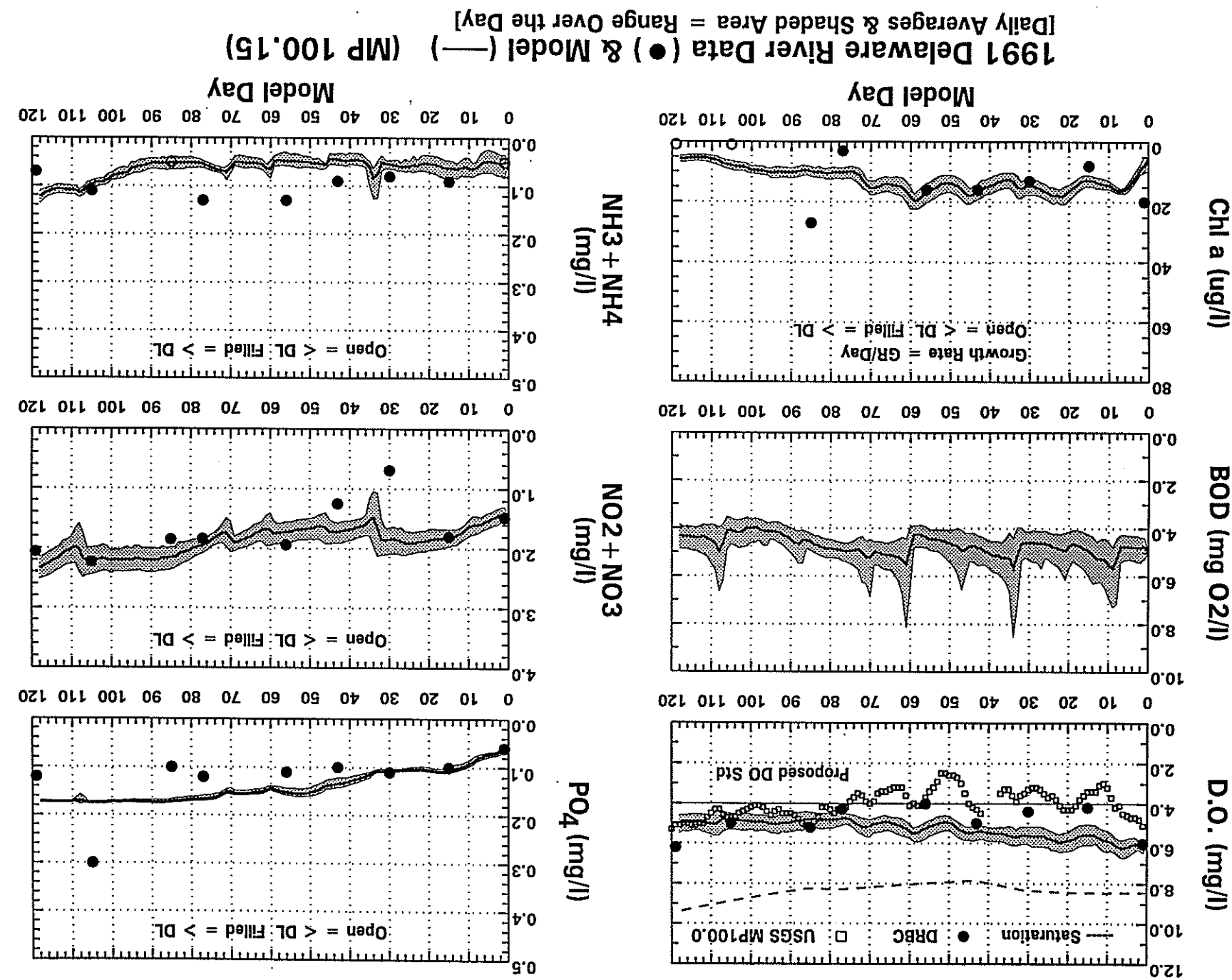


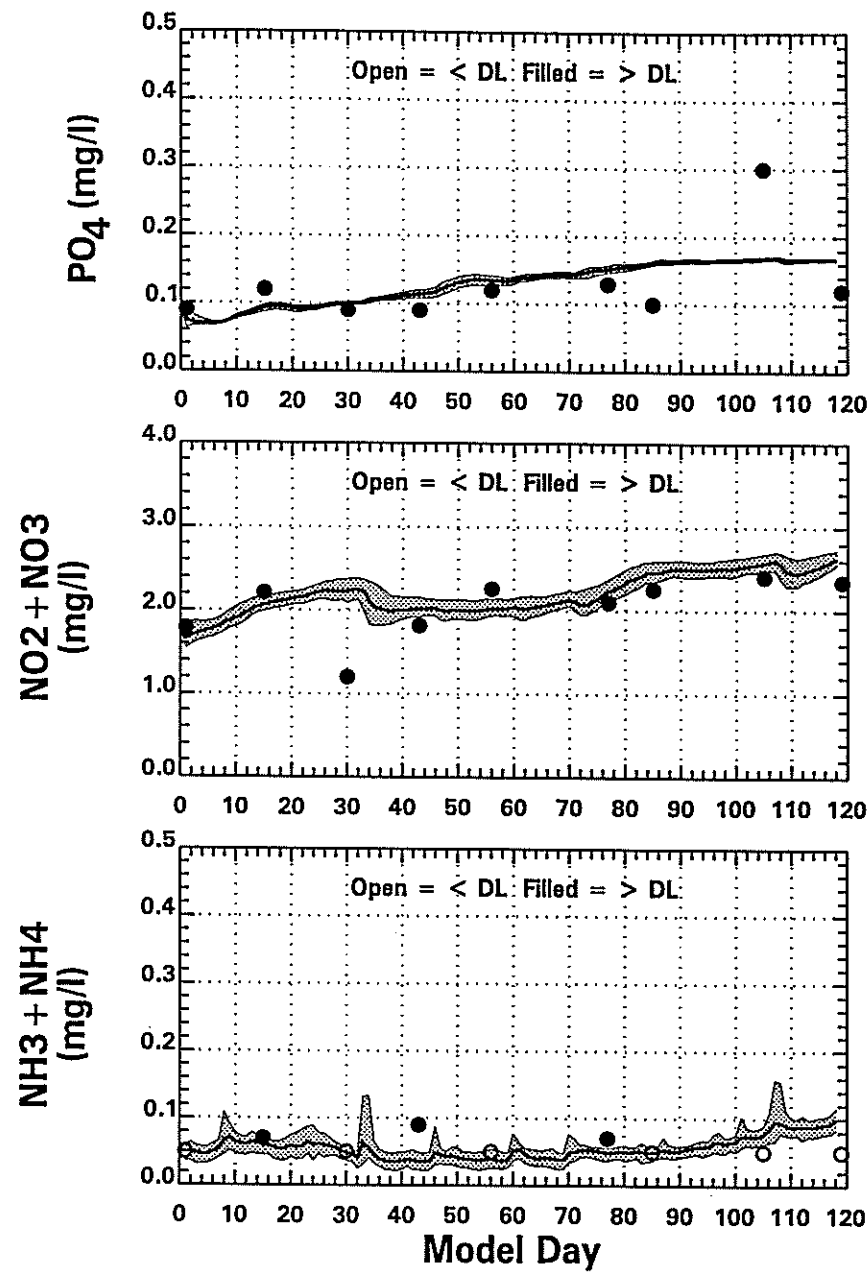
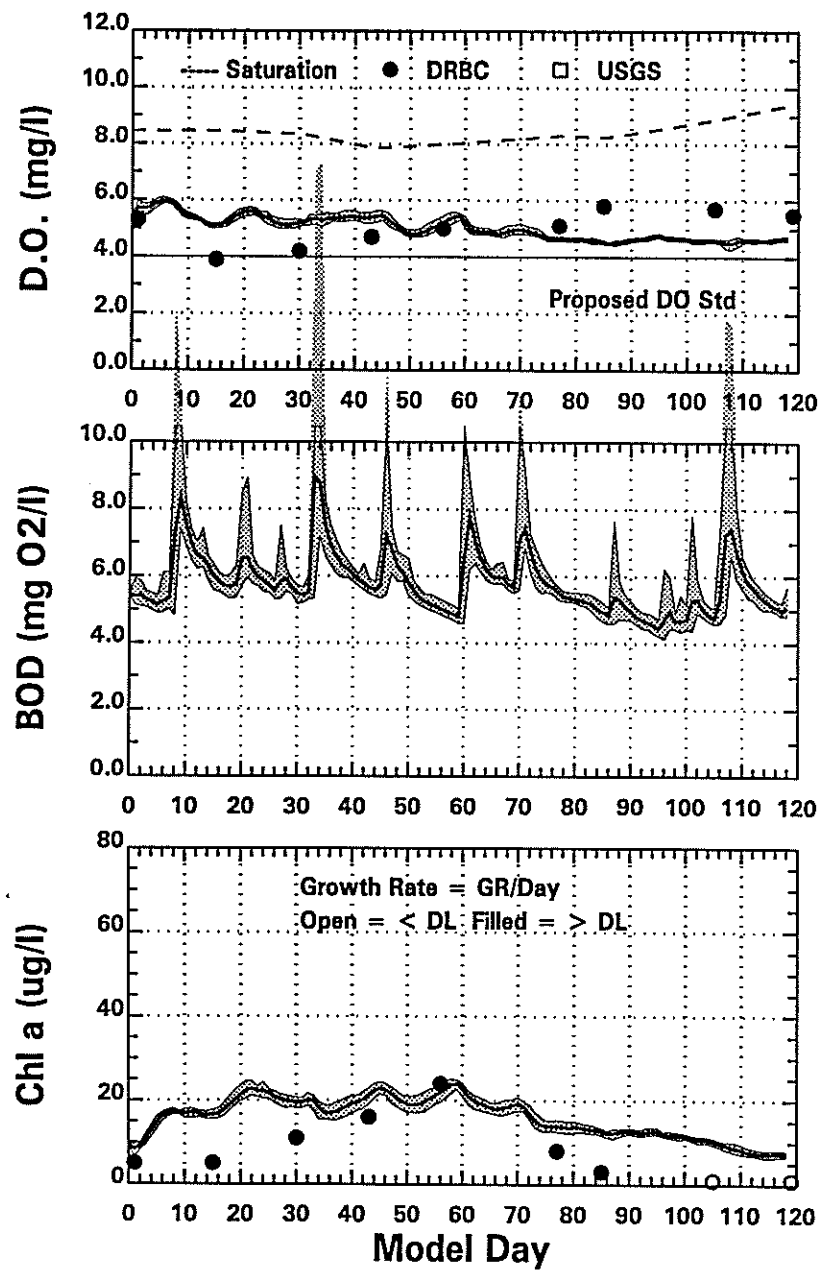
1991 Delaware River Data (●) & Model (—) (MP 117.80)
[Daily Averages & Shaded Area = Range Over the Day]



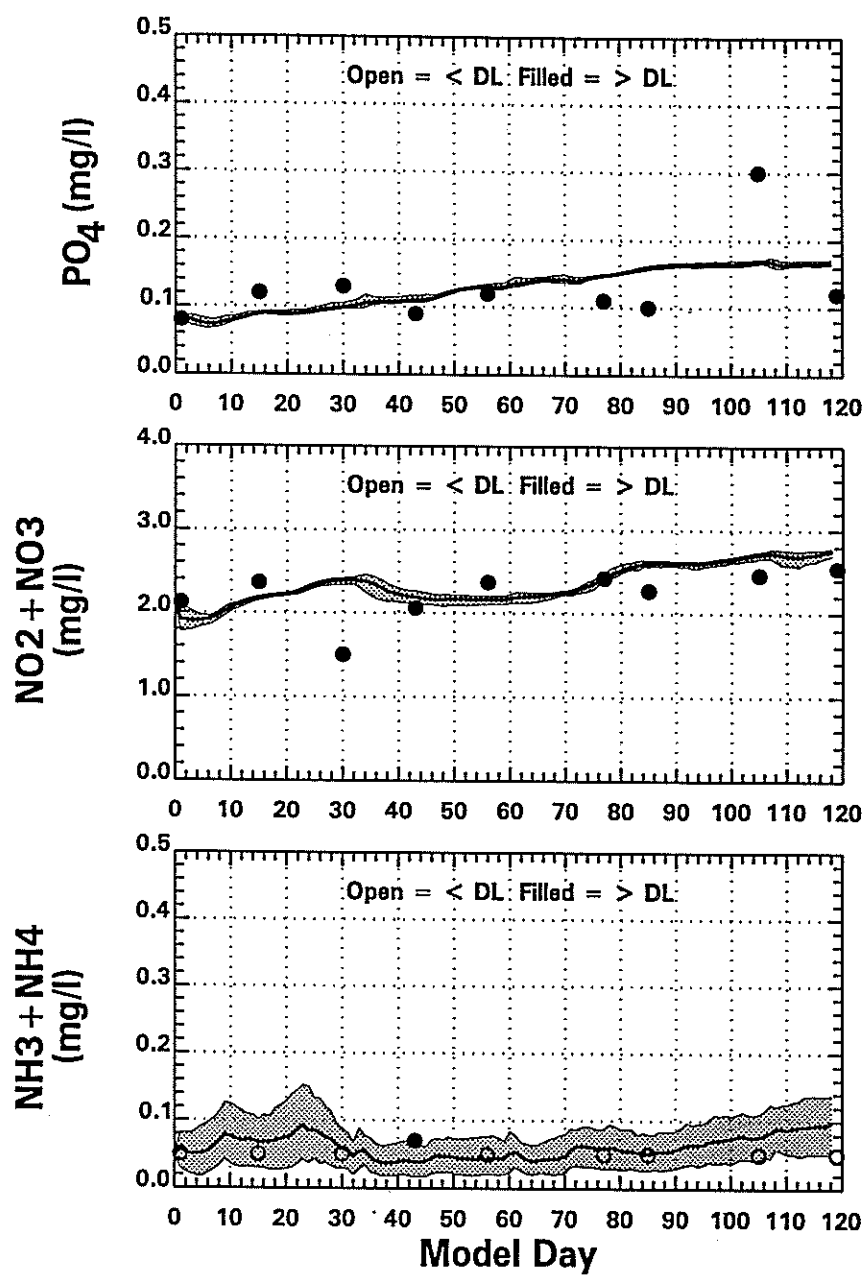
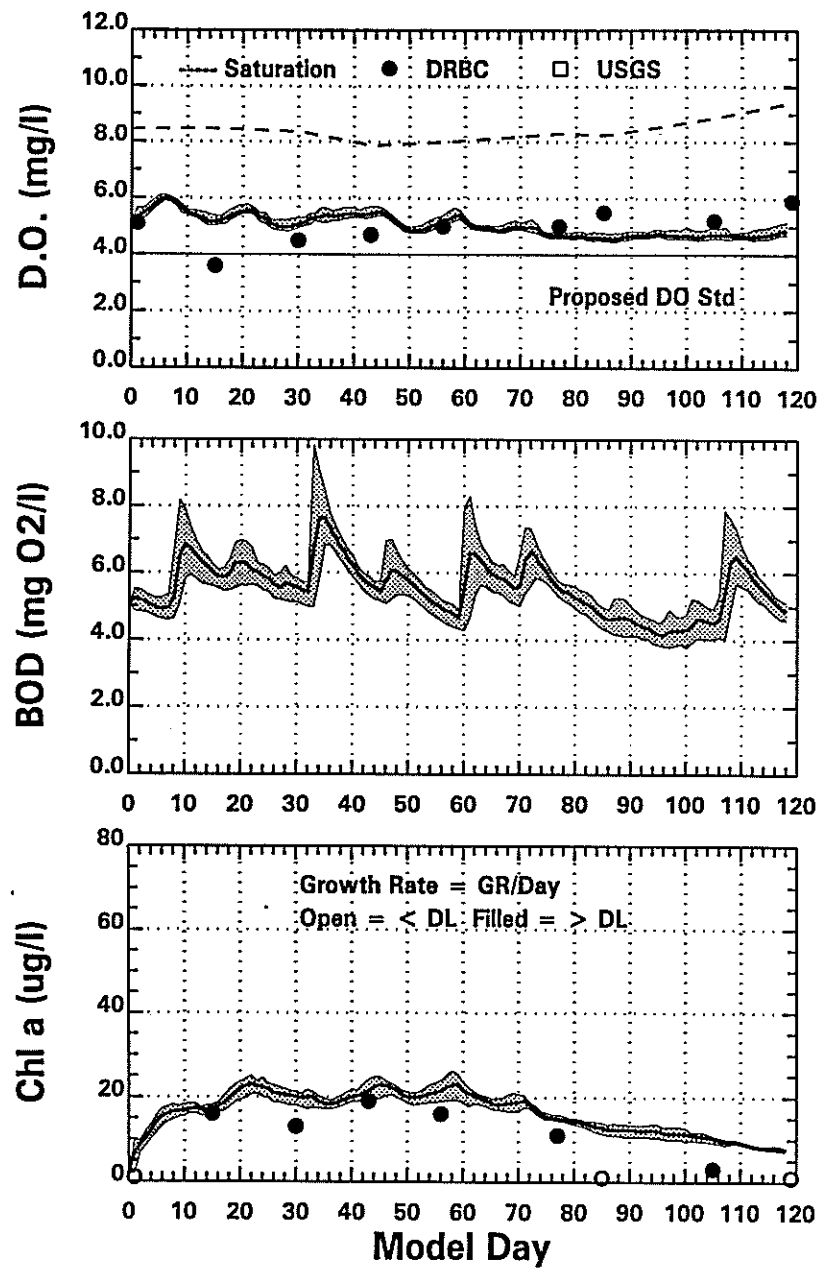


1991 Delaware River Data (●) & Model (—) (MP 104.90)
 [Daily Averages & Shaded Area = Range Over the Day]

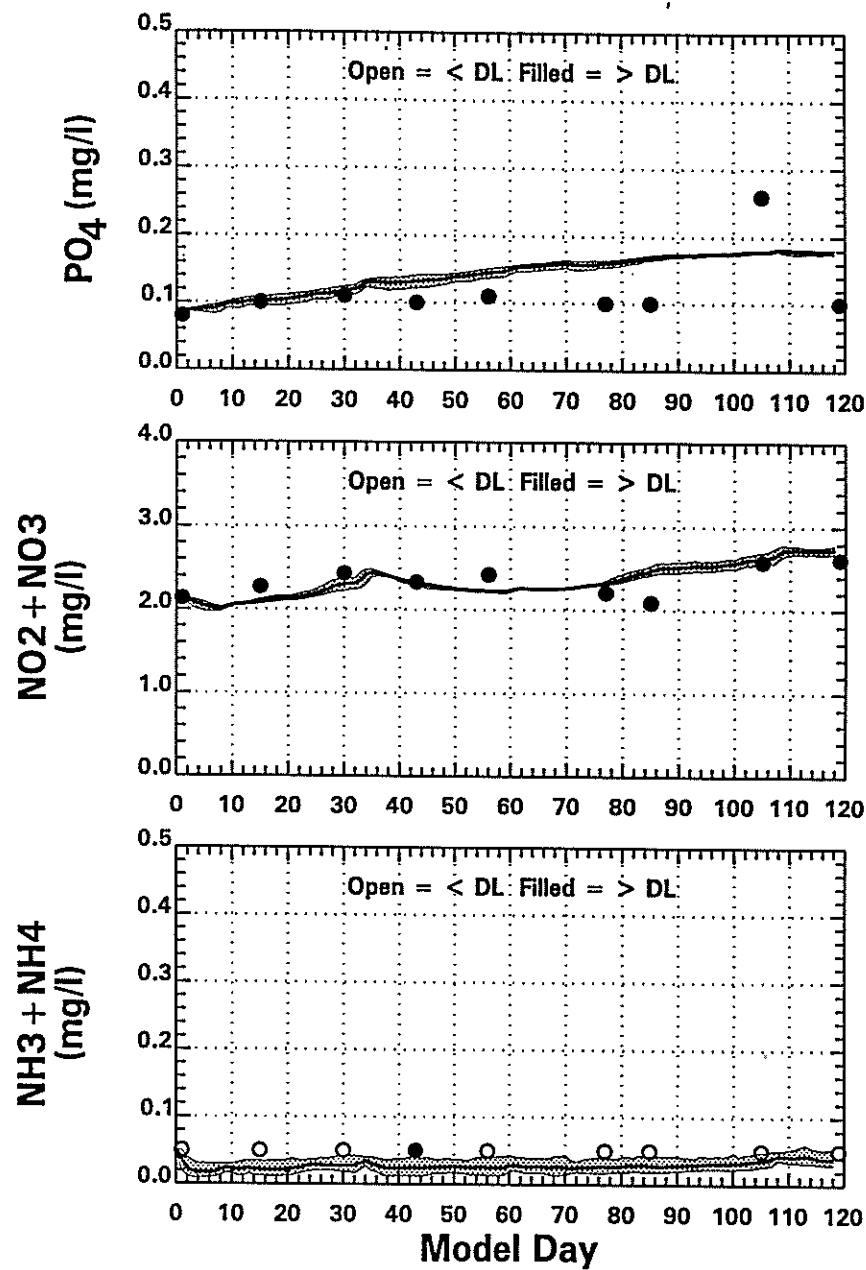
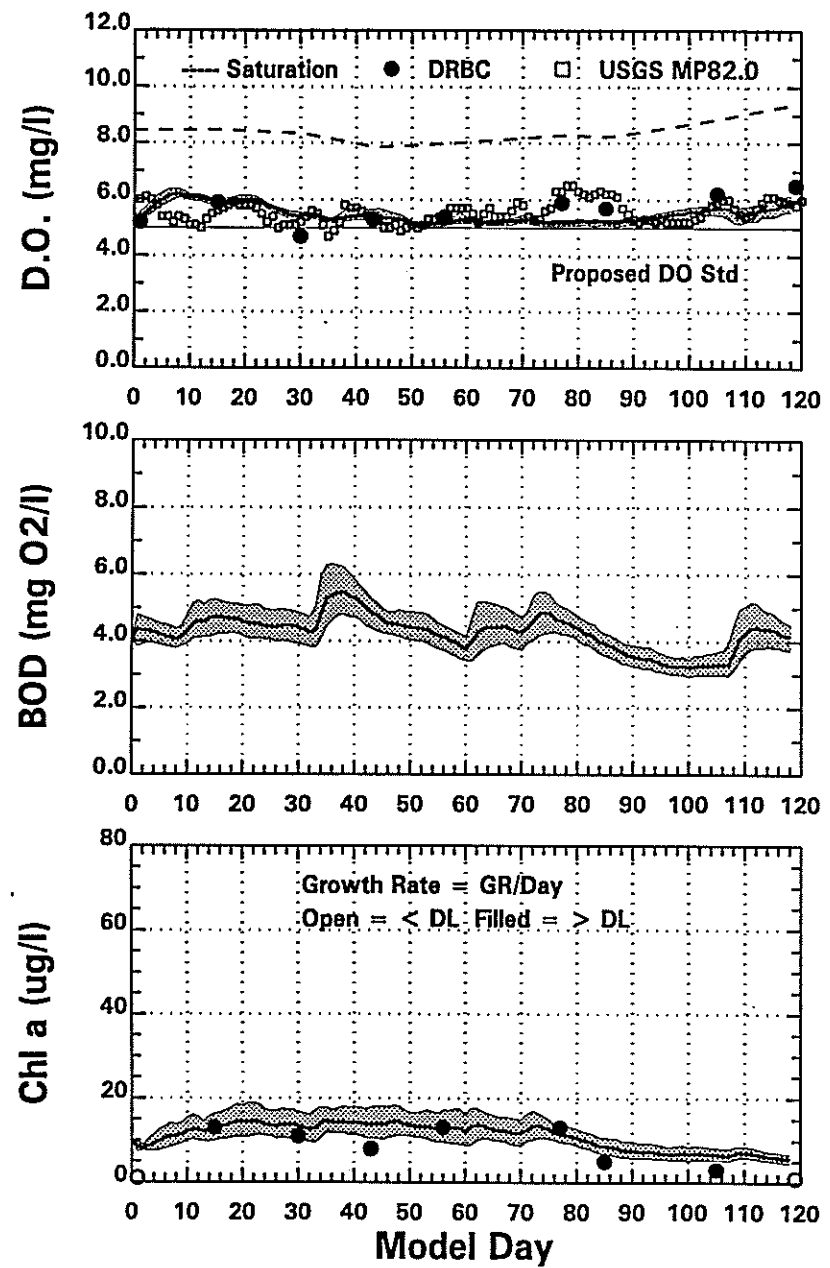




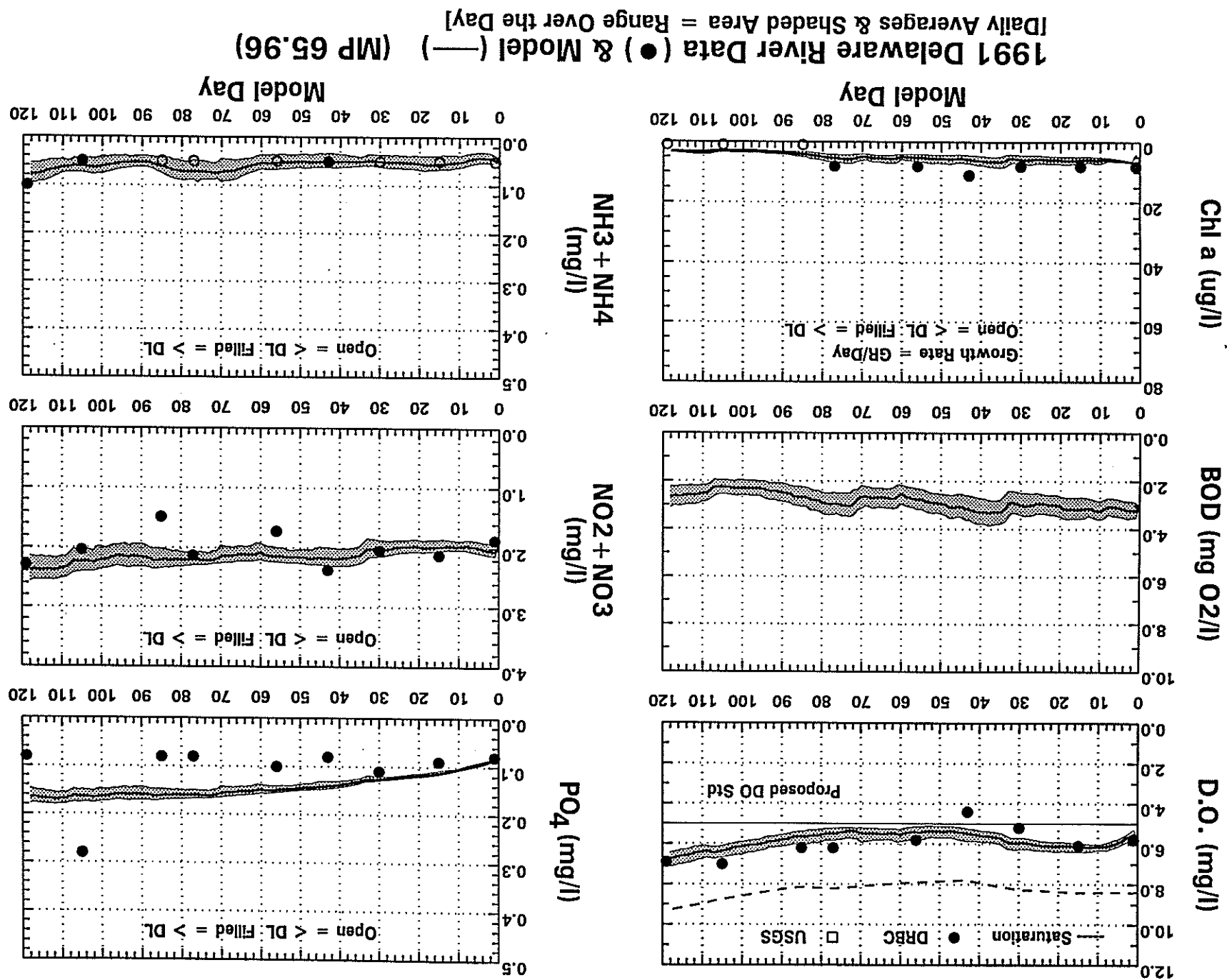
1991 Delaware River Data (●) & Model (—) (MP 93.18)
[Daily Averages & Shaded Area = Range Over the Day]

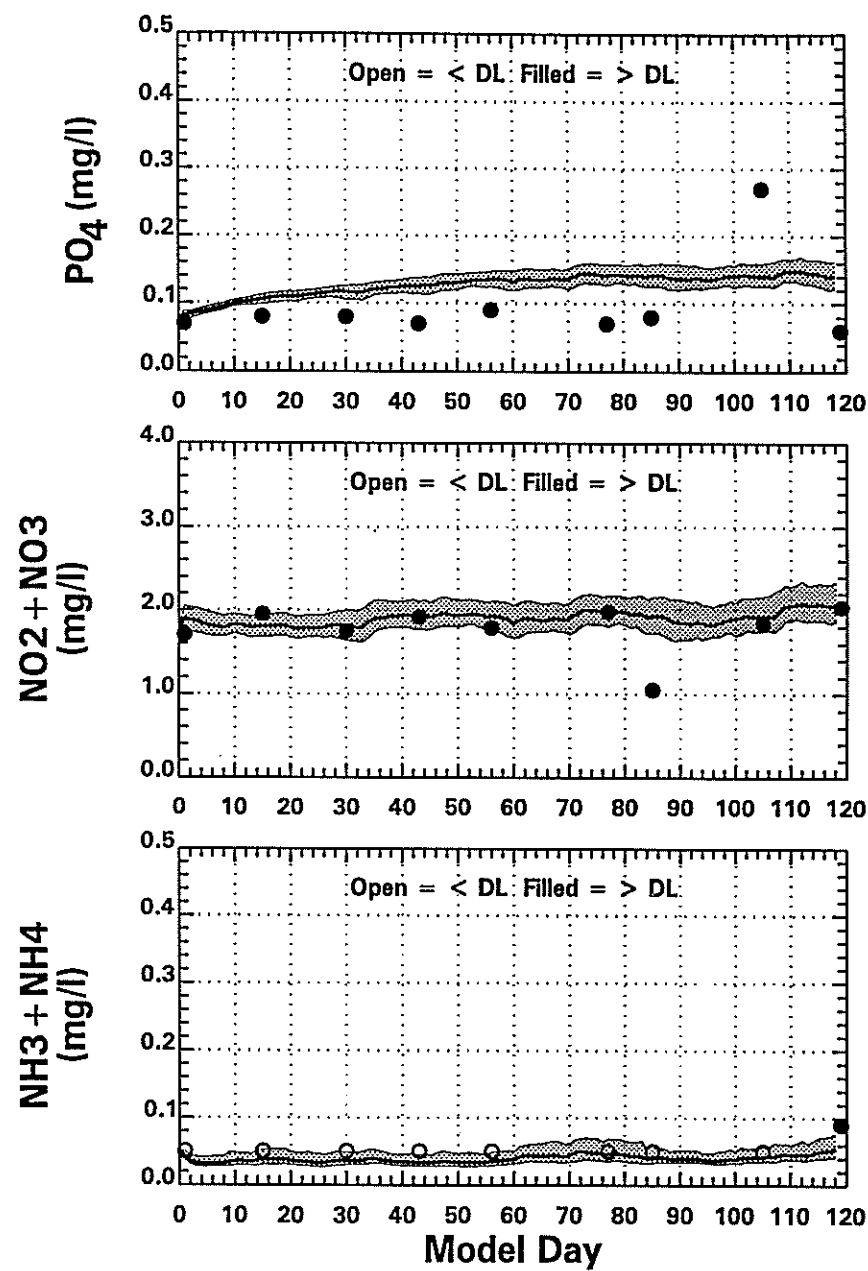
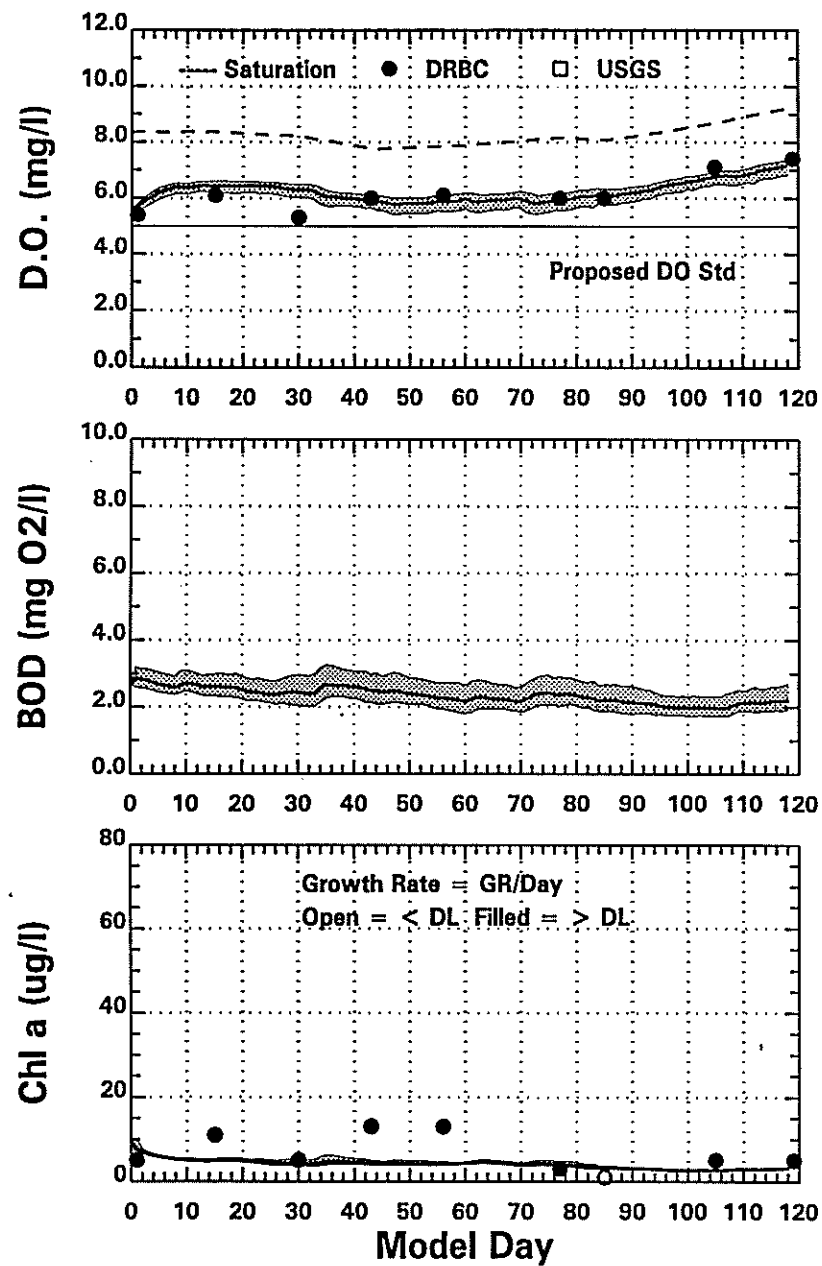


1991 Delaware River Data (●) & Model (—) (MP 87.90)
 [Daily Averages & Shaded Area = Range Over the Day]

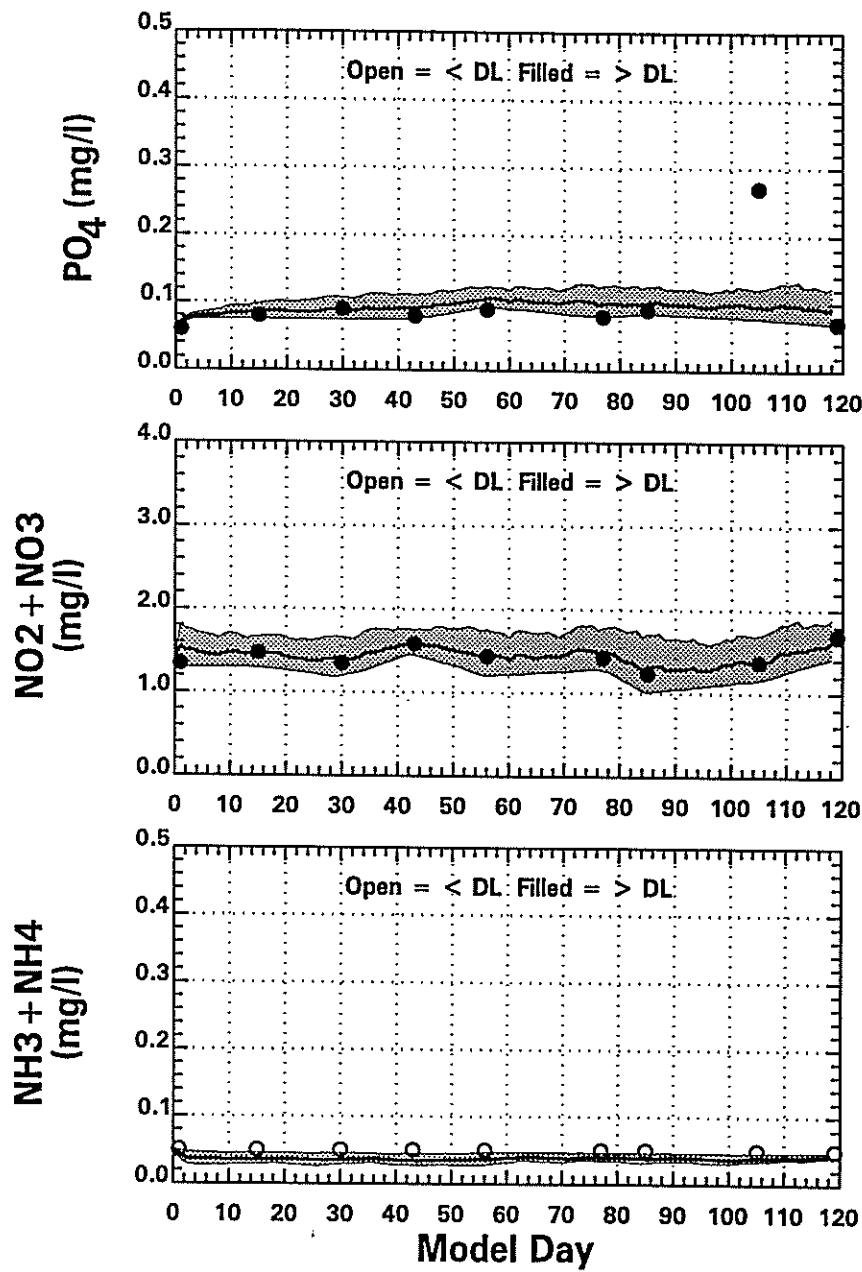
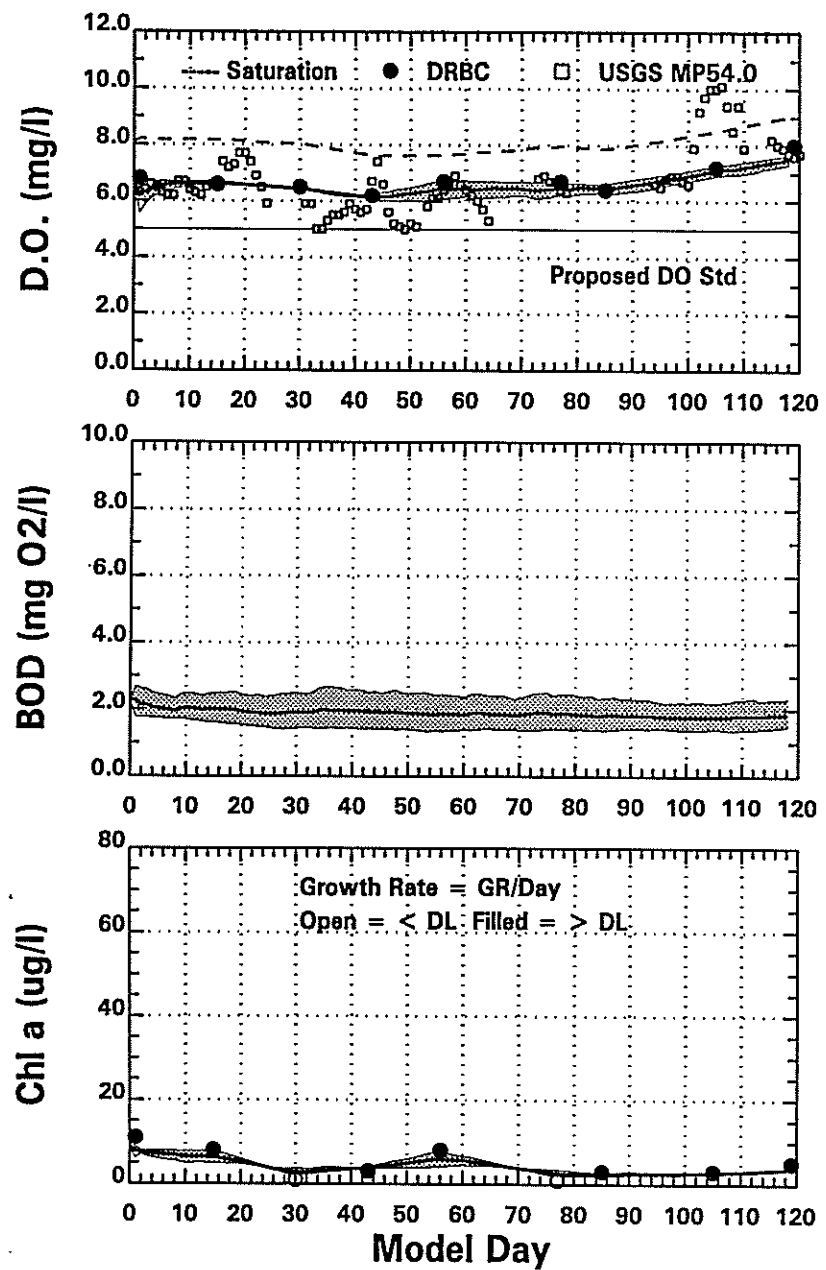


1991 Delaware River Data (●) & Model (—) (MP 78.07)
 [Daily Averages & Shaded Area = Range Over the Day]

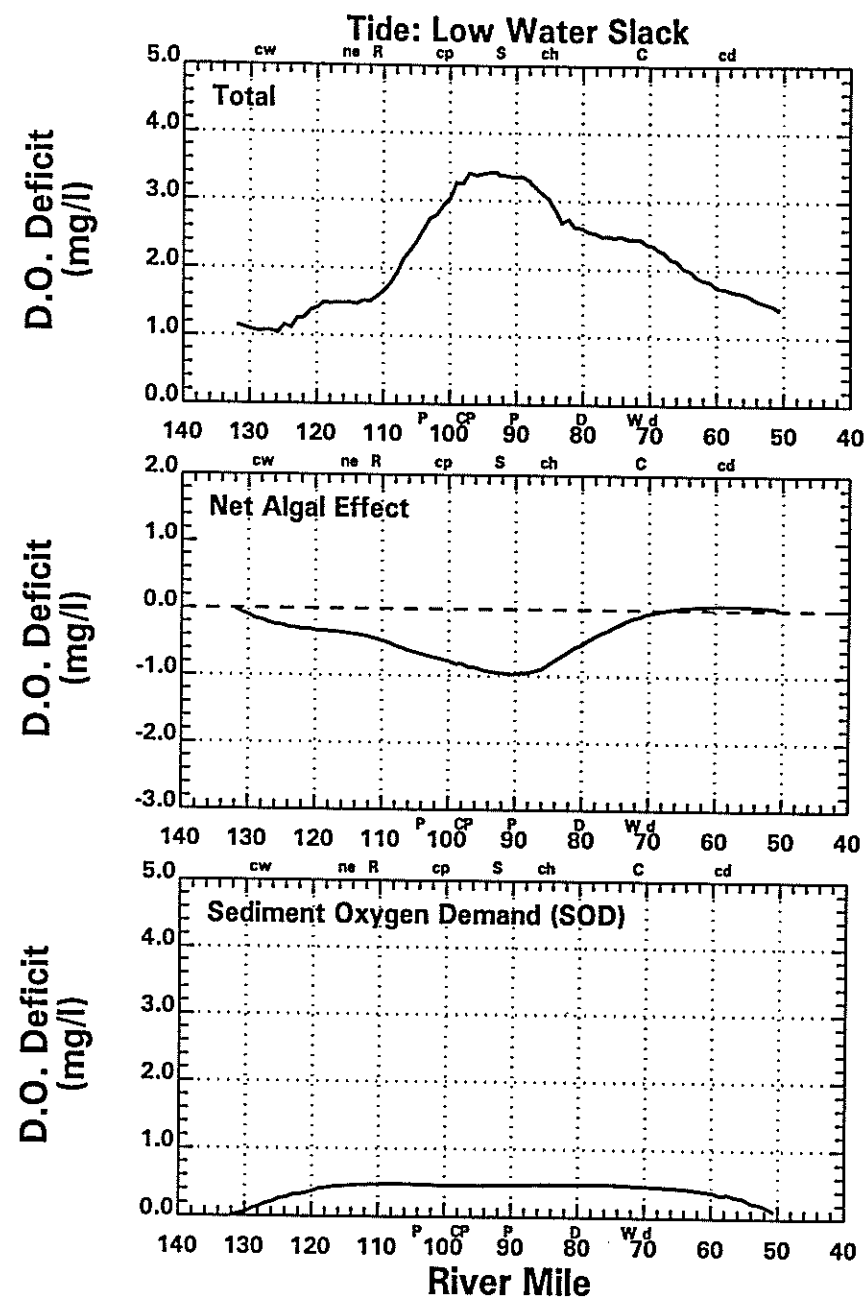
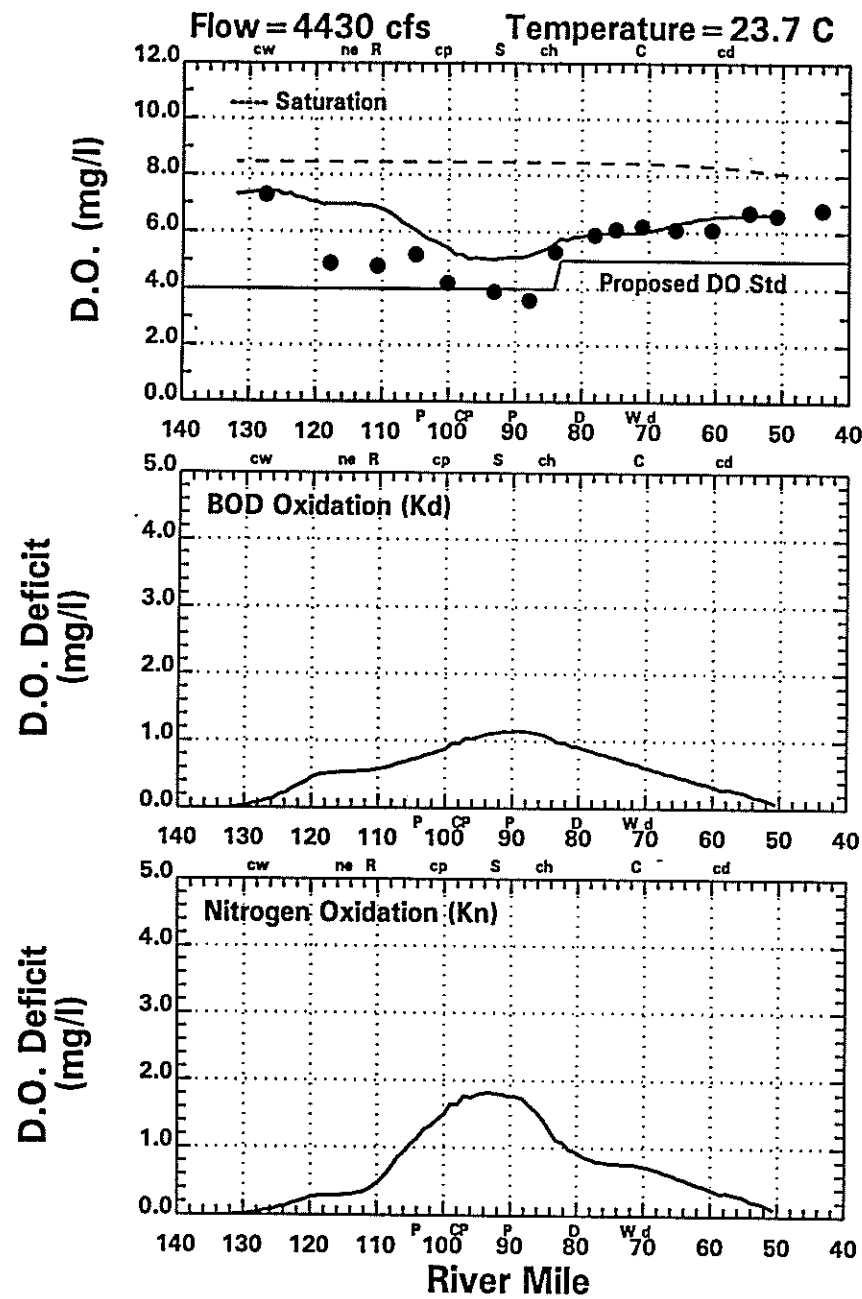




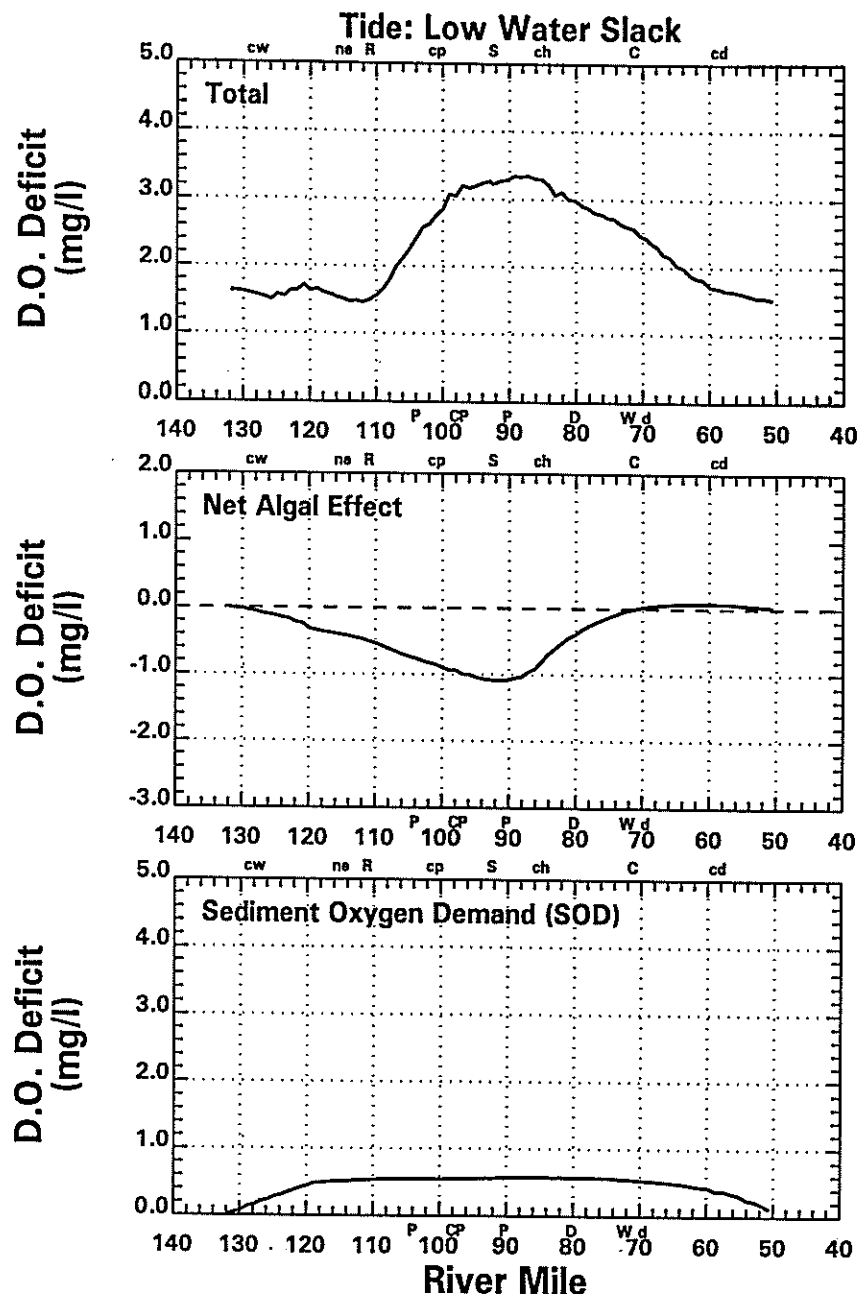
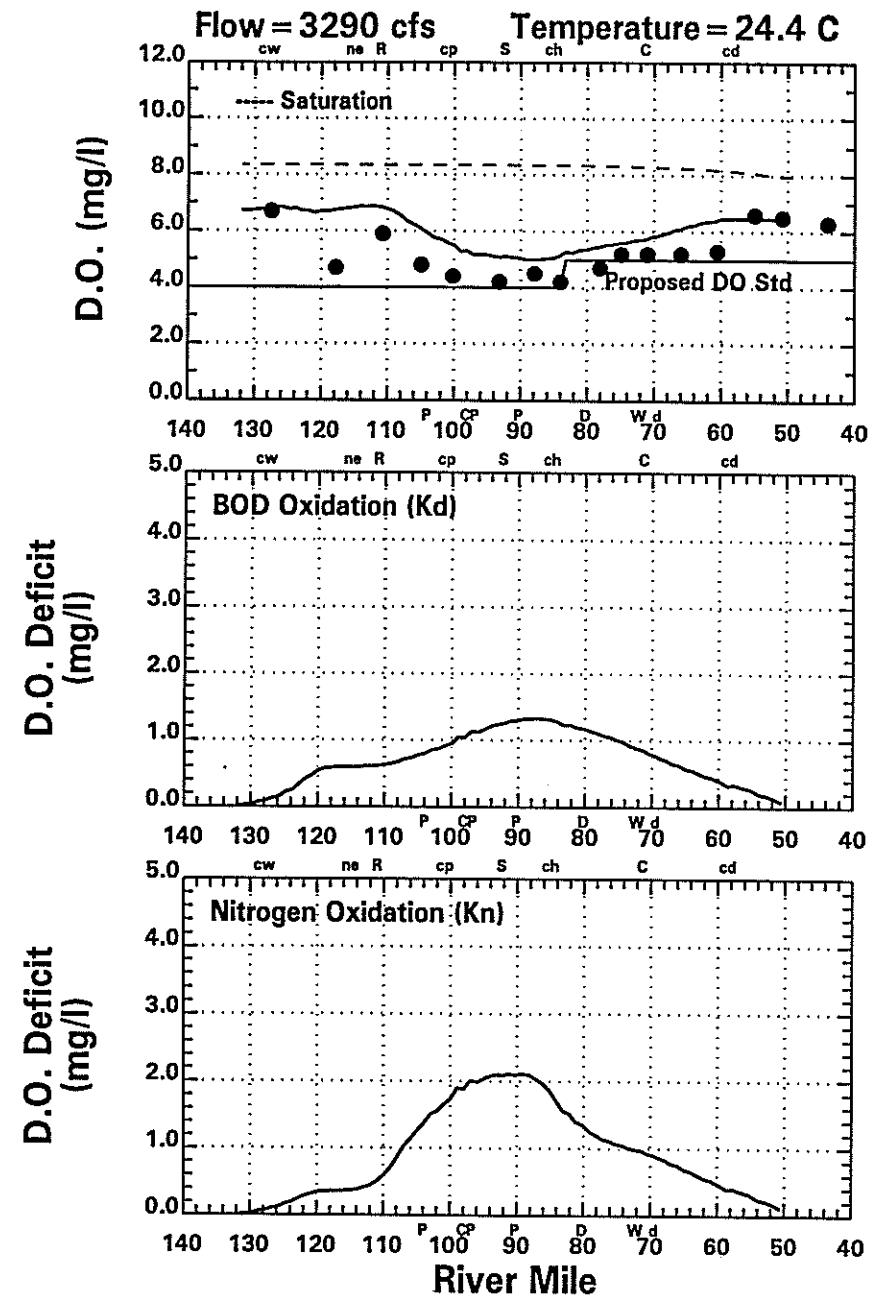
1991 Delaware River Data (●) & Model (—) (MP 60.55)
[Daily Averages & Shaded Area = Range Over the Day]



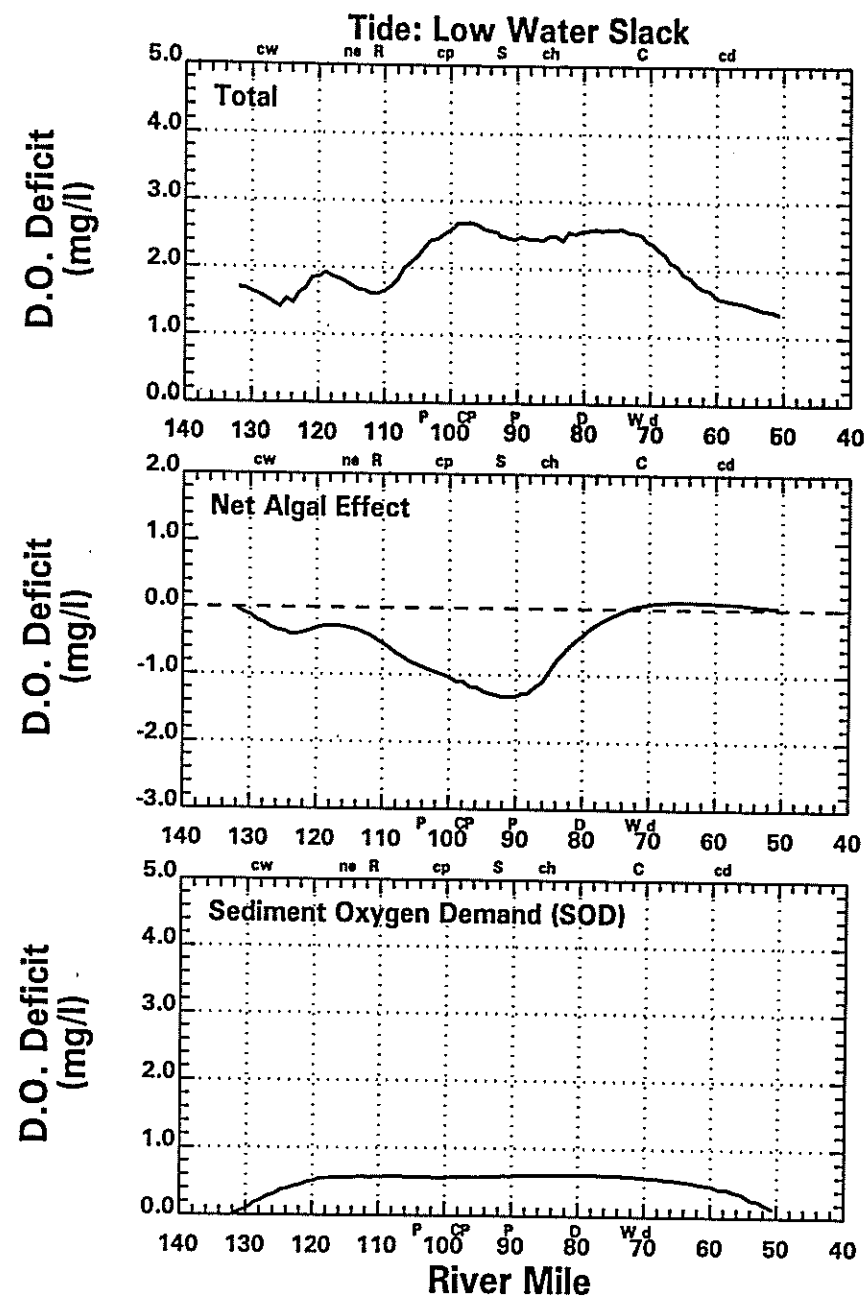
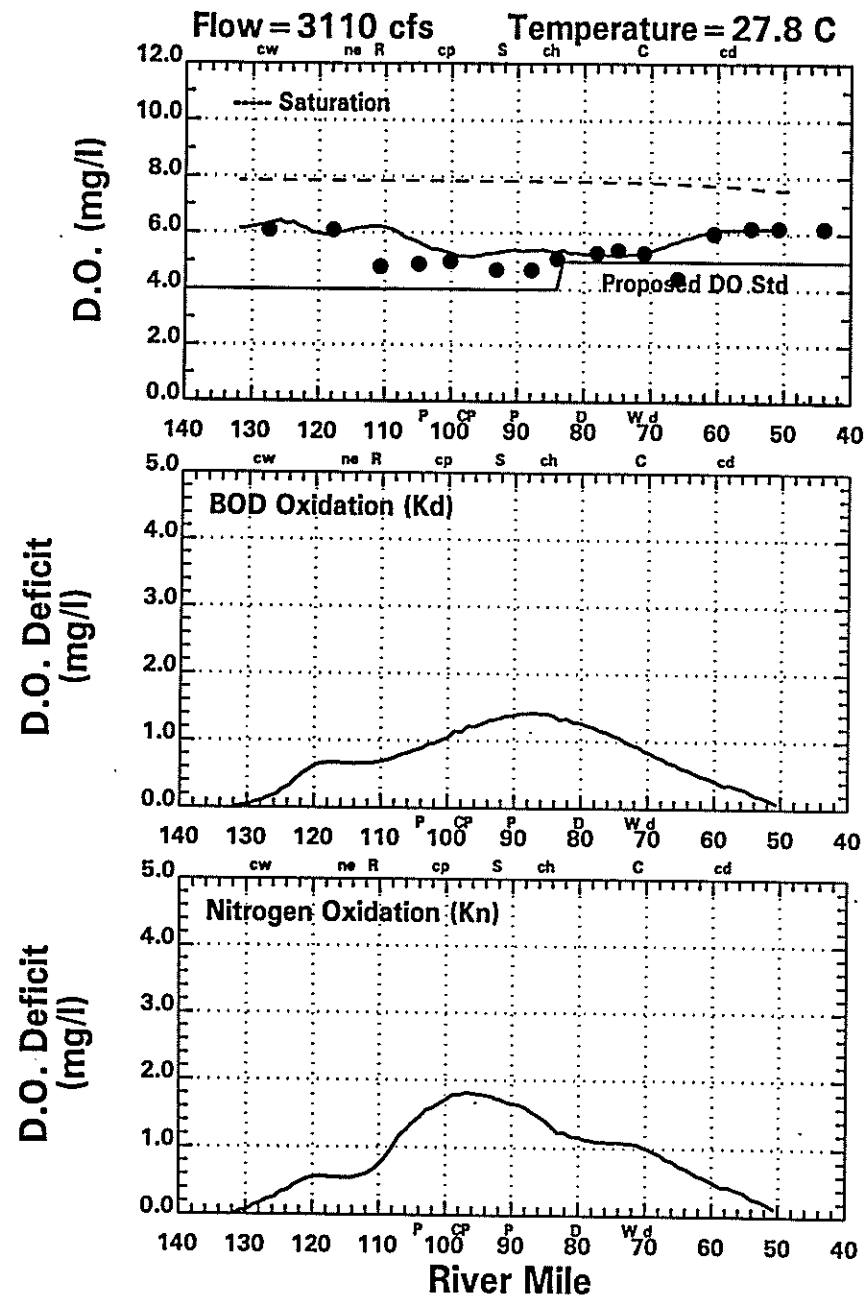
1991 Delaware River Data (●) & Model (—) (MP 50.80)
[Daily Averages & Shaded Area = Range Over the Day]



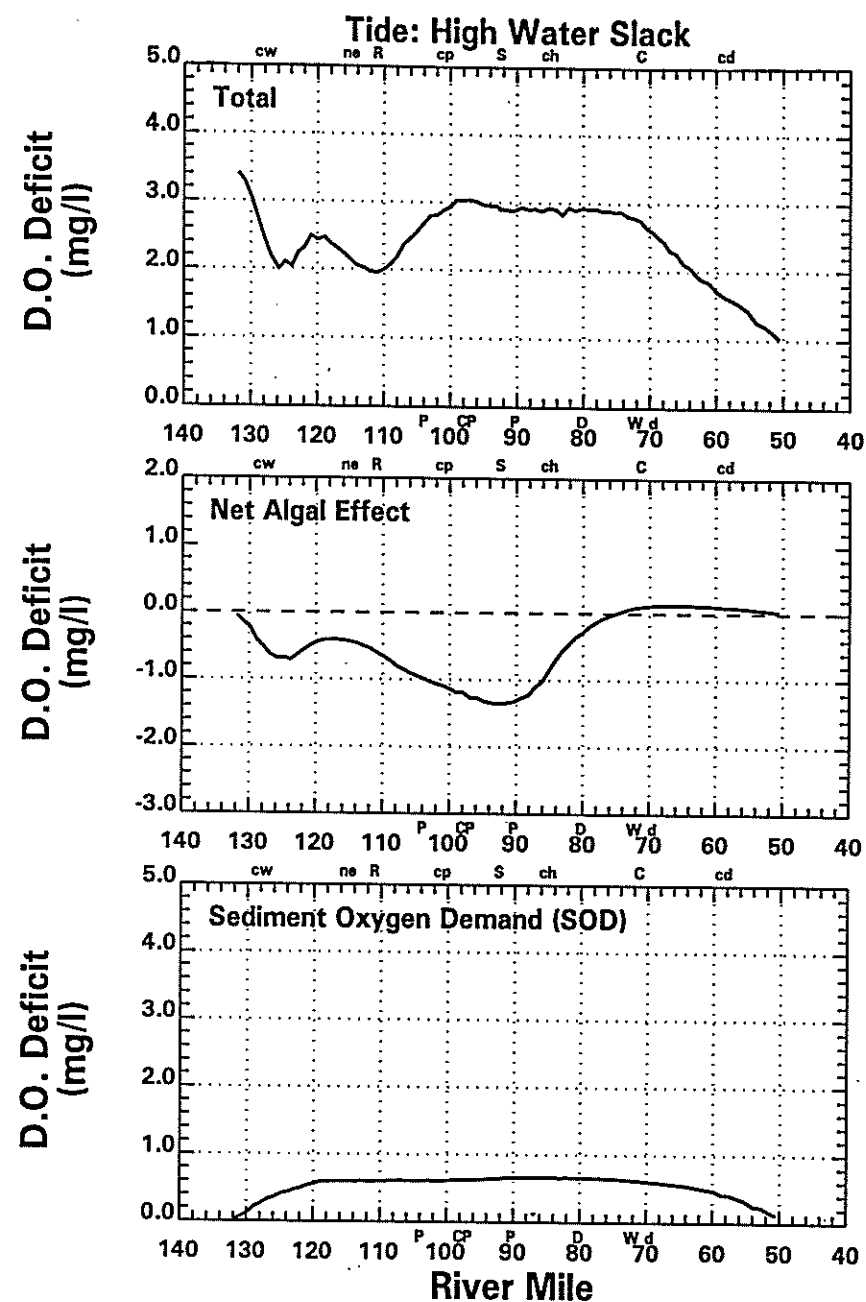
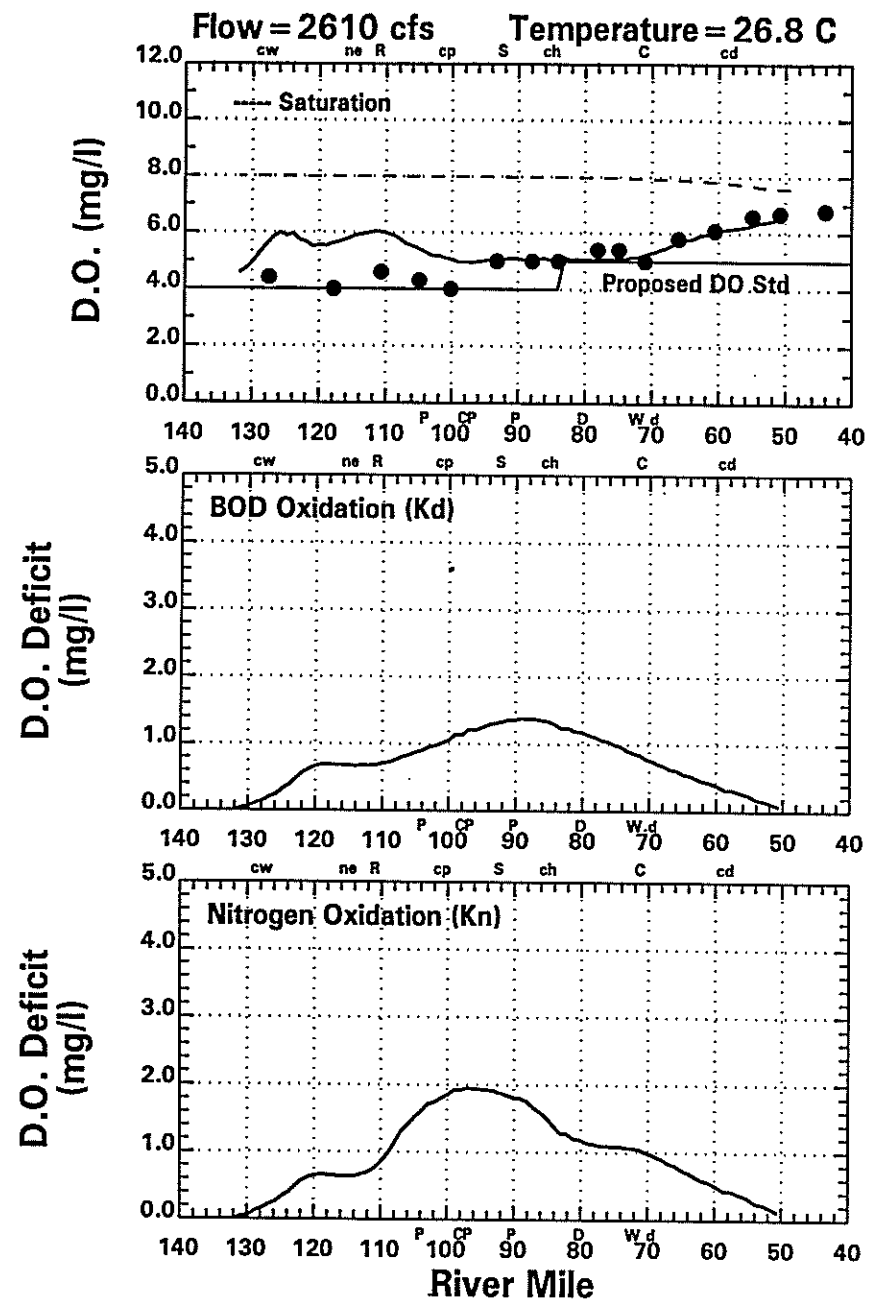
Delaware River Data (●) & Model (—) 6/25/91 (Model Day 15)
 [Temporally, Vertically and Laterally Averaged]



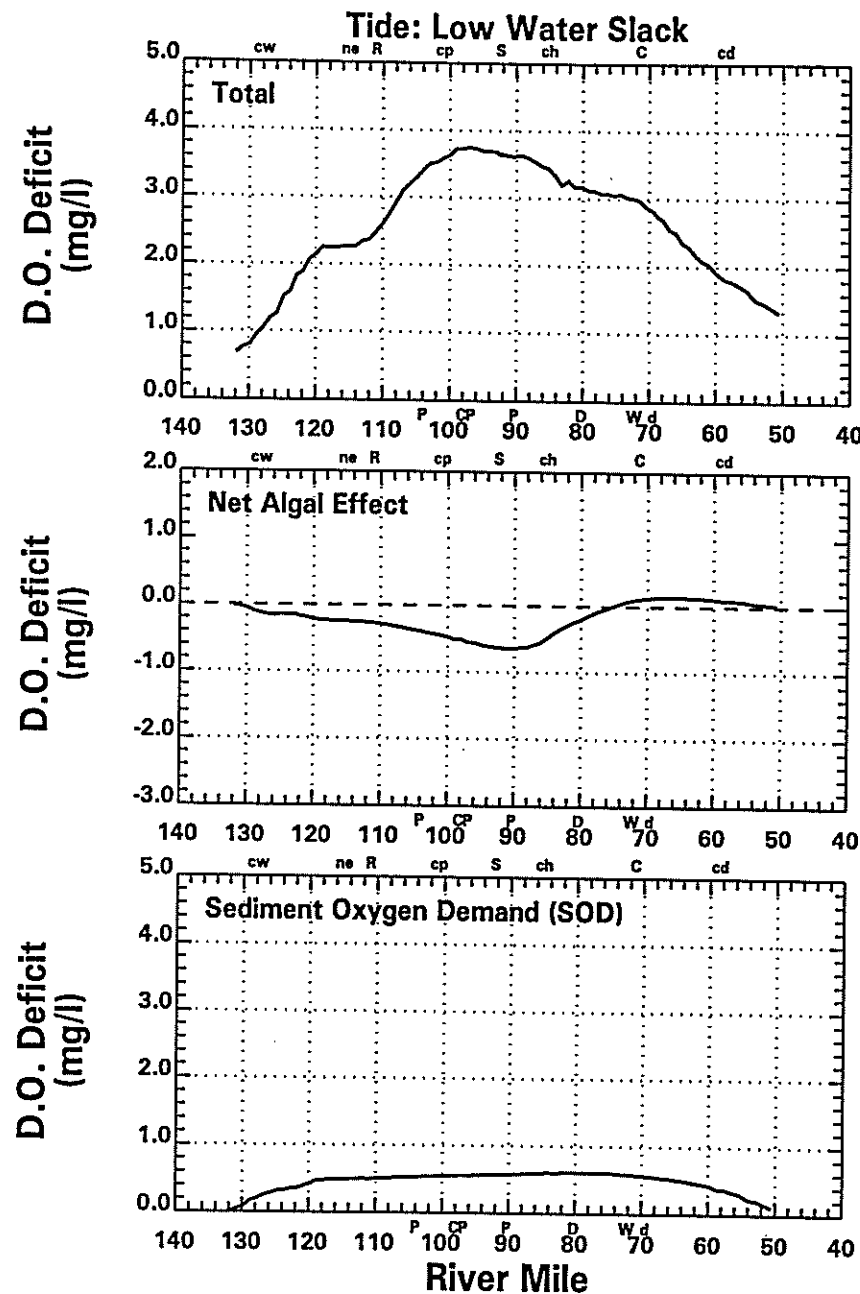
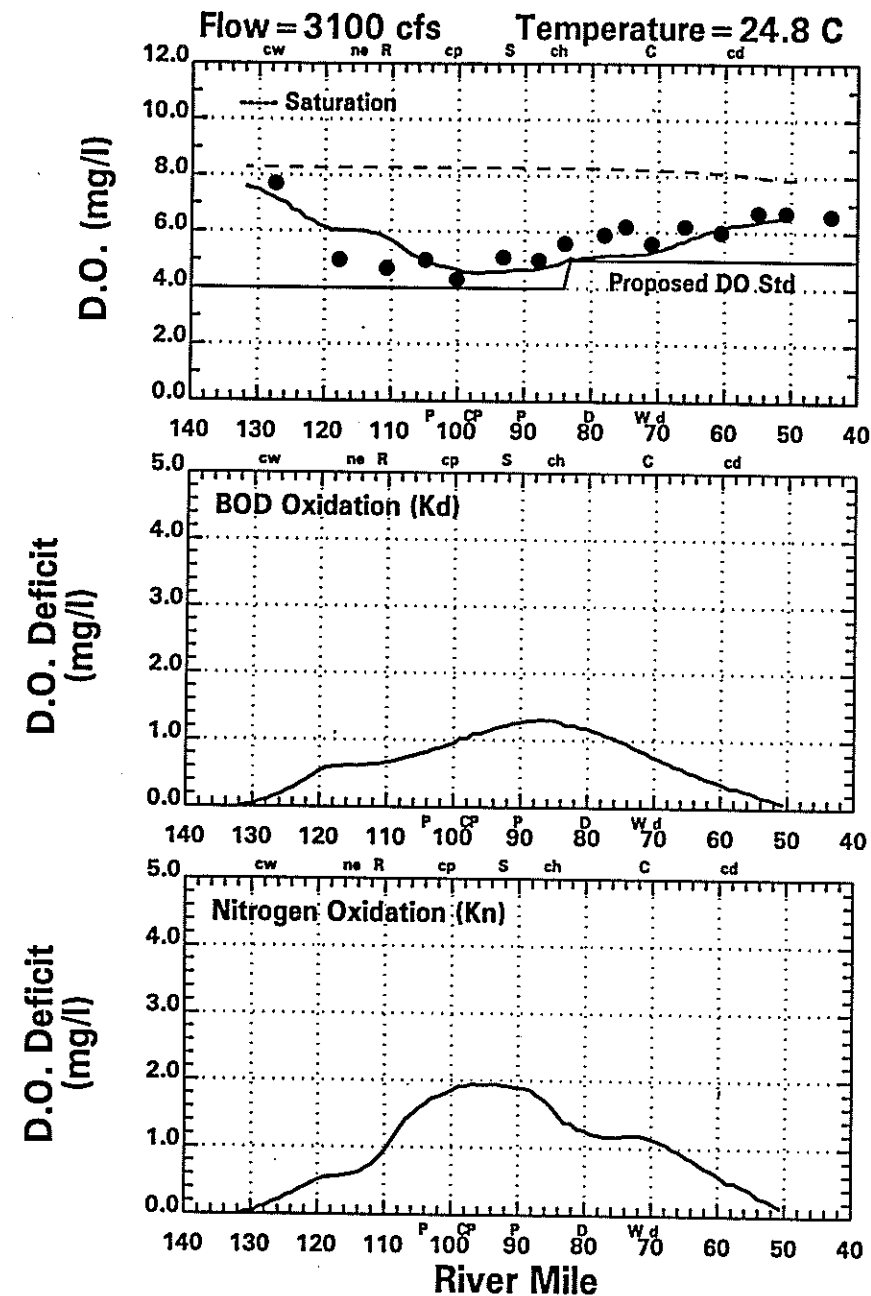
Delaware River Data (●) & Model (—) 7/10/91 (Model Day 30)
 [Temporally, Vertically and Laterally Averaged]



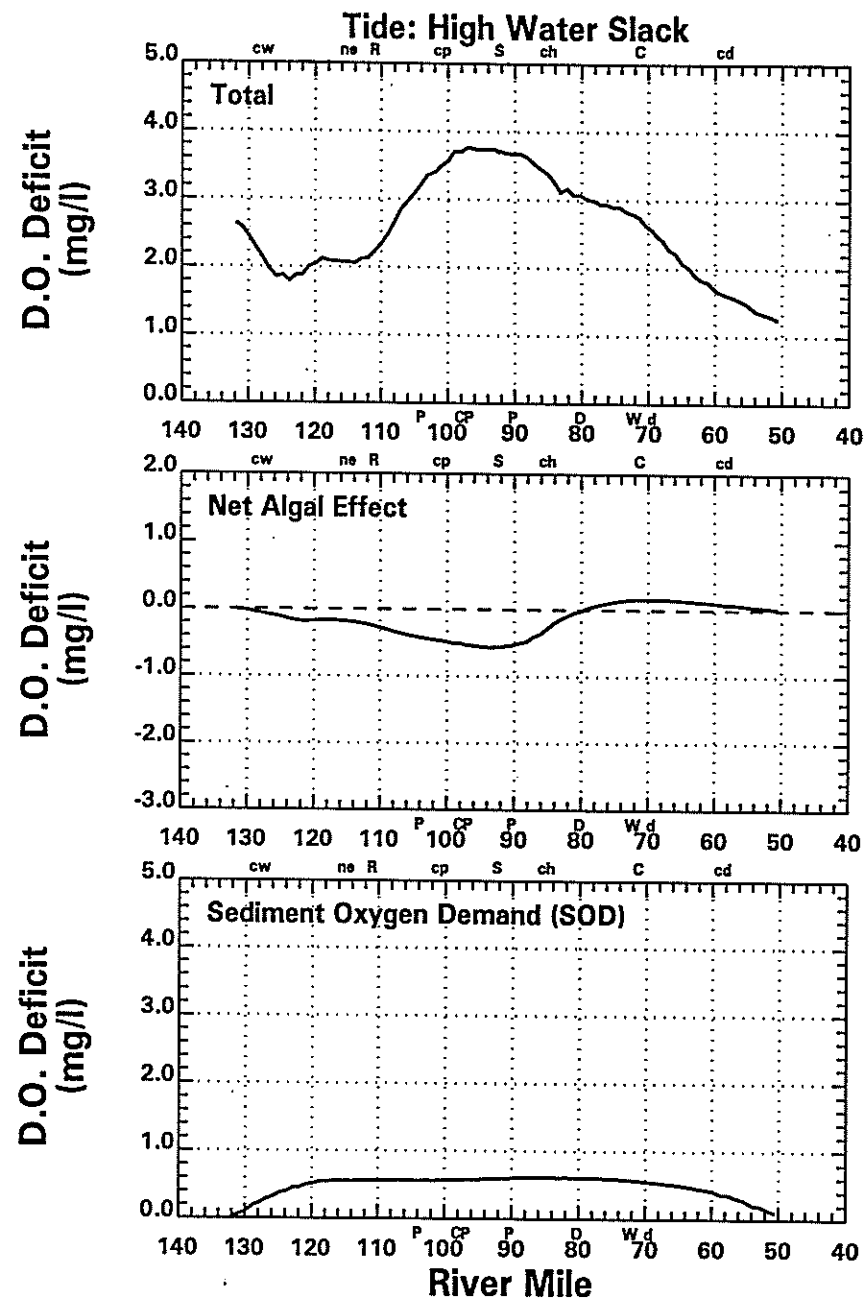
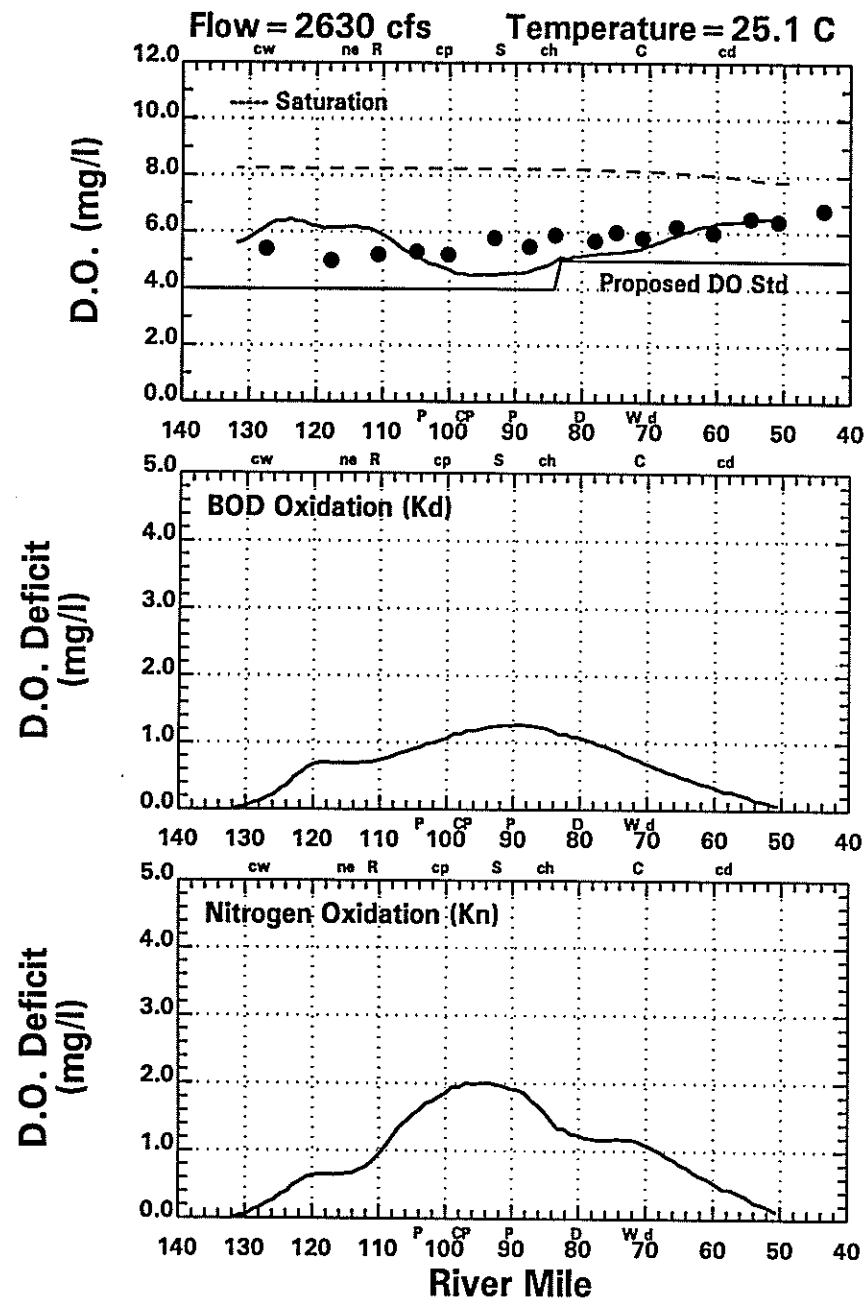
Delaware River Data (●) & Model (—) 7/23/91 (Model Day 43)
 [Temporally, Vertically and Laterally Averaged]



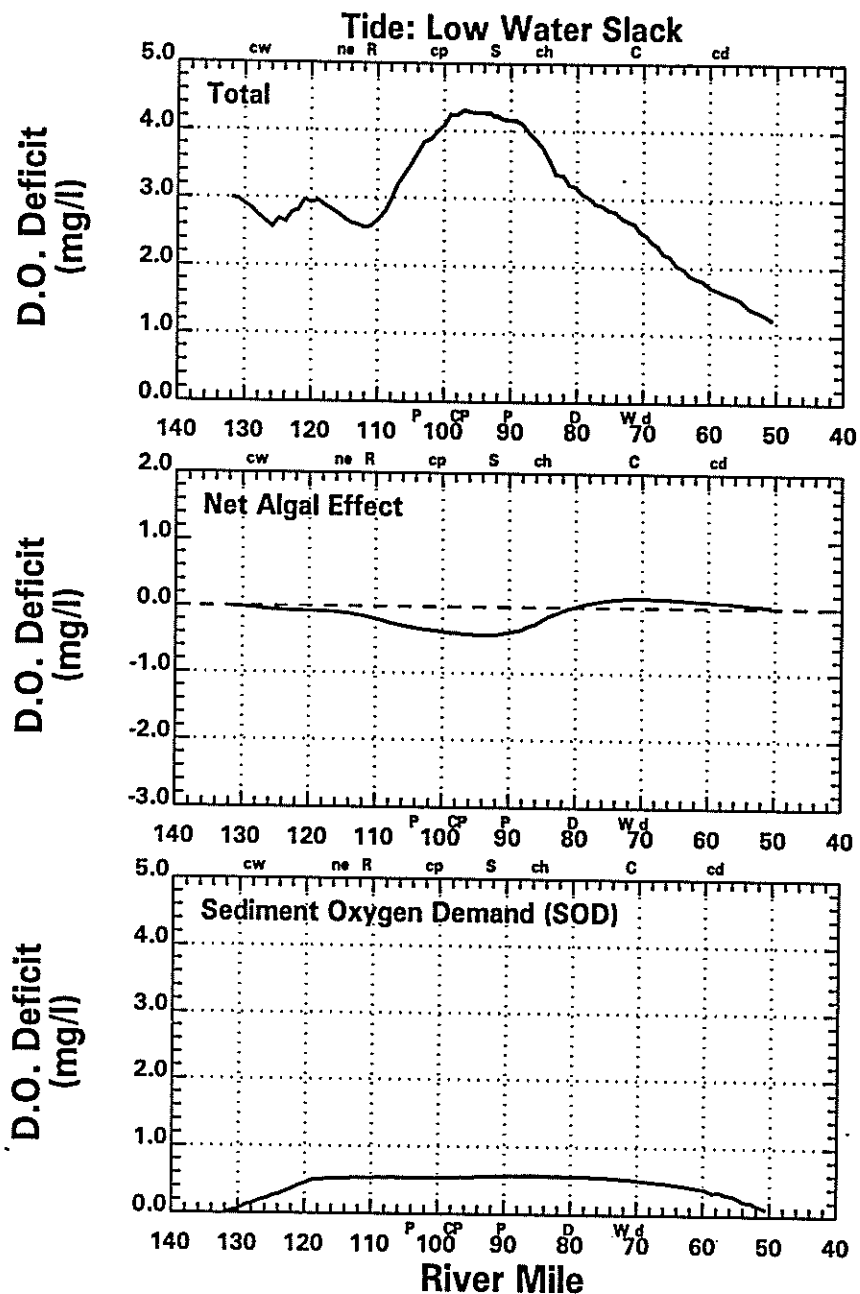
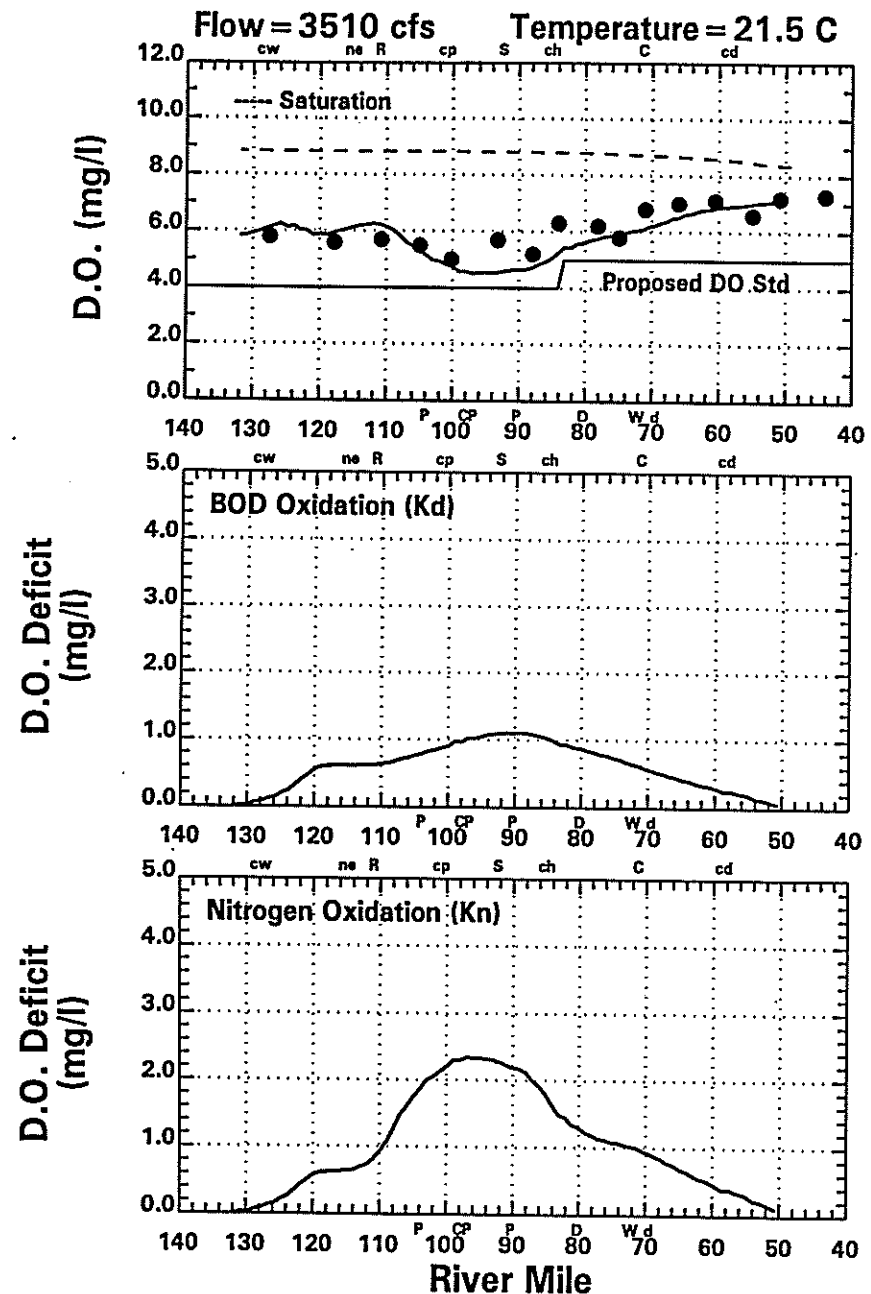
Delaware River Data (●) & Model (—) 8/5/91 (Model Day 56)
 [Temporally, Vertically and Laterally Averaged]



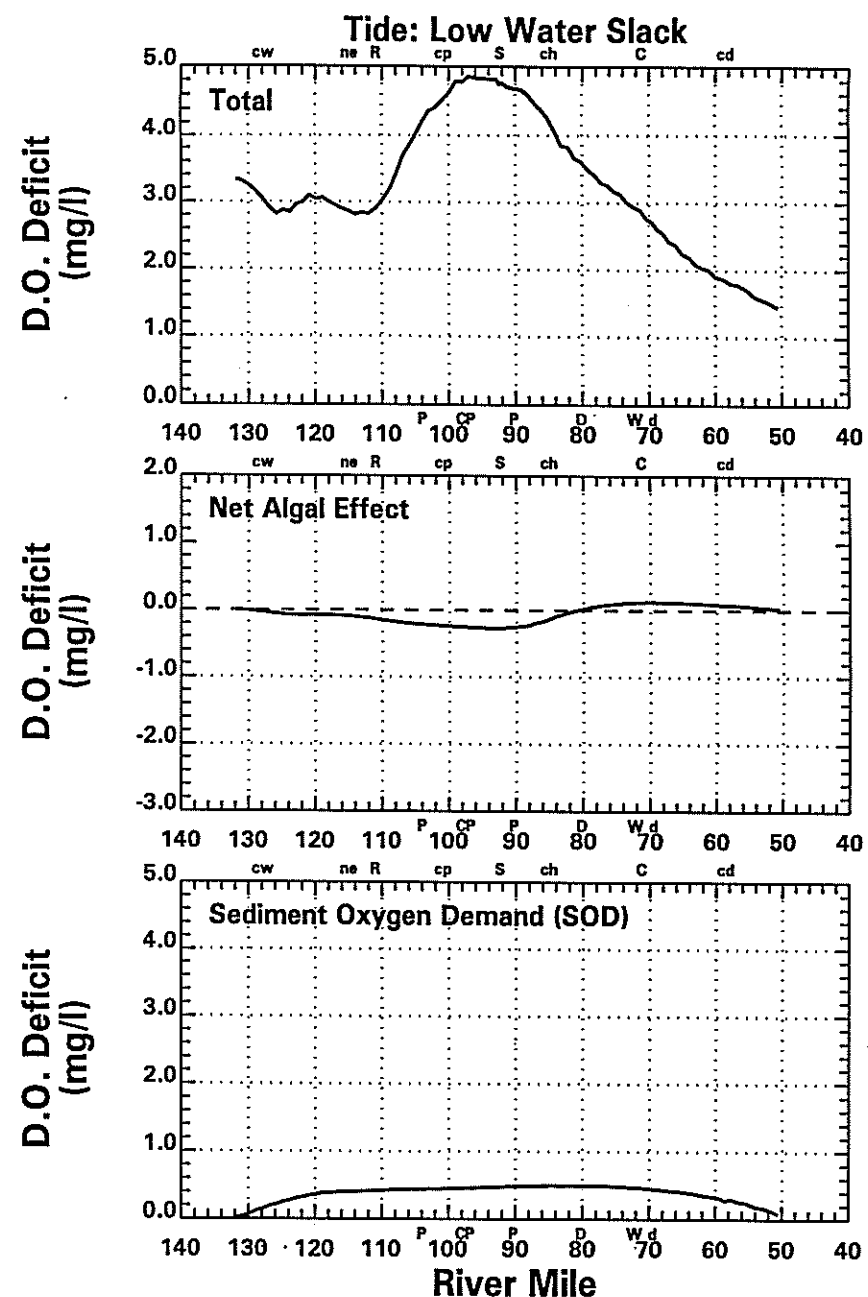
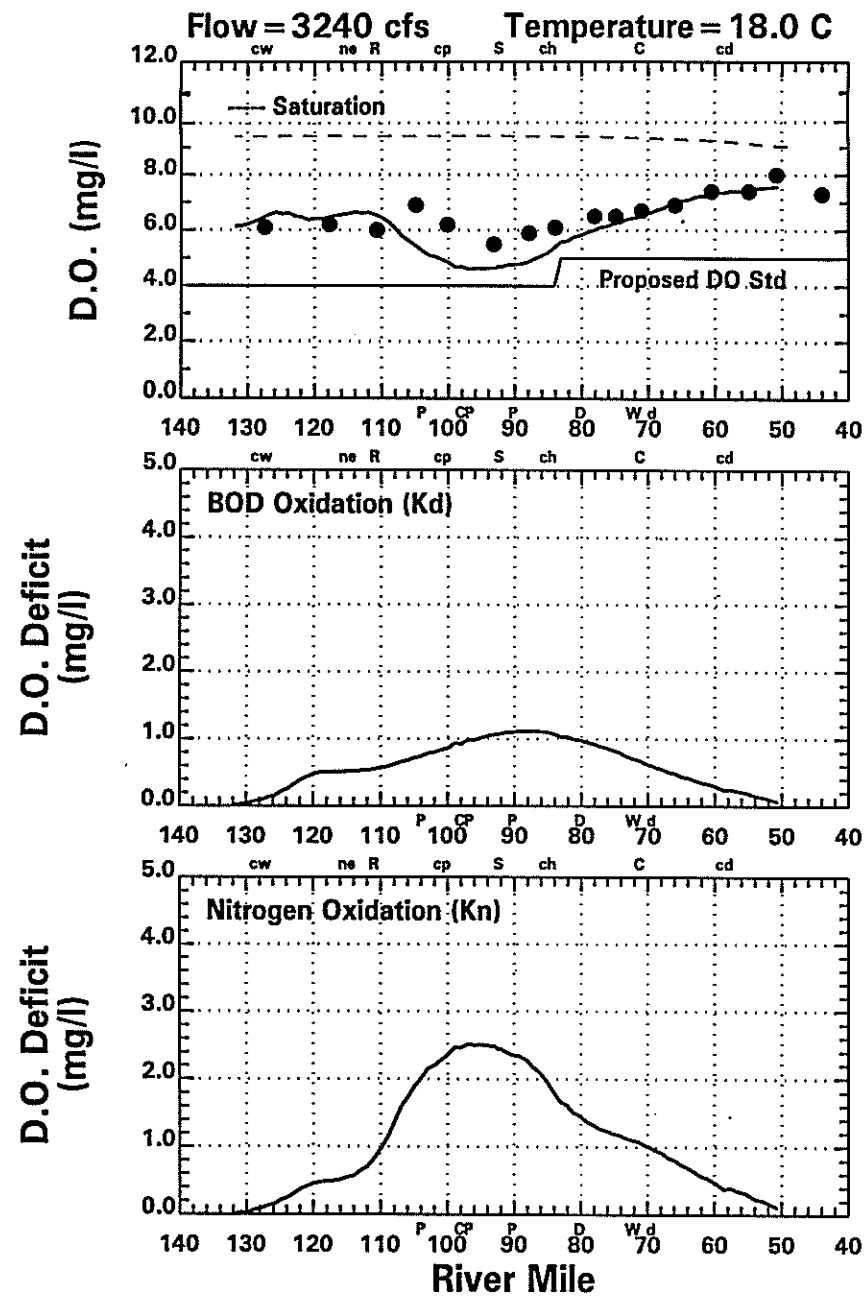
Delaware River Data (●) & Model (—) 8/26/91 (Model Day 77)
 [Temporally, Vertically and Laterally Averaged]



Delaware River Data (●) & Model (—) 9/3/91 (Model Day 85)
 [Temporally, Vertically and Laterally Averaged]



Delaware River Data (●) & Model (—) 9/23/91 (Model Day 105)
 [Temporally, Vertically and Laterally Averaged]



Delaware River Data (●) & Model (—) 10/7/91 (Model Day 119)
 [Temporally, Vertically and Laterally Averaged]

